ENERGY-SAVING NON-METALLIC CONNECTORS FOR PRECAST SANDWICH WALL SYSTEMS IN COLD REGIONS

A Thesis
Submitted to the Graduate Faculty
of the
North Dakota State University
of Agriculture and Applied Science

By

Austin James Allard

In Partial Fulfillment of the Requirements
for the Degree of
MASTER OF SCIENCE

Major Department:
Civil and Environmental Engineering

July 2012

Fargo, North Dakota

North Dakota State University
Graduate School

Title

Energy-Saving Non-Metallic Connectors for Precast Sandwich Wall Systems in Cold Regions

By

Austin James Allard

The Supervisory Committee certifies that this ***disquisition*** complies with North Dakota State University's regulations and meets the accepted standards for the degree of

MASTER OF SCIENCE

SUPERVISORY COMMITTEE:

Dr. Sivapalan Gajan
Chair

Dr. Frank Yazdani

Dr. Xiangfa Wu

Approved:

11-20-2014
Date

Dr. Dinesh Katti
Department Chair

ABSTRACT

Conserving energy in large structural buildings has become very important in today's economy. A number of buildings today are constructed with sandwich wall panels. Steel connections are most commonly used in these panels. The problem with steel is that it has a tendency to reduce the thermal resistance of the insulation.

This project considers glass fiber reinforcing polymers (GFRP) and carbon fiber reinforcing polymers (CFRP) as an alternate material to steel. An experimental sandwich wall panel was constructed and subjected to freezing temperatures.

The results of the experimental program were compared to a theoretical model using the ANSYS computer program. The model was verified using current analytical methods that determine the heat flux of a sandwich wall panel. The methods investigated include the parallel path, zone, parallel flow, and isothermal planes methods. The results suggest that the GFRP connectors perform slightly better than the steel and CFRP connectors.

ACKNOWLEDGEMENTS

I would like to thank my advisor, Dr. Yail J. Kim, for his leadership and instruction. He continued to guide me along the correct path for the research presented in this Master's thesis.

I would like to give a special thank you to my committee members, Dr. Sivapalan Gajan, Dr. Frank Yazdani, and Dr. Xiangfa Wu, for their technical guidance and expertise throughout the research process.

I would also like to thank Mechanical Engineering Professors, Dr. Iskander Akhatov and Dr. Michael Stewart, for answering my technical questions and help with designing the experiment. Thanks to fellow graduate students, Thomas Shanandore and Dallas Brown, for help preparing the experiments.

I also appreciate the funding from ND EPSCoR, and samples obtained from Wells Concrete.

Lastly, but most definitely not least, I would like to thank my wife, Kayla. Without whose love and support, I would not have been able to complete this thesis.

TABLE OF CONTENTS

LIST OF TABLES

LIST OF FIGURES

Figure Page

Figure Page

LIST OF ABBREVIATIONS

C_{Ave}..... Average Conductance

C_n..... Undetermined Constants

C_1..... Conductance of Part 1

C_2..... Conductance of Part 2

d..... Distance from the Panel Surface to the Connector

k_{con}..... Concrete Conductivity

k_{ct}..... Metal Wythe Connector Conductivity

k_{in}..... Insulation Conductivity

m..... Diameter of the Connector

P..... Percent of Steel

W..... Zone Width

W_n..... Revised Zone Width

LIST OF APPENDIX FIGURES

CHAPTER 1. INTRODUCTION

1.1. Introduction

Sandwich wall panels are becoming an increasingly more popular system for large structural buildings. They are commonly used as building envelopes. They are usually constructed using two outer layers of precast concrete and an inner layer of insulation material (Figure 1-1). These three layers are typically held together using metal connectors. Some responsibilities of the sandwich wall panel include insulation, supporting gravity loads, resisting wind loads, and aesthetics. This thesis will focus on the insulation properties of the panel.

Sandwich wall panels are typically manufactured in a lab to help control the quality. They are usually constructed with a height of 45 ft. and a width of 12 ft. The concrete layer thickness can range from 2 in. to 6 in. The insulation layer thickness can also change depending on the level of thermal protection that is required by the designing engineer or owner. This is determined by considering the thermal properties of the insulation being used and comparing it to the thermal loads the structure is exposed to.

There are additional benefits that contribute to the quality of the sandwich wall panel design. One of the main benefits includes making the structure more energy efficient. The walls are designed in a manner that makes certain the insulation is evenly distributed throughout the area of the panel. The insulation runs from edge to edge to ensure the concrete wythes don't connect. The insulation also cannot move after the panel has been fabricated, so there will be no gaps in

thermal performance throughout the life of the structure. The insulation is restricted in movement because it is sandwiched between two layers of concrete that are connected by ties. With the combination of the friction of the concrete and the connectors penetrating the insulation, the insulation will be unable to translate while in service. When a minimum required amount of thermal connectors are used, the design dictates approximating the wall as a panel with continuous insulation without connectors. When there are no connectors present, this will lower the energy costs of the structure. It is beneficial that concrete has a high thermal mass, because it is able to absorb large amounts of energy and resist increases in temperature (Designer's Notebook). Because this property acts in cohesion with insulation's resistance to temperature change, the overall thermal resistance of a sandwich wall panel is significant.

There are other advantages of using sandwich wall panels that are not related to its thermal performance. One of these advantages includes a reduced life cycle cost of structures using this material. This is attributed to the speed of erection and a decreased long-term maintenance cost (Designer's Notebook). The panels also provide design flexibility because they act as a loadbearing component and have an aesthetically pleasing outer finish. Furthermore, buildings constructed using these panels meet safety requirements, because the walls provide adequate strength to the structural system. Lastly, sandwich wall panels are durable as they have been subjected to long-term tests regarding impact, corrosion, freeze-thaw

conditions, abrasion, and extreme weather in harsh environments (Designer's Handbook), and have proved to be resistant to all of these damaging conditions.

1.2. Research Significance

Sandwich wall panels are commonly constructed using metal ties used to connect the two outer layers of concrete to the interior insulations layer. Recent research and engineering practice has shown an interest in substituting the metal tie connectors for carbon fiber reinforcing polymer (CFRP) or glass fiber reinforcing polymer bridges (GFRP). There have been a number of reports stating the structural benefits of using CFRP/GFRP in sandwich wall panels (Frankl et al. 2011). There hasn't been as much information on the beneficial thermal properties of CFRP/GFRP could have on the overall thermal performance of the system.

The current problem with using metal tie connectors in sandwich wall panels is they reduce the efficiency of the insulation. When designing a panel, the engineer decides if the wall should be non-composite, partially-composite, or fully composite. A fully composite wall offers the benefits of increasing the overall strength of the structure, because two layers of concrete act in cohesion while distributing stresses throughout the wall. The downside of this type of system is more metal connectors must be used to achieve composite action in the panel. As more connecters are used, the thermal efficiency of the wall becomes compromised. This is due the steel material having a large thermal conductivity. This property affects how fast heat can flow through a material. Energy travels through a path of least resistance, so heat begins to flow through the steel instead than being resisted by the insulation

layer. GFRP has a much smaller thermal conductivity than steel (Ashby, 13). This implies that GFRP could be used to achieve composite action without the negative effects on the thermal resistance of the structure.

1.3. Objectives

The objective of the research conducted was to evaluate the differences in the thermal performances of a sandwich wall panel using ties with various thermal properties and geometries. The main objectives addressed in the thesis presented include:

1. Construct a finite element analysis model to compare the heat flux in a sandwich wall panel.
2. Use experimental methods to validate computer model and perform a parametric study.
3. Determine the thermal efficiency of a sandwich wall panel using various connector materials and shapes.

1.4. Design Approach

This thesis will focus on the relationships between the thermal performance of a sandwich wall panel using steel, CFRP, and GFRP connectors. Each material will be compared using models constructed using finite element software. Three different shapes of thermal connectors are commonly used in practice, such as the W-shaped, Z-shaped, and J-shaped geometries, were considered. The properties of

each of these shapes will be changed to signify a different material in the model, and the effect on the thermal flux will be compared.

The model was verified for accuracy using experimental data. Miniature sandwich wall panel samples were constructed. The sides of the sample were insulated and one face was exposed to freezing temperatures. The change in temperature through the metal ties was recorded with time. This data was compared to the finite element analysis model for accuracy.

The value for the flux that the model found was also compared to some analytical methods that are currently being used to find the thermal resistance of a sandwich wall panel. These methods were modified to increase the accuracy of the methods to make them comparable to the research results.

1.5. Thesis Outline

A brief outline of the thesis is presented below:

Chapter 2: presents a literature review of research on the structural performance on CFRP/GFRP sandwich wall panels, and information on the thermal abilities of the panels.

Chapter 3: provides a description of the experimental work conducted. It includes the design and procedure used to record the temperature within the sample with time.

Chapter 4: describes the process involved with the predictive models. This includes a description of the finite element analysis and the current numerical methods used to determine the thermal resistance.

Chapter 5: presents the results and discussion of the research. It includes a comparison of the different materials along with several geometries.

Chapter 6: presents a summary and conclusion of the research and provides a recommendation for future work involving FRP sandwich wall panels.

References.

Appendix: provides additional figures.

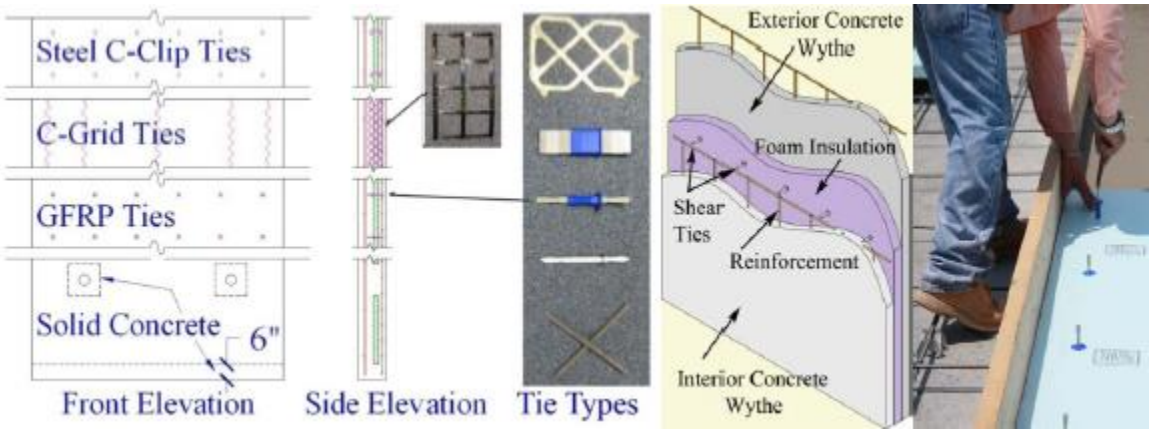

Figure 1-1: Sandwich Wall Panel (Naito et al. 10)

CHAPTER 2. LITERATURE REVIEW

2.1. Introduction

This chapter presents a review of literature related to sandwich wall panels. It includes reports about the structural efficiency of sandwich wall panels constructed with FRPs. The impact of the strength of the connectors is also discussed. The thermal performance of the panels is evaluated. A new FRP geometry that has been developed is discussed. Finally, a revised method to determine the R-value is discussed.

2.2. Structural Efficiency

There has been research done evaluating the structural efficiency of sandwich wall panels. The most recent research consists of trying the make the panels more structurally and thermally efficient. To be able to accomplish this, the sandwich panel must have three characteristics. The first component is composite action must be achieved through the connectors. Secondly, the thermal resistance of the connectors must be high. Lastly, the concrete should not penetrate through the insulation layer. The first two can be fulfilled by using FRPs, because of their low thermal conductivity. The last one is accomplished by ensuring quality throughout the manufacturing process.

A study conducted by the University of Nebraska provided some results pertaining to the structural efficiency of sandwich wall panels using FRP bars. There were four different types of geometries tested (Figure 2-1). Results of a shear

test showed that the FRP connector's axial strength governed the shear strength. The concrete also successfully bonded to the insulation to produce a more uniform material. This showed that the insulation contributed roughly 10% of the shear capacity.

2.2.1. Small Scale Flexural Experiments

Small scale flexural testing was also performed on the FRP specimen (Einea et al. 1994). The results showed that the panels exhibited non-composite action during the elastic stress level (Figure 2-2). Though, the panel's ultimate strength was close to that which could be achieved through composite action, so structural efficiency was accomplished with this design. Composite action means the structural member is obtaining the most load resistance that it can from the materials being used. Since the panel was non-composite at early stages and composite at failure, this leads to the conclusion that the connectors slip at the beginning of loading, but they eventually fail when the ultimate strength is reached. The slipping could help reduce the effect of bowing that occurs in the panels because of temperature differences.

2.2.2. Large Scale Flexural Experiments

Large scale flexural testing experiments were also conducted to show the practicality of the panels and to simulate conditions that would be actually applied in the field (Einea et al. 1994). The results of the experiment showed that longer sandwich panels show more composite properties than shorter panels (Figure 2-3).

2.2.3. Finite Element Analysis Model

The results of the full scale model were verified using a finite element program. The results of the analysis were very similar to the outcome of the experiments (Figure 2-4). The model is slightly stiffer because the program did not account for the slippage of the FRP bar.

The research at the University of Nebraska showed that sandwich wall panels constructed with FRP rods are structurally efficient, because they show composite action to achieve maximum strength. It was also noted that even though FRP is a brittle material, the overall performance of the sandwich panels showed ductile behavior. It is also suggested that the FRP be anchored into the concrete of the panels.

2.3. Strength of the Connectors

Research has been conducted about the strength of the connectors used in sandwich wall panels. To obtain composite action, and thus, achieve the maximum structural efficiency of the panels, the shear force must be transferred through the connector ties in a direction that is perpendicular to the loading. This makes the design of the connectors a critical component in the overall efficiency of the sandwich panels. The design of these ties is most commonly done using the method recommended by the Precast/Prestressed Concrete Institute.

2.3.1. Types of Connectors

There are various types of materials used to construct the shear connector ties. A few of these materials are carbon steel, stainless steel, carbon fiber

reinforced polymer (CFRP), glass fiber reinforced polymer (GFRP), and basalt fiber reinforced polymer (BFRP). Stainless steel is usually favored over steel when corrosion resistance is required. CFRP, GFRP, and BFRP are preferred over metallic materials if thermal resistance is a high priority (Naito et al. 2010). This is because the former materials offer lower thermal conductivity values.

There are a number of different geometries that can be used for the connectors. These include trusses, pins, rods, and grids. Since the materials have different properties, the deformation related to each material used will also change. Because FRP is a brittle material and steel is ductile, this will affect the flexural abilities of the sandwich panels. This was discussed in the previous section.

2.3.2. Connector Experiment

An experiment was designed to determine the structural performances of connectors with various materials and geometries in sandwich wall panel construction (Figure 2-5)(Figure 2-6). The experiment was done following standards specified in ASTM E488 with the exception that the insulation was also taken into account. The samples were tested under a simulated uniform pressure load.

The results showed each connector type differed in strength, stiffness, and deformation. The FRP truss connection showed elastic-brittle behavior. Other sandwich wall panels constructed with FRP connections showed elastic-plastic behavior, and failed from tension. Elastic-plastic behavior was shown by the steel wire truss. Elastic-plastic behavior was shown in the steel M-clip and C-clip, and failed from pullout of the concrete (Figure 2-7).

The flexural deformation was also measured during the experiment. A shear force diagram was used to determine that the ends of the sandwich wall panel have the highest shear deformation values, while the middle has zero. It was also shown that if the connector is too flexible, the two concrete layers will not act together to resist flexure. A stiff tie will increase the initial strength of a sandwich panel by changing the strain energy. This leads to the conclusion that flexible ties lead to a decreased post-cracking flexural stiffness, but the overall strength remained fairly close. The results of the experiments were verified using a model (Figure 2-8).

2.4. Thermal Performance

Recent research conducted at Lehigh University focused on improving the thermal performance of sandwich wall panels (Lee and Pessiki, 2005). The panels are typically constructed using two writhes of concrete separated by one layer of insulation. This research focused on using three writhes of concrete separated by two staggered layers of insulation. Concrete was used as the thermal connector instead of the usual steel material. The process used to evaluate the thermal efficiency in the research was also used in this thesis.

2.4.1. R-value

Research indicates the shear tie connectors of concrete that penetrate the insulation could reduce the thermal performance of a sandwich panel by as much as 40% (McCall 1985). This reduction in thermal performance is commonly evaluated by determining a panel's thermal resistance or R-value. The R-value is the ability

of a material to resist the flow of heat energy. A material with a high R-value would be more efficient at keeping a building warm during winter months.

2.4.2. Evaluation of Thermal Performance

There are three common practices used to evaluate the thermal performance or resistance of a sandwich wall panel. The first method is found in the American Society of Heating, Refrigerating, and Air-Conditioning Handbook (ASHRAE). These use electric-circuit analogies to determine the R-value, and will be discussed in Chapter 4.

The second way to evaluate is by experimental methods. The most commonly used experiment is the Guarded Hot Box apparatus. During the experiment, the panel is placed in a box where warm air is applied on one face and cold air on the other. The remaining four sides are insulated to direct the heat transfer through the sample under observation. Once steady state is reached, the total heat flow of the system can be found. The overall thermal resistance can be determined by taking the difference of the air temperatures, multiplying by the area of the sample, and dividing by the heat flow.

The third method used to evaluate the thermal performance of a sandwich panel is a finite element analysis approach. The finite element analysis of the two and three wythe panels were performed using the SAP 90 Heat Transfer Analysis Program (Lee and Pessiki 2006). This program estimates the R-value of a panel. This was the primary source of evaluation of the panels. A similar program was used for the analysis in this thesis and is described in Chapter 4.

2.4.3. Three Wythe Panels

Two wythe sandwich panels were constructed using two different techniques for the concrete connectors. The first included drilling holes in the appropriate locations of the insulation. The second involved leave space around the edges of the insulation to provide space for the concrete connections (Figure 2-9). The purpose of these connections includes holding the insulation in place and to aid in achieving composite action. Experiments using the Guarded Hot Box Method have shown that R-value was reduced by 45% when these concrete connections were added compared to a sample without connections.

In an attempt to help improve the thermal performance, a three wythe sandwich wall panel was developed. The panel has three wythes of concrete and two layers of insulation that are staggered to insulate the entire area of the panel. If the top layer has a section with a gap in the insulation, the bottom layer will cover it to prevent a thermal bridge (Figure 2-10).

2.4.4. Advantages

The first advantage of the three wythe panel is the increased thermal performance. Another, is the concrete between the layers of insulation help accomplish composite action to improve the strength. Some potential advantages that need to be investigated include an increase in span length because of the increased thickness of the panel. Since the concrete is thicker in regions between staggered concrete, there are more places to put equipment that is needed for the construction of wall panels in structures. It is also a possibility that prestressing

could be done on the middle concrete wythe. This would reduce the amount of steel in the system, provide better corrosion protection against the steel, and prestressing would only have to be done once.

On the downside, the three wythe panel system could also increase production time and costs.

2.4.5. Thermal Performance Results

It was shown that the thermal performance of the three wythe panels were better than the two wythe panels (Figure 2-11). This is due to the longer path the heat energy has to take to get through the panel. As the amount of concrete that is penetrated through insulation is decreased, the R-value of the panel is increased. When the thickness of the concrete is increased, the R-value doesn't change much, but when more insulation is used, there is a greater increase in the R-value. When high R-value insulation is used, three wythe sandwich panels have a greater impact on the total R-value of the system (Figure 2-12).

2.5. Nu Sandwich Panel

Since the invention of the sandwich wall panel, there have been continuous improvements to the efficiency of the system. One of the newest improvements is the NU-tie system (Maximos et al. 2007). This system implements a glass fiber reinforce polymer connector system. It has proven to have high structural performance, low thermal conductivity (higher R-value), and is easy to install.

2.5.1. Evolving design

NU-ties were designed using glass fiber reinforced polymers because they have efficient thermal and mechanical properties that are ideally suited for sandwich wall panels. The NU-tie has gone through five design changes since it was first constructed (Figure 2-13). This was done to ensure the most efficient design is to be implemented in the field.

2.5.2. Thermal Efficiency

GFRP connectors have a small thermal conductivity (0.2-5 W/mK) compared to steel (15-50 W/mK). The NU-tie also has a small cross sectional area (3/8 in. diameter) penetrating the insulation. These properties reduce the effects of thermal bridging and will increase the thermal efficiency of the panels.

The thermal performance of the panels was calculated by finding the R-value for three systems. The first was a sandwich wall panel with metal connectors. The second used insulated concrete form. The third sandwich panel type implemented the Nu-ties. The revised zone method was used to find the R-values. This method will be discussed in the next section.

The results of the thermal evaluation showed that insulated concrete form had 44% more thermal efficiency than the panels with metal ties (Figure 2-14). The NU-tie system was 75% better than the metal tie panels. The thermal characteristics of the GFRP used were beneficial to the thermal performance.

2.5.3. Ease of Production

The NU-tie panels are manufactured similar to sandwich wall panels with metal connectors. The lone exception is how the tie is placed into the insulation. When a Nu-tie is used, a slot is melted into the foam. Then the Nu-tie is placed into the recently formed slot. Foamed insulation is used in the remaining parts of the insulation to ensure there is no thermal bridging. After that is done, the insulation with the NU-ties can be placed in between the concrete wythes in the usual steps of the manufacturing process (Figure 2-15).

2.5.4. Structural Efficiency

Full scale tests were conducted using sandwich wall panels that included the latest generation of NU-tie design. The variable in the experiment was the number and location of the NU-ties. The test was performed to evaluate the effect the spacing of the ties had on the flexural capacity and stiffness of the panels.

A load-deflection relationship was created based on the results of the experiments (Figure 2-16). The graphs show that sandwich panels made with three rows of NU-tie connectors close to the edge of the panels exhibit almost four times the flexural capacity.

The results of the experiment were compared to the theoretical values that can be calculated using the PCI Design Handbook. The comparison showed the experimental results of the panel with two rows of NU-tie connectors achieved only 76% of the theoretical value. These panels did not exhibit composite behavior. The experimental values of the panels with three rows of NU-tie connectors exceeded

the theoretical values. When the experiment was being designed, the PCI Design Handbook method for determining the number of connectors to achieve composite action suggested three rows of connectors. The PCI Design Handbook is an efficient resource for designing sandwich wall panels with NU-ties.

The deflections measured in the experiment were verified using the truss model, beam model, and FE models. The truss and FE models provided the most accurate estimations of the actual performance. The truss model was preferred for deflection measurements based on simplicity.

2.6. Revised Zone Method

Research has been done to improve the analytical methods used to design a sandwich wall panel for a specific R-value (Lee and Pessiki 2008). The current analytical methods are found in the ASHRAE Handbook and will be discussed in Chapter 4. The improvements to the zone method will be discussed here.

2.6.1. Purpose of Revision

One important component of the zone method is called the zone width, W. The zone width is calculated based on the geometry of the sandwich panels. The zone width parameter was originally designed to be applied to metal frame structures, and it is not accurate when applied to metal connectors. The revision of the zone method begins with a new zone width, W_n. The new zone width was determined by comparing a series of finite element analysis models to evaluate the important parameter affecting the R-value of the sandwich panels. It was

determined that the metal connector size and material conductivities were the most influential variables.

2.6.2. Proposed Zone Width

After performing a parametric study using the finite element analysis software, the heat flow could be found for the panels. The flow was used to calculate the R-value. Then, the R-value was used to back calculate the zone width using the Zone Method. Equation 2-1 was the first assumption used to find the new zone width. The constants, C_n, were found through varying the connector sizes, cover distance, and conductivity. This process leads to the simplified Equation 2-2. The process was simplified further by inputting common thermal conductivity values to create Equation 2-3. The resulting equation is slightly different from the original zone width calculation. The new version places a higher priority on the thickness, m, of the metal connectors. The cover thickness, d, has an insignificant effect on the new zone width. The overall change to the R-value calculation is small, but the change increases the accuracy of the method.

$$W_n = (C_1 k_{con} + C_2 k_{in} + C_3 k_{ct} + C_4)m + C_5 k_{con} + C_6 k_{in} + C_7 k_{cl} + C_8 + C_9 d \quad (2\text{-}1)$$

$$W_n = (0.17k_{con} - k_{in} + 0.0026k_{ct} + 2.24)m + 0.02k_{con} - 0.6k_{in} + 0.0024k_{ct} + 2.35 - 0.15d \quad (2\text{-}2)$$

$$W_n = 4.9m + 3.5 - 0.15d \quad (2\text{-}3)$$

2.6.3. Verification

The Revised Zone Method was verified by comparing the results of the finite element analysis to the new method. Various parameters were varied to study how the new method handled the change. One of the first parameters studied was the metal connector spacing (Figure 2-17). As the tie spacing increased, the R-value also increased because of less metal connectors used. The Revised Zone Method accurately modeled this increase, whereas, the Zone Method overestimated the R-value.

Other parameters considered were connector diameter, cover distance, concrete conductivity, insulation conductivity, and metal wythe connector conductivity. These all showed similar results as the first parameter. The Revised Zone Method was accurate and the Zone Method overestimated. The percent difference between the finite element analysis and both methods was determined (Figure 2-18). This shows that with various concrete and insulation thicknesses, the total error with the Revised Zone Method was at most 1%. The error with the Zone Method was up to 6%.

Overall, the Revised Zone Method is the most accurate technique to predict the R-value of a sandwich wall panel with metal tie connectors.

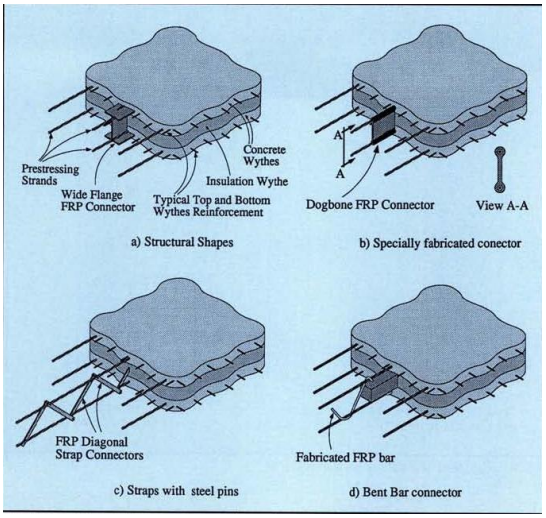

Figure 2-1: Various FRP geometries tested by the University of Nebraska (Einea et al. 1994)

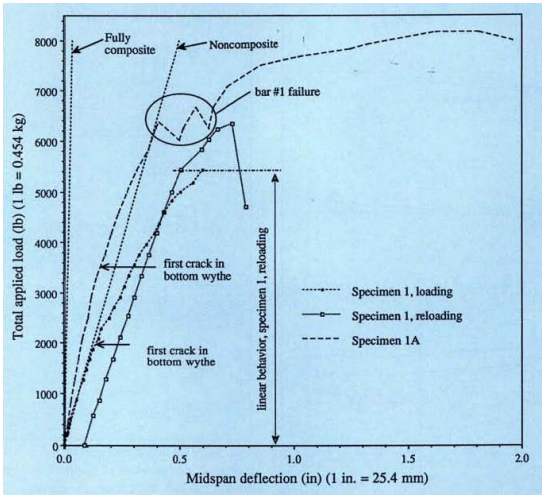

Figure 2-2: Results of the Small Scale Test at the University of Nebraska (Einea et al. 1994)

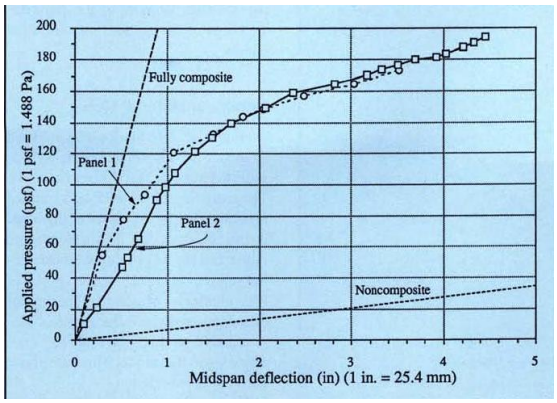

Figure 2-3: Results of the Full Scale Test at the University of Nebraska (Einea et al. 1994)

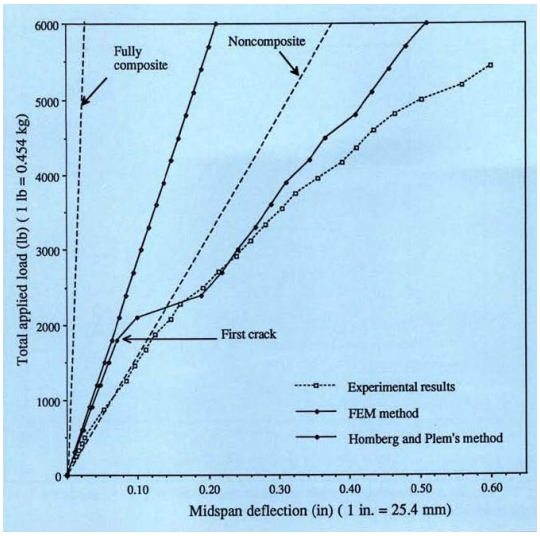

Figure 2-4: Comparison of the Model and Full Scale Test at the University of Nebraska (Einea et al. 1994)

Table 1: Shear Tie Matrix (Note: 1 in. = 25.4 mm)				
ID	Company	Tie Type	Material	Size
A	Dayton	Delta Tie	GFRP Grid	Standard
B	THERMOMASS	Composite Tie	GFRP Pin	CC 150-50-50-50
C		Non-Composite Tie	GFRP Pin	MC 20/50
D-1[1]	Altus Group	C-Grid w/ EPS	CFRP Grid	C50 – 1.8 X 1.6
D-2		C-Grid w/ XPS	CFRP Grid	C50 – 1.8 X 1.6
E	Universal Building Products	TeploTie	GFRP Tie	10 mm dia. x 150 mm
F		RockBar	Basalt FRP Bar	7 in. x 5/16 in.
G	TSA Manufacturing	C-Clip	Galvanized Steel	5 in. x 1.5 in. wide
H-1[2]	Dayton Superior	C-Clip	Galvanized Steel	4 in. x 1.5 in.
H-2[3]		C-Clip	Stainless Steel	4 in. x 1.5 in.
I		M-Clip	Galvanized Steel	0.25 in. dia. – 6 in. tall
J	Meadow Burke	Welded Wire Girder	1008 Steel	0.25 in. dia. wire
K	Dayton Superior	Single Wythe Truss	Hot Dipped Galvanized Steel	See Figure 3
L		Single Wythe Ladur	Hot Dipped Galvanized Steel	See Figure 3
[1] Two tests conducted, [2] One test conducted, [3] Four tests conducted				

Figure 2-5: Experimental Test of Connectors (Naito et al. 2010)

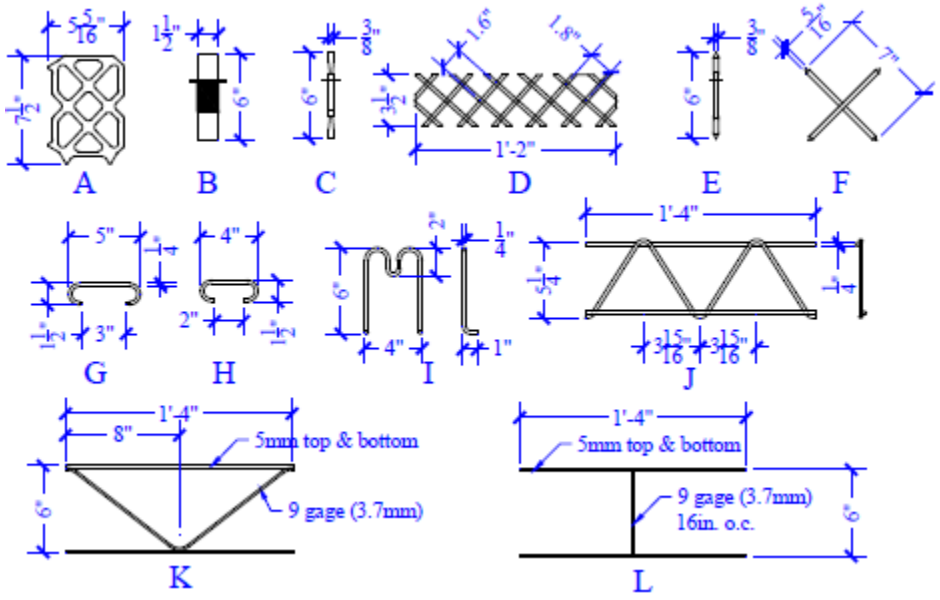

Figure 2-6: Experimental Test of Connectors (Naito et al. 2010)

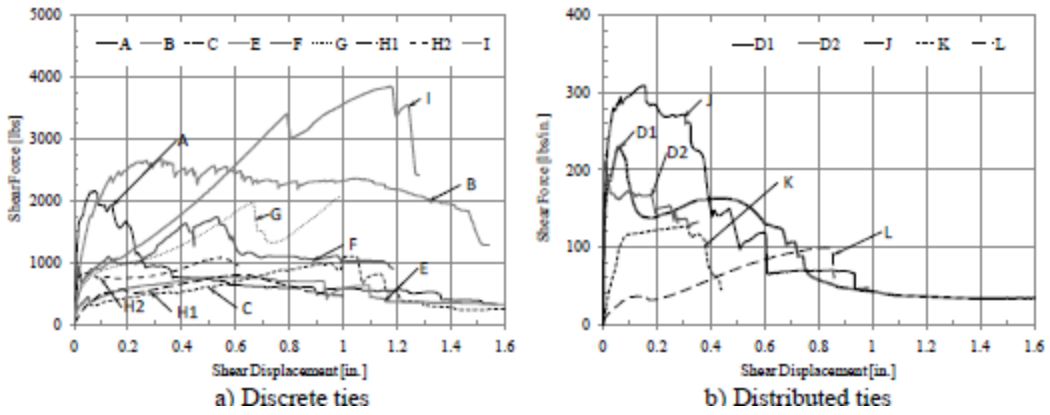

Figure 2-7: Experimental Test of Connectors (Naito et al. 2010)

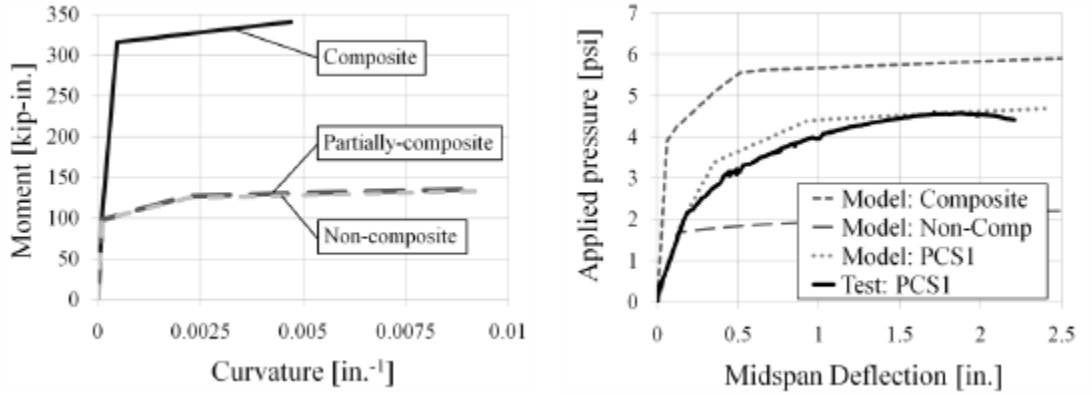

Figure 2-8: Model of Connectors (Naito et al. 2010)

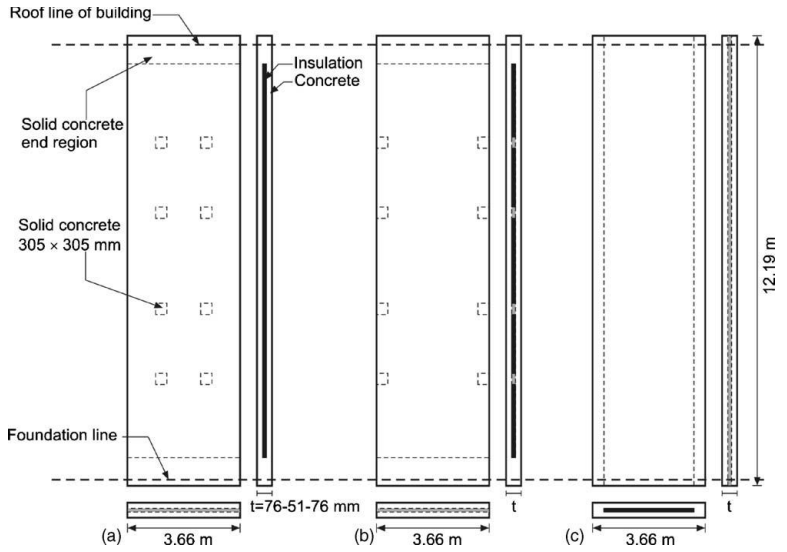

Figure 2-9: Two Wythe Sandwich Wall Panels (Lee and Pessiki 2006)

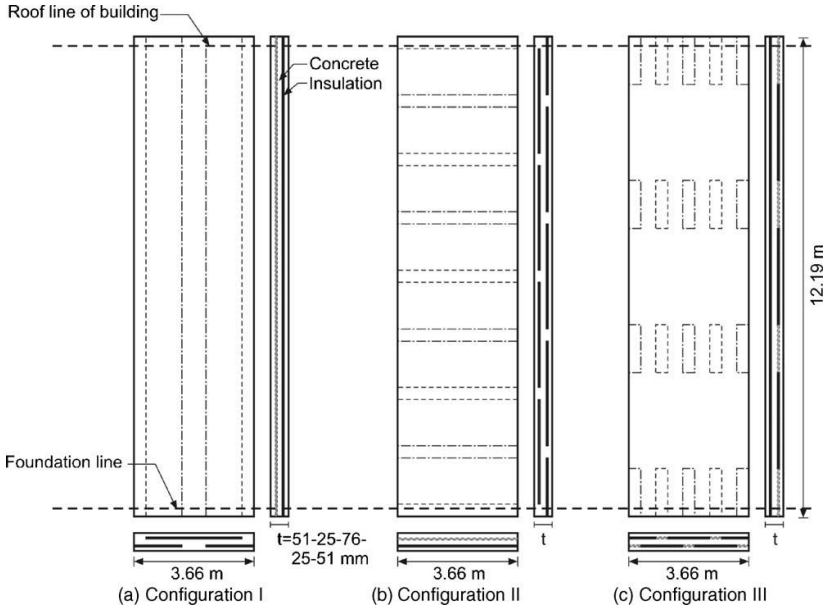

Figure 2-10: Three Wythe Sandwich Wall Panels (Lee and Pessiki 2006)

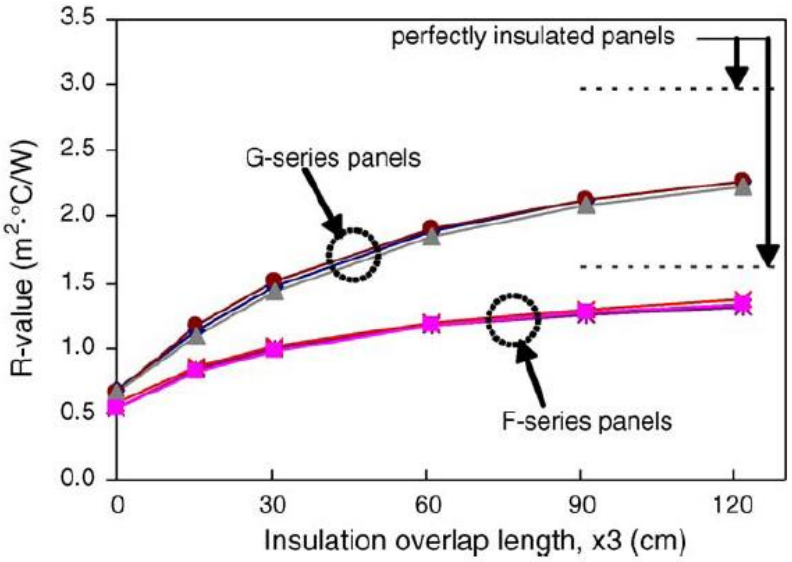

Figure 2-11: Thermal Performance (Lee and Pessiki 2006)

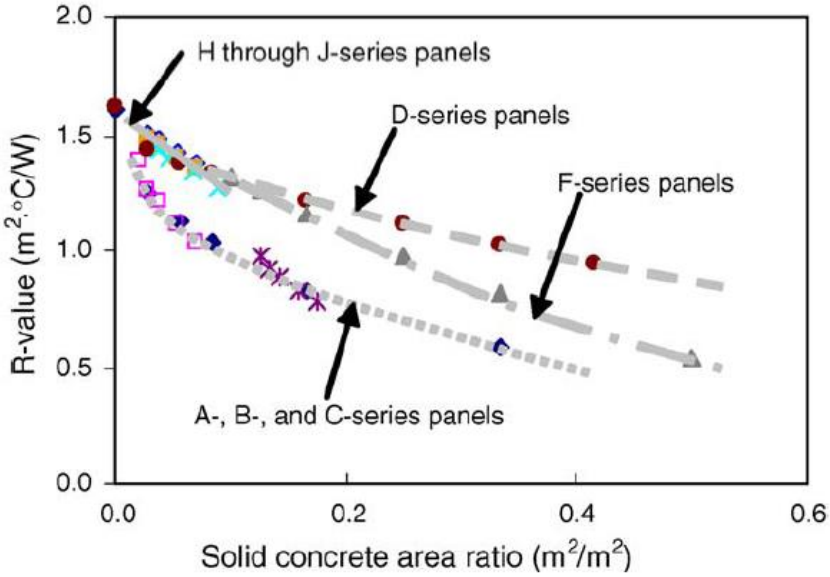

Figure 2-12: Thermal Performance (Lee and Pessiki 2006)

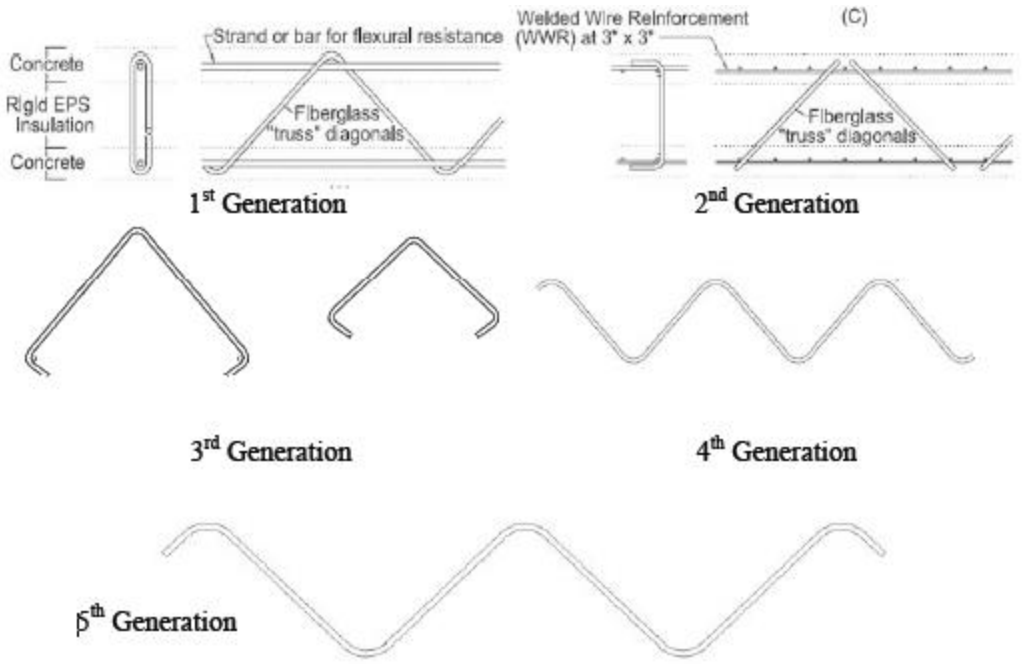

Figure 2-13: Five NU-tie Generations (Morcous et al. 2010)

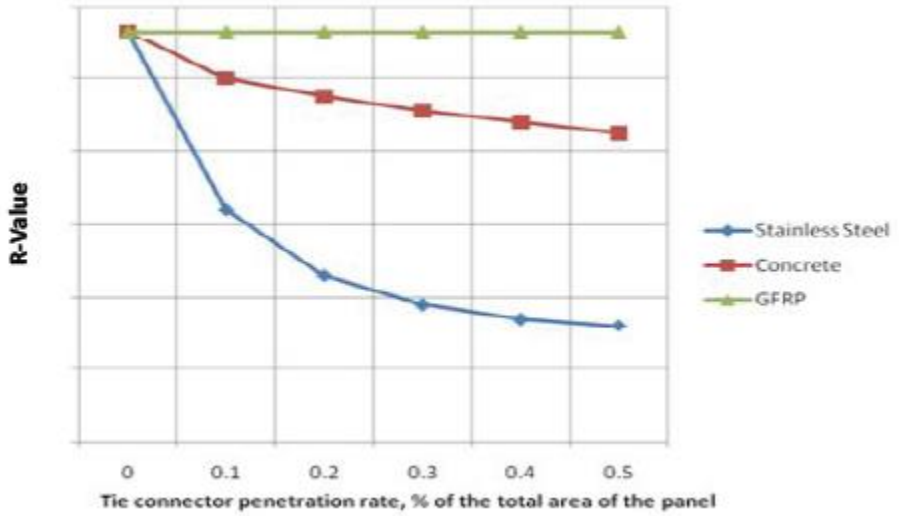

Figure 2-14: Thermal Performance of NU-Ties (Morcous et al. 2010)

Figure 2-15: NU-tie Manufacturing Process (Morcous et al. 2010)

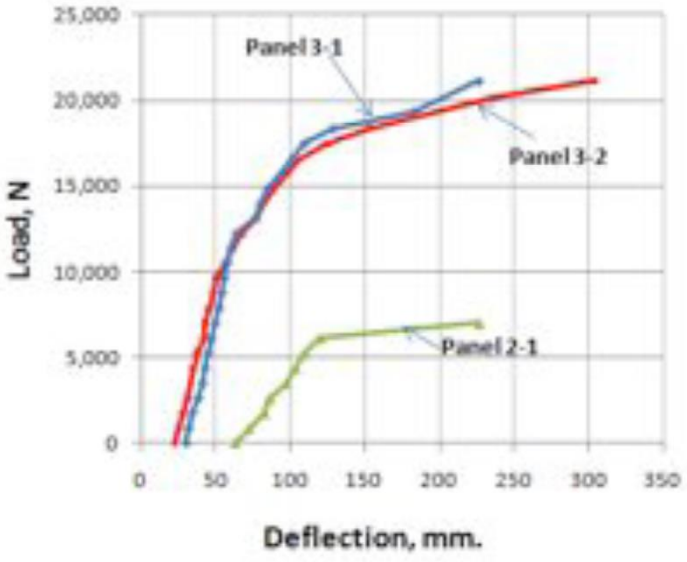

Figure 2-16: Load-Deflection Relationship (Morcous et al. 2010)

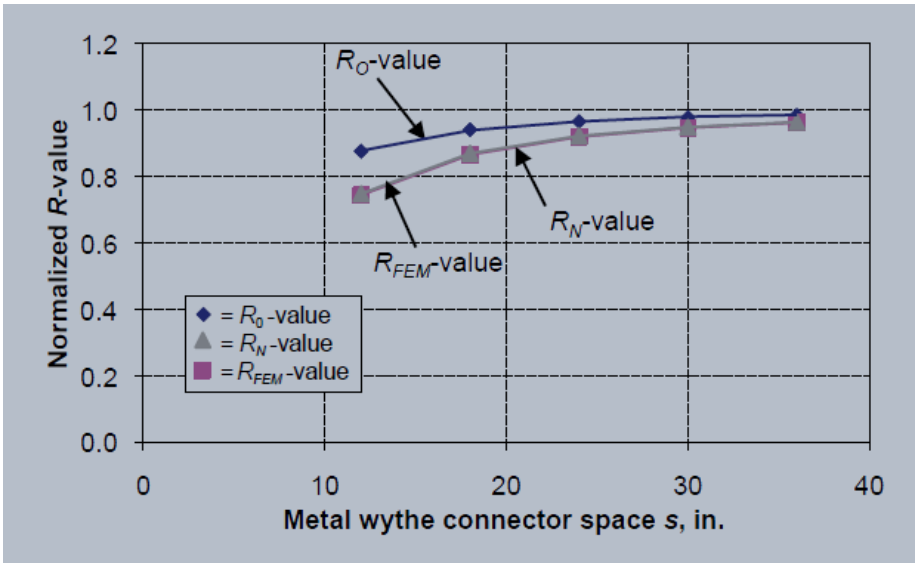

Figure 2-17: Revised Zone Method Verification (Lee and Pessiki 2008)

Panel wythe thickness, in.-in.-in.	Finite element method	Zone method with Eq. (1)		Zone method with Eq. (3)	
	R_{FEM}-value, $\frac{hr \times ft^2 \times °F}{BTU}$	R_0-value, $\frac{hr \times ft^2 \times °F}{BTU}$	R_0/R_{FEM}	R_N-value, $\frac{hr \times ft^2 \times °F}{BTU}$	R_N/R_{FEM}
2-1-2	4.9	5.0	1.03	4.8	0.99
3-1-3	5.0	5.2	1.03	5.0	1.00
4-1-4	5.2	5.3	1.03	5.2	1.00
2-2-2	8.3	8.6	1.04	8.2	0.99
3-2-3	8.4	8.8	1.05	8.4	1.00
4-2-4	8.5	9.0	1.05	8.6	1.01
2-3-2	11.6	12.2	1.05	11.5	1.00
3-3-3	11.7	12.4	1.06	11.7	1.00
4-3-4	11.8	12.6	1.06	12.0	1.01
Note: 1 in. = 25.4 mm; $1 \frac{hr \times ft^2 \times °F}{BTU} = 0.1761 \frac{m^2 \times °C}{W}$.					

Figure 2-18: Revised Zone Method Verification (Lee and Pessiki 2008)

CHAPTER 3. EXPERIMENTAL WORK

3.1. Introduction

This chapter presents the experimental work performed for this thesis. Usually, sandwich wall panels are evaluated by determining the R-value using the Guarded Hot Box method, but instead, an original experimental method was developed to evaluate the thermal performance of the panels in a different way. The experimental work focused on the rate at which the temperature changed through the center of the panels where the connectors were placed. This chapter will focus on the materials used for test specimen, description of the samples, the experimental setup, instrumentation used, and the thermal tests performed.

3.2. Materials Used for Test Specimen

Sandwich wall panels are traditionally constructed with concrete, insulation, and metal connectors. These three core materials were used in the experiment. In addition to the conventional metallic connectors, the performance of GFRP and CFRP connectors were evaluated in the experiments.

3.2.1. Steel Connectors

Steel connectors were obtained from a manufacturer of sandwich wall panels. The steel connectors used included three different geometries. The W-shaped connector had a diameter of 2.56 mm (Figure 3-1a). The Z-shaped (Figure 3-1b) and J-shaped (Figure 3-1c) connectors had a diameter of 4.65 mm. All three connector types were 6 in. (152.4 mm) in the longitudinal direction. Each connector was used

in its own sandwich wall panel specimen. There were two specimens constructed with each connector type. One had a single connector in the center, and the other had four connectors spaced evenly apart (3 in. between connectors and 3 in. to each edge).

3.2.2. GFRP Connector

A glass fiber reinforced polymer (GFRP) dowel was also used in the testing (Figure 3-1d). The dowel was smooth, and had a diameter of 16 mm. The dowel was also 152.4 mm tall. The GFRP dowel used is not a design shape that would be implemented in the field because it doesn't provide a surface for the concrete to easily bond to. It was used solely for the purpose of evaluating the results with a model that will be discussed in Chapter 4 and comparing with the steel and CFRP connectors.

3.2.3. CFRP Connector

Carbon fiber reinforced polymer (CFRP) connecters were evaluated. Two different geometries were used. The first was a rectangular shaped strip (Figure 3-1e). The dimensions were 16 mm x 2.5 mm x 152.4 mm. The second geometry used was a circular bar (Figure 3-1f). It had a diameter of 6.75 mm and a depth of 152.4 mm. These CFRP connectors, just like the GFRP connectors, were used solely for the purpose for comparison with the model, and would not typically be used in the field.

3.2.4. Insulation

The type of insulation most commonly used in sandwich panels is called cellular insulation. This material is rigid and provides ideal properties for the panels. A few of these beneficial properties are moisture absorption, dimensional stability, and a favorable compressional and flexural strength (Losch et al. 2011). The insulation thickness chosen for the experiment was 1.5 in. Insulation thickness in sandwich wall panels used in actual construction can vary from 1 to 4 in.

3.2.5. Geometry

Nine different small scale sandwich wall panels were constructed for this research. All nine samples had two concrete wythes that were 3 in. thick each. The insulation thickness of each was 1.5 in. The cross sectional area of each panel was 9 in. x 9 in. The connectors were varied in each sample. There were two panels of W-shaped, two of Z-shaped, two of J-shaped, and one GFRP dowel, CFRP strip, and CFRP bar. Two thermocouple wires were placed on the connectors. The locations of the wires were on both sides of the insulation. The thermocouples were placed in these locations to determine if the insulation slowed the heat transfer of the connectors.

3.3. Experimental Setup

The small scale sandwich panels were constructed in a manner similar to the construction of large scale panels. First, a wood form was built with the interior dimensions of 9 in. x 9 in. x 7.5 in. (3 in. concrete, 1.5 in. insulation, 3 in. concrete). A concrete mix was prepared with design strength of 20 MPa. The mix included 4.3

Kg of water, 8.8 Kg of cement, 20.1 Kg of course aggregate, and 16.8 Kg of fine aggregate. The concrete mix was poured into the form up to the three inch thickness. The connectors were pushed through the 9 in. x 9 in. x 1.5 in. insulation layer. One thermocouple was bonded to connector on the inside portion of the insulation, and another was bonded on the outside portion (Figure 3-2). The insulation with the connector and two thermocouples were placed on top of the wet concrete. Then, an additional three inches of concrete was poured on top of the insulation (Figure 3-3).

For the experiment, an insulation box was constructed. The box was 4.5 in. thick of insulation. This thickness was used because it would have a significantly greater R-value than the concrete sandwich wall panels. This was determined by comparing the resistance of 4.5 in. of concrete to the resistance of a sandwich panel without connectors. Since the connectors reduce the R-value of the panel, it is a conservative comparison. By comparing the R-values, it would help to ensure the heat was flowing through the panel opposed to being lost through the walls of the box. The 4.5 in. thickness included three 1.5 in. thick layers of insulation. One side of the box was left open to place the concrete panel specimen into (Figure 3-4a). The various test specimens could be interchanged in the box between tests. Insulating foam was also used to decrease the heat lost through the space between the insulation box and the wall specimen.

3.4. Instrumentation

The thermocouple wires from the sandwich panels were connected to a module that was controlled by a computer. The computer ran on the DATAQ software. It was accurate to +/- 1 degree Celsius. The temperatures recorded give the approximate temperature of the connectors, concrete, and insulation intersections.

3.5. Thermal Tests

The insulation box with the sandwich wall panels and thermocouples were placed into a freezer that was set at a temperature of -30 degrees Celsius (figure 3-4b). The temperature of the freezer fluctuated +/- 3 degrees over the length of each experiment. Each test was run over a period of 12 hrs. This was done to determine the rate at which the temperature changed throughout the panels.

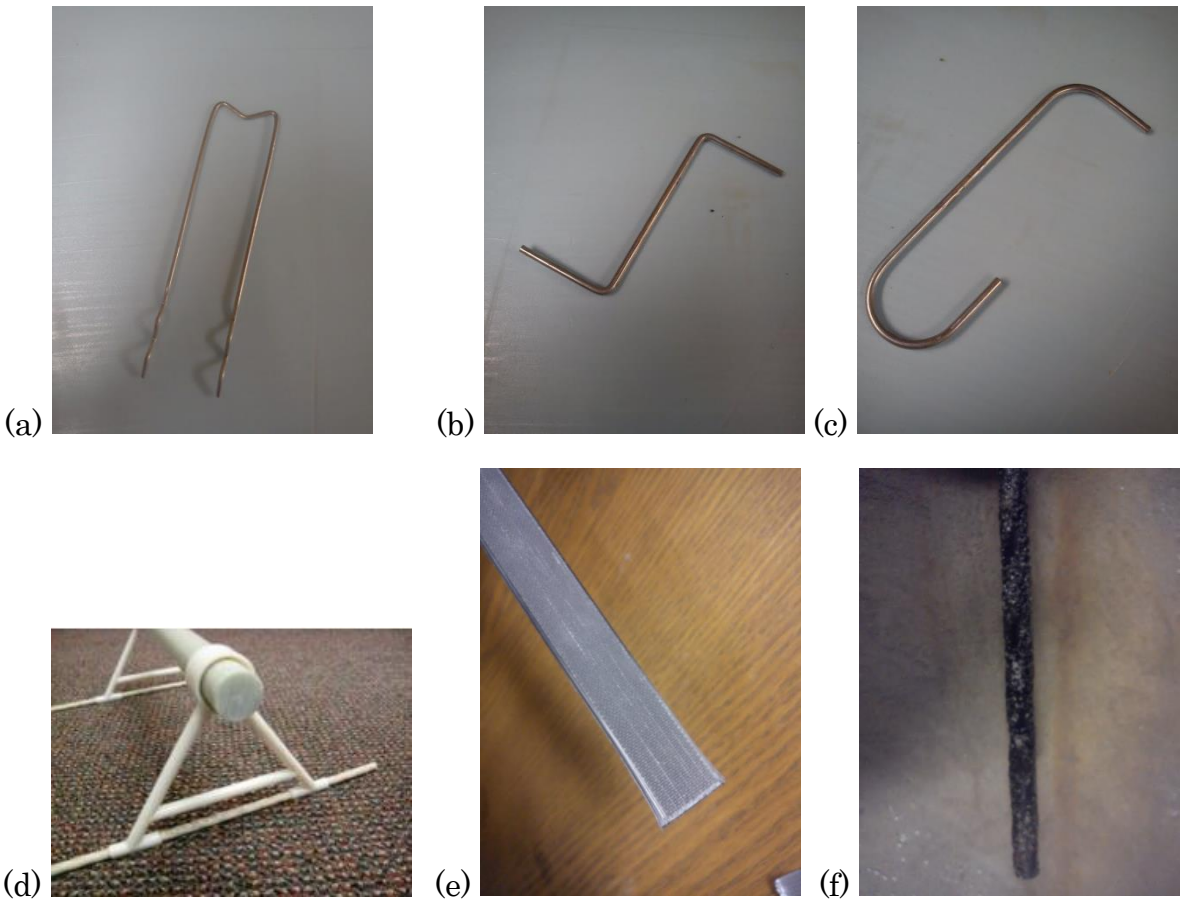

Figure 3-1: Shear Tie Connectors; a: Steel W-Shaped Connector, b: Steel Z-Shaped Connector, c: Steel J-Shaped Connector, d: GFRP Dowel (Aslan FRP 2012), e: CFRP Strip, f: CFRP Bar

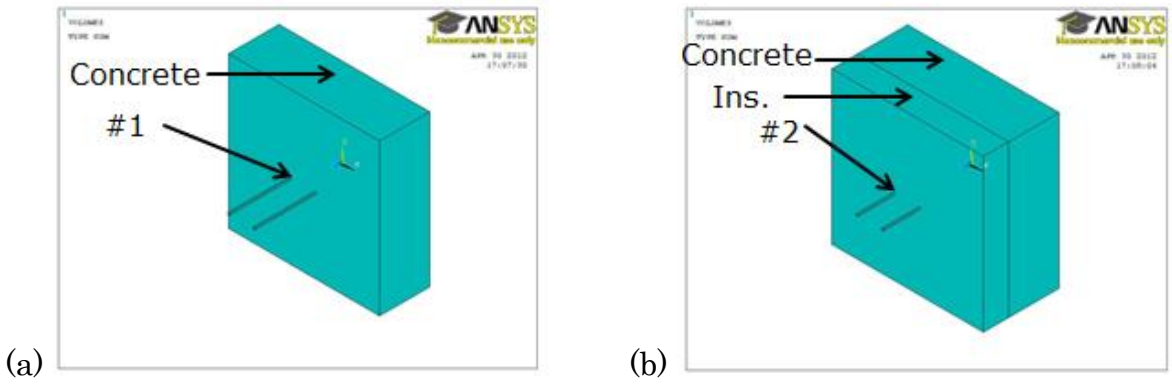

Figure 3-2: Positions of the Thermocouple; a: Position 1, b: Position 2

(a) 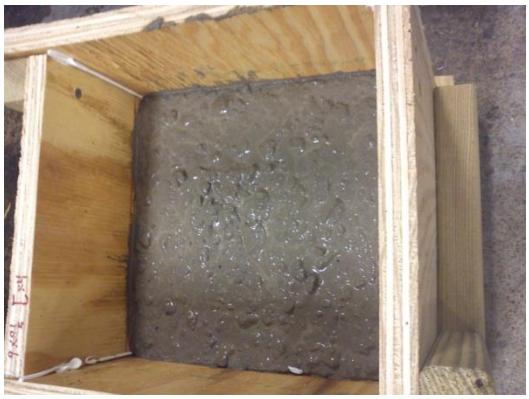 (b) 

(c) 

Figure 3-3: Experimental Setup; a: Three inches of concrete, b: Additional insulation, c: Additional three inches of concrete

(a)  (b) 

Figure 3-4: Experimental Test; a: Sandwich wall panel inside the insulation box, b: Sandwich wall panel inside the freezer

CHAPTER 4. PREDICTIVE MODELS

4.1. Introduction

This chapter presents the predictive modeling done to compare with the experimental study. A parametric study was also done to examine the effect of GFRP connectors on the thermal efficiency of the panels. The analytical analyses discussed are the Zone, Parallel Flow, and Isothermal Planes Methods. A computational analysis was also done using finite element analysis software to evaluate the analytical and experimental data.

4.2. Analytical Analysis

Common methods to determine the R-value of a designed sandwich wall panel are to use the numerical equations provided in the American Society of Heating, Refrigerating, and Air-conditioning Engineers (ASHRAE) Handbook (ASHRAE 2001). These methods are called the Zone Method, Parallel Flow Method, and Isothermal Planes method. These methods determine the R-value of a sandwich panel by treating the materials as electrical resistance analogies that are organized in parallel, series, or a combination of the two. The new Revised Zone Method for estimating the R-value of the panels was discussed in Chapter 2.

4.2.1. Parallel Flow Method

The R-value is determined by first finding the percentage of steel occupied in the transmission area, *P*. The side view of the sandwich panel is separated into two parts (Figure 4-1a). One part has only the concrete and insulation, and the second

part includes just the connector and the concrete. The total resistance, R, is found for each part. If thermal bridging is not considered; the resistance would be from part 1. The conductance, C_{ave}, could be found from the resistance (Equation 4-1). If thermal bridging is taken into account, then the conductance including the connectors can be found (Equation 4-2). The R-value can be found from Equation 4-1.

$$C_{ave} = C_1 = {}^{1}/_{R_1} \tag{4-1}$$

$$C_{ave} = ([1 - P] * C_1) + (P * C_2) \tag{4-2}$$

4.2.2. Isothermal Planes Method

Finding the R-value is similar to the parallel flow method. The sandwich panel is broken into two parts, and the R-value is calculated for each part. The total R-value can be calculated (Equation 4-3). If the conductance is needed, Equation 4-1 can be used.

$$R_{T(av)} = R_{con} + \frac{1}{\left({}^{(1-P)}/_{R_1}\right) + \left({}^{P}/_{R_2}\right)} + R_{con} \tag{4-3}$$

4.2.3. Zone Method

According to the ASHRAE Handbook, the zone method contains two calculations. The sandwich wall panel is separated in to two sections. Zone A contains the highly conductive part of the panel close to the steel connectors. Zone B is the remaining portion that contains simpler construction without connectors (Figure 4-1). The two calculations can be combined by using the parallel flow

method described previously. The area conductances can be added in parallel, and the area resistances can be added in series.

The effective surface shape for Zone A is found by an empirical formula (Equation 4-4). The equation is based on a relationship between the connector diameter, *m*, and the distance of the tip of the connector to the surface of the panel, *d*. If the connector is not placed in the center of the sandwich panel, then two W values (Eq. 4-4) are calculated and the larger value is used. The W value can be used to calculate the area of Zone A, which, in turn, can be used to calculate the area of Zone B. The modified zone method was discussed in Chapter two and the difference in calculating W is shown in Equation 2-3.

$$W = m + 2d \tag{4-4}$$

4.3. Computational Analysis

A computational analysis was done using finite element analysis software. The ANSYS computer software was used for the analysis. The model was developed to predict the experimental findings. It was also done to evaluate the accuracy of the analytical analysis. After verification was complete, a parametric study was conducted to further study the effect of FRP connectors on the thermal performance of the sandwich panels.

4.3.1. Properties

The properties required by the finite element program are material properties and the element type. The type of element used was a solid, tetrahedral

element with 10 nodes. This was chosen because it could model the various angles of the connectors the most accuracy. All ten nodes have three degrees of freedom each. The triangular shape of each side gives the element the ability to model irregular meshes.

The material property required to determine the R-value of the panes is the thermal conductivity. The additional properties that are required to determine the change in temperature with time are the density and specific heat of each material. These values were obtained from literature (Ashby 13, Chowdhury et al. 2007, Pardini and Gregori 2010) and can be found in Table 4-1.

4.3.2. Geometry

The initial geometry modeled followed the experimental dimensions. This includes a 9 in. x 9 in. cross sectional area. It has two 3 in. layers of concrete, and one 1.5 in. layer of insulation. The models contained either 1 or 4 steel connectors. All connector types, W-Shaped, Z-Shaped, J-Shaped, GFRP Dowel, CFRP Bar, and CFRP Strip, were all modeled (Figure 4-2).

The model was created by first constructing the connectors. The layers of concrete and steel were added over the connectors. The program operations overlap and glue were used to connect the panel.

4.3.3. Meshing

Meshing is aspect of the finite element program where the panel is divided into elements that will be individually evaluated. This is also where specific properties can be assigned to various volumes in the model. All connector

geometries were modeled using the three material properties (steel, CFRP, and GFRP). The size of the mesh can determine the maximum value obtained in a specific location on the model. It can also make contour plots of the results look smoother. However, a larger mesh size will increase the computational time required to find a solution. A mesh refinement was conducted to find an optimal mesh size. The mesh used for the modeling is shown (Figure 4-3).

4.3.4. Boundary Conditions

For the models that focused on determining the R-value of the panels, a different temperature was applied on both faces of the panel. This included a room temperature, 20 °C, and a freezing temperature of -30 °C. The four remaining sides of the panel were considered to be insulated. This is done by setting the convection coefficient to zero on the necessary areas. After solving the current ls, the thermal flux contour plot can be found at a steady state. The heat flux at specific nodes can be found by using the Subgrid Solu option. From there, the R-value of the model can be determined by averaging the flux values and solving Equation 4-5. The heat flux, Q, temperature, T, and resistance, R, are used to solve the equation.

$$Q = \frac{T_1 - T_2}{R} \tag{4-5}$$

The models that determined the change in temperature on the connector required additional steps. An initial temperature of 20°C was applied to the entire model using the Apply; Initial Temperature option and picking every node. This ensured that the entire model began at an initial temperature of 20°C. Then, the freezing temperature of -30°C was applied to one face. This was done by using the

option Apply- Thermal- Temperature- On Area, and picking the front area. The locations of specific nodes were chosen to record data. These nodes are located where the thermocouple wires were placed on the experimental panels (Figure 4-4). The change in temperature at these nodes was recorded over a period of 12 hrs.

4.3.5. Parametric Study

After the results of the model were compared to the results obtained from the experimental study and the analytical analysis, a parametric study was conducted. The parametric study focused on the W-Shaped, Z-Shaped, and J-Shaped connectors. These are the connectors that are commonly used in the industry. All of these connector shapes were evaluated using steel, CFRP, and GFRP properties. More realistic geometries were evaluated. The spacing of the connector was varied from 1 to 4 ft. The concrete thickness was changed from 2 to 6 in., and the insulation layer was varied from 1 to 4 in. A large scale model was also evaluated to observe the differences the change in connector shapes and properties made to the thermal efficiency of the system.

a)

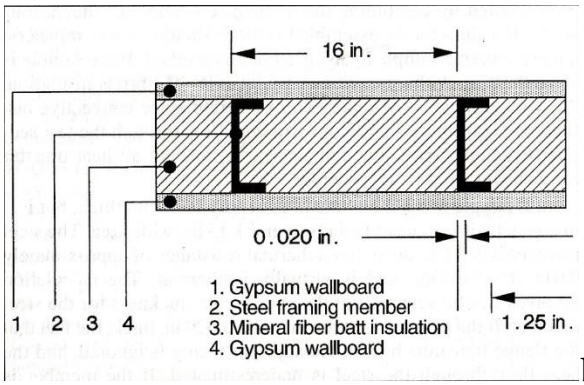

b)

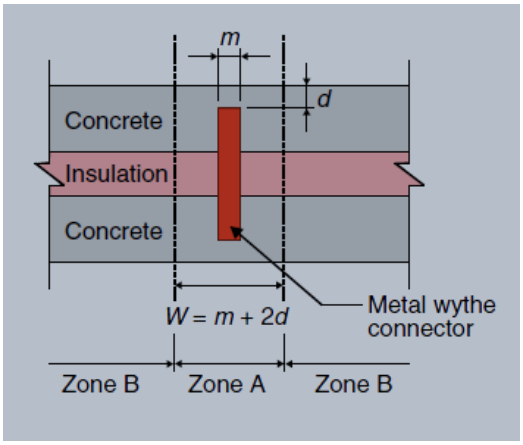

Figure 4-1: Analytical Methods; a: Parallel Flow Method (ASHRAE 2001), b: Zone Method (Lee and Pessiki 2008)

Table 4-1: Material Properties (Ashby 2013, Chowdhury et al. 2007, Pardini and Gregori 2010)

Material	Conductivity (W/mK)	Specific Heat (J/kgK)	Density (kg/m^3)
Concrete	0.8-3.5	800-1200	2400
Insulation	0.02-0.065	1000-1200	15-30
Steel	15-50	400-500	8000
GFRP	0.2-5	1000-1200	1750-2000
CFRP	45-130	900-1050	1500-1600

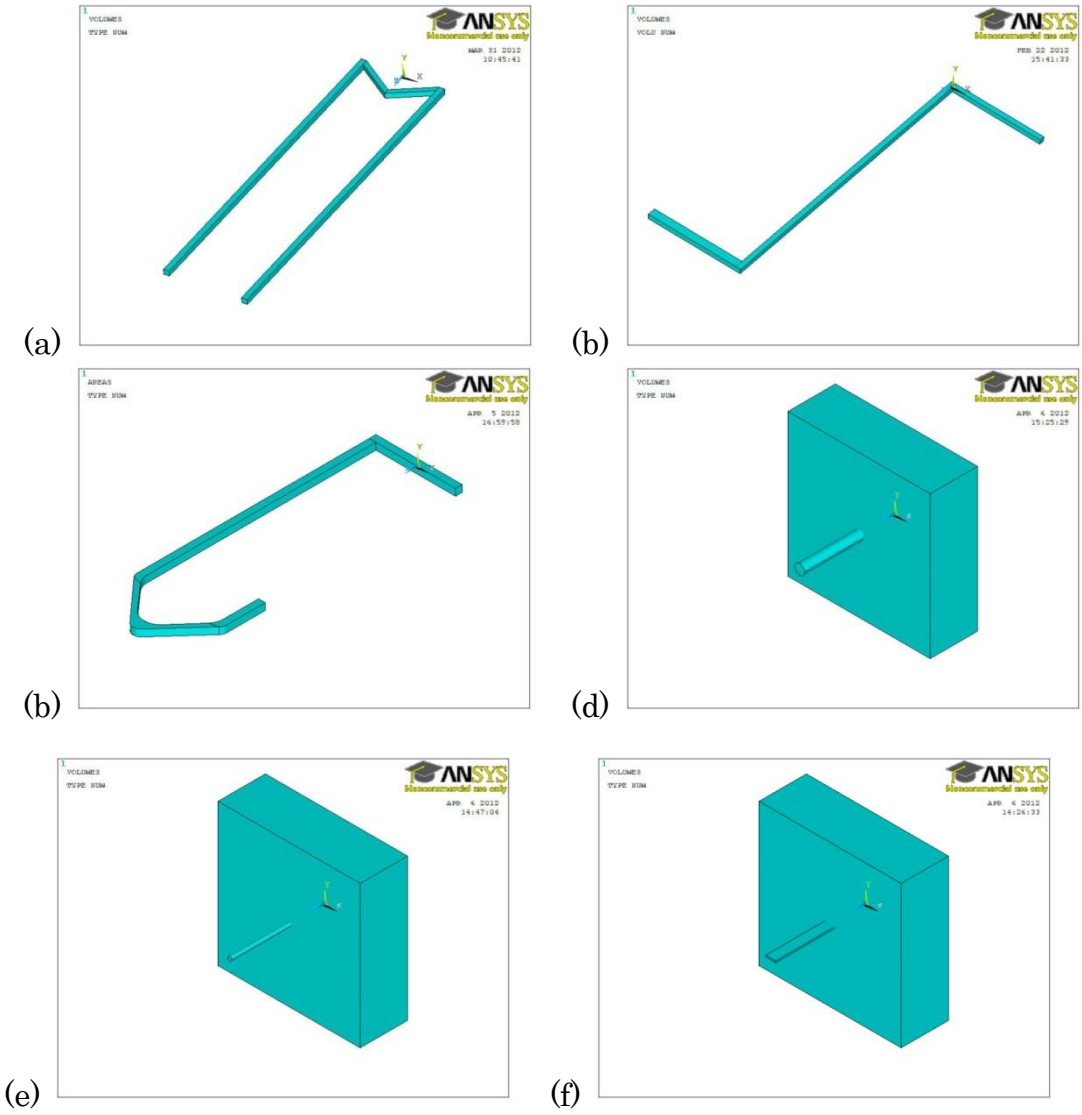

Figure 4-2: Connector Types; a: W-Shaped, b: Z-Shaped, c: J-Shaped, d: GFRP Dowel, e: CFRP Bar, f: CFRP Strip

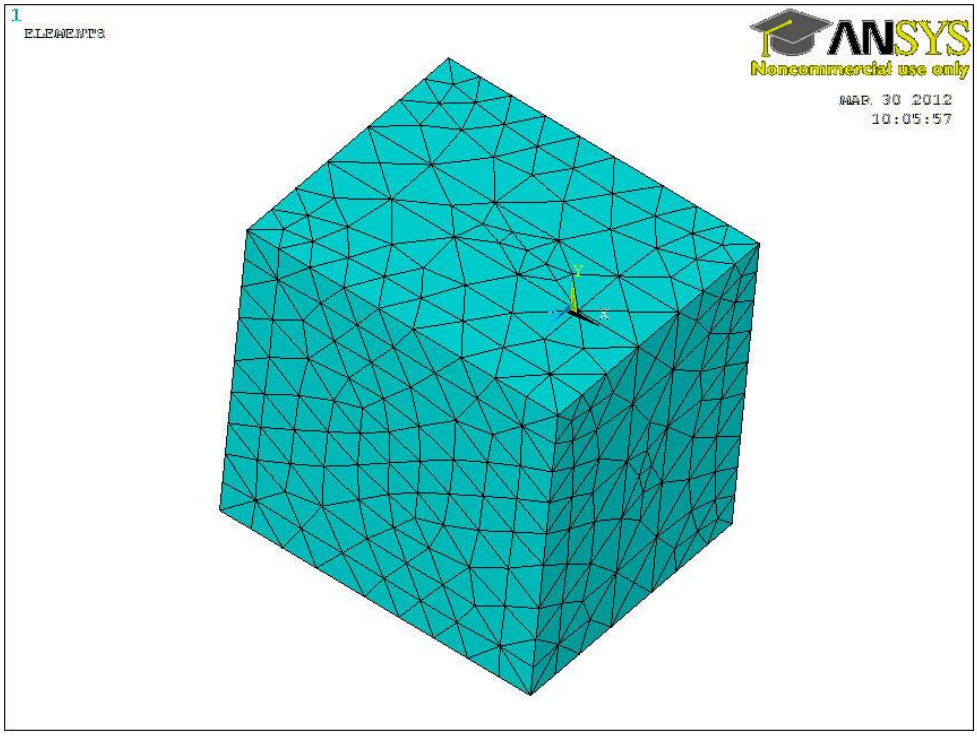

Figure 4-3: Finite Element Model Mesh

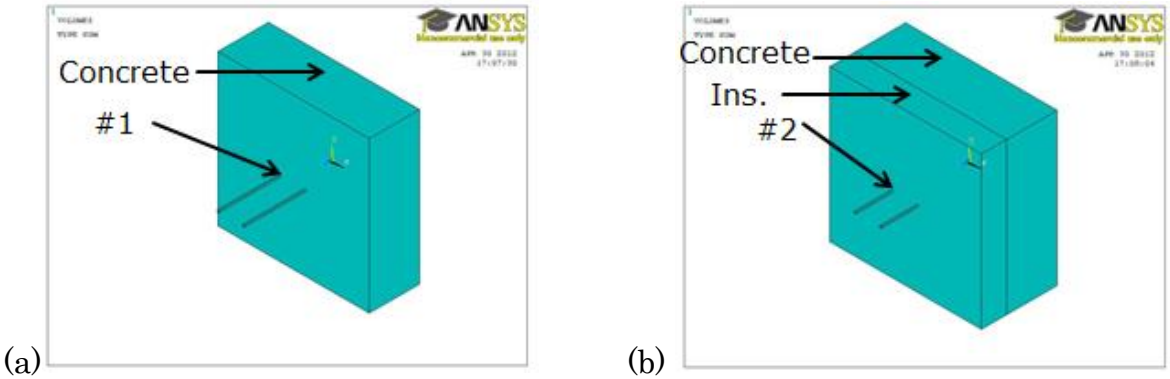

(a) (b)

Figure 4-4: Node Positions; a: Position 1, b: Position 2

CHAPTER 5. RESULTS AND DISCUUSSION

5.1. Introduction

This chapter will cover the results and discussion determined by the conducted research. The findings from the small scale experiments will be presented. This was compared to a finite element model consisting of geometry similar to the experiment. The model was evaluated through the use of numerical methods found in the ASHRAE Handbook. The overall thermal performance of sandwich wall panels was examined through a parametric study of the finite element analysis model. These results were compared to the methods found in the ASHRAE Handbook and the Revised Zone Method for accuracy purposes.

5.2. Experimental Results

The experiment consisted of 6 sandwich wall panels with steel connectors, 1 with a GFRP dowel, and 2 with CFRP connectors, as discussed in Chapter 3. The sample size remained constant for each panel tested at 9 in. x 9 in. with two 3 in. wythes of concrete and one 1.5 in. of insulation. The temperature was recorded on two different positions of the connectors. The panel was insulated on the four sides to ensure heat flow through the center of the panel containing the connectors. Each sample was subjected to a temperature of -30oC for a period of 12 hrs.

5.2.1. Steel W-Shaped Connectors

Two panels were constructed with the steel W-shaped connectors. One panel had one connector in the center, while the other panel had 4 ties spaced evenly

apart. Figure 5-1 shows the temperature vs. time graph for the sandwich wall panel with one connector at the position closest to the freezing temperature. After a 12 hr. period, the temperature at position one was -20°C. The experiment was repeated 3 times and the results of each test are shown in the figure. The results of the finite element analysis model are also given in the figure. The temperature decrease appeared to follow an exponential curve. The results of the three experiments and the model varied by +/- 3 degrees.

Figure 5-2 gives the temperature vs. time graph for the panel at the position closer to the insulated side of the box originally at room temperature. After a 12 hr. period, the temperature at this position was just under 0°C. This is warmer than the temperature at position one. This is due to position one being closer to the applied cold air and position two being on the opposing side of the insulation. The insulation prevents the connector from losing heat as fast. This graph also varied by less than 3 degrees. The shape of the graph showed a more linear shape than at position one. Figure 5-3 shows the temperature vs. time graphs of both positions using the average experimental values.

To give supplemental information in a 'what-if' scenario, the finite element model was used to change the material properties of the connector from steel to GFRP and CFRP. Figure 5-4 shows the comparison of the steel, GFRP, and CFRP connectors at position one. It is shown that the GFRP and CFRP models conclude with a temperature that is five degrees lower than the steel model. This is due to the various changes in the conductivity, specific heat, and density between the

different materials. A lower thermal conductivity is proportional to higher thermal resistance, and a higher specific heat will lead to the material needing more energy to change temperature. Figure 5-5 shows the comparison of the materials at position two. In this case, the GFRP and CFRP reach a minimum temperature that is five degrees higher than the panel made with steel connectors.

Figure 5-6 shows the temperature vs. time comparison of the three materials at both positions (Figures 5-4 and 5-5). It is interesting to see that the GFRP and CFRP deceased in temperature faster on the side that is closer to the subjected freezing temperature. When examining these two materials on the opposing side of the insulation, they reached a final temperature that was warmer than the steel material. This may mean that the GFRP and CFRP connectors work more efficiently with the insulation to prevent thermal bridging. A reason for this is that they have over twice the specific heat value as steel.

The second panel constructed with W-shaped connectors increased the number from one to four. Each of these connectors were spaced evenly apart at 3 inches apiece. Figure 5-7 shows graphs similar to those shown for one W-Shaped tie. Position two concludes at -20^{o}C, while position one levels out at -5^{o}C after 12 hrs. The general shapes of the graphs are comparable, and the variability between the experiments and the finite element model is small. Figure 5-8 gives the results of the temperature vs. time graphs using the substituted GFRP and CFRP materials. Similar to the graph with one connector, the GFRP model in position one is colder than the steel values, but at position two, it is significantly warmer after

12 hrs. The behavior of the CFRP model is different from what was seen in the previous graphs. In position one, the model is very close to the temperature values for the steel model. In position two, the model is only slightly warmer than the steel model. This could mean the thermal bridging resistance of CFRP is not as effective when more connectors are implemented.

5.2.2. Steel Z-Shaped and J-Shaped Connectors

The steel Z-shaped and J-shaped connectors are similar in a number of ways. They both have a diameter of 4.65 mm (0.183 in.). This diameter is thicker than the W-shaped ties. Since there are two extensions for this connector, the overall effect of the three different ties is roughly the same because the overall area is similar. The experimental panels constructed with the Z-shaped and J-shaped connectors are similar to the W-shaped ties. Each connector type had a panel created with one tie in the center, and an additional panel with four ties spaced evenly apart at 3 inches apiece.

Figures 5-9 and 5-10 show the results of the panels with a single Z-shaped connector. The results of the experiment are similar to the W-shaped connectors. The temperature at position one (closer to the cold) is -15°C, and the temperature at position two is 0°C. The accuracy of the model using this new shape is still relatively close to the experimental results. The graph with the Z-shaped connectors with CFRP and GFRP properties doesn't deviate much from the previous path. The GFRP acts similar to the steel material, but the CFRP is warmer than the steel model at position 1. A slightly thicker diameter CFRP has improved the

initial resistance of the panel. The CFRP at position two is comparable to the steel curve.

Figures 5-11 and 5-12 give the graphs of the temperature vs. time comparison of the sandwich panels with four steel Z-shaped connectors. The GFRP material is colder than steel at position 1, but is significantly warmer in position 2. The CFRP material is warmer than steel at position 1, but performs nearly identical at position 2. The main difference between this shape and the previous results with a single connecter is the temperature at position one is -20°C, and at position two it is -5°C. This is a decrease of 5°C which shows that that more steel is creating a thermal bridge that is diminishing the effect the insulation is having on the transfer of the heat through the panel.

Figures 5-13, 5-14, 5-15, and 5-16 give the results of the J-shaped connectors. Overall, the results are comparable to the Z-shaped connectors with one exception. The accuracy between the model and the experiments is slightly reduced. This accuracy reduction is attributed to the geometry of the model. The curved portion of the model is not perfectly round which does not match the actual shape of the connector. The model did show that the steel shape performed slightly better than the GFRP and CFRP shapes at position two when there was only a single connector. When there were four connectors being examined, the steel decreased dramatically to match the CFRP at position two while the GFRP only decreased slightly. The thermal bridging seemed to have a greater effect on this shape than on the previous two.

Graphs comparing the sandwich wall panels with one connector with the panels containing four connectors can be found in the Appendix.

5.2.3. Glass Dowel

The glass dowel was done to obtain experimental data on the GFRP sample that was available. The dowel has a 16 mm (0.63 in.) diameter, which is nearly 3.5 times larger than the steel samples.

Figure 5-17 shows the temperature/time graphs for the experiment and the model. The model had some difficulty predicting the rate of decreasing temperature of the experiment at position one. There was a max difference of temperature of 15°C between the model and the experiment. The model did conclude at approximately the same value as the experiment, which was 0°C. The model was more accurate at predicting the temperature change at position two. The model and experiment both reached a final temperature of -20°C.

Figure 5-18 shows the graph of the 'what-if' scenario using the dimensions of the glass dowel. In addition to GFRP, the steel and CFRP properties were used in the temperature vs. time graphs. The increased diameter increases the effects of the properties so a clearer picture of how the various properties affect the thermal performance can be seen. At position one, the CFRP and steel are almost equal throughout the duration. The GFRP model ends up almost 10 degrees colder than the other two models. At position two, the CFRP and steel models remaining similar, but the CFRP model finishes slightly warmer. The GFRP model concludes the time duration over 10 degrees warmer than other two. For the previous shapes,

the difference between these values was at most 5 degrees. This shows the effect the larger diameter had on the thermal efficiency of the system.

5.2.4. Carbon Bar and Strip

The carbon bar had a diameter of 6.75 mm (0.266 in.). This would make it almost 50 percent larger than the steel samples. The carbon strip had dimensional properties of 16 mm x 2.5 mm (0.63 in. x 0.098 in.), which is over twice the area of the steel connectors.

Figures 5-19 and 5-20 show the results of the carbon rod experiments and models. The model was accurate in determining the temperature change for both positions. The model varied by at most 4 degrees from the experimental results. For position one, the temperature settled at -15°C, and for position two, the temperature was -5°C at the end of the 12 hr. time period. Since this model used a geometry that was similar to the overall area of the steel shapes, the results are close to what has been seen in the previous materials and geometries. The steel and CFRP provided nearly identical values while the GFRP connector was cooler in position one and warmer in position two.

Figures 5-21 and 5-22 give the graphs of the carbon strip analysis. Resembling the carbon rod analysis, the model was accurate for both positions. The values were nearly identical and they concluded on comparable temperatures. The material comparison model continued the trend of GFRP taking the highest and lowest values for both positions, whereas, the CFRP performed slightly worse than the steel. The carbon was three degrees cooler than the steel at position two.

5.3. Analytical Results

The analytical analysis focused on determining the heat flux of a sandwich wall panel using three methods given in the ASHRAE handbook. The three methods are the Zone Method, Parallel Flow Method, and the Isothermal Planes Method. These values will be compared to the values obtained from the finite element analysis model. The graphs that will be shown give value of the heat flux at specific locations on a line across the surface of the panel. There are three lines from which the heat flux were measured on. The first line is directly across the center of the surface of the panel. The second line is between the center of the middle line and the edge of the panel. That is, it is ¼ from the edge of the panel. The third line is located on the edge of the panel. Since the samples are symmetric, the flux values from the center to the edge of the face are identical on either side of the panel. The provided graphs give the value of the flux at a specific distance that is given as a percentage across the line. A higher flux value signifies more heat flowing through that portion of the panel. It will indicate numerically how well each material or geometry is performing, and how it is affecting the concrete and insulation around the connector.

5.3.1. W-Shaped Connectors

To stay consistent with the experiments, the analytical analysis was done using the same connector types and geometries as the experiments. Steel, GFRP, and CFRP connectors were considered during this analysis. Figure 5-23 shows the results of the analysis. Line 1 on all three graphs shows the largest peak. This is

where the connector is located inside the panel, so this result is expected. On the steel graphs, the flux peaks at 90 W/m/m on the first line. The flux peaks at 75 W/m/m on the second line. The third line stays almost constant at 67 W/m/m. All three lines start and finish around 66 W/m/m.

The CFRP tie has almost the same thermal conductivity as the steel connectors. This leads to comparable results between the two. The fluxes from the CFRP model are almost identical to the steel model (Figure 5-24). GFRP has a low thermal conductivity. This leads to a minimal change in the flux. The flux only varies from 65 W/m/m to 67 W/m/m in the first line.

The ANSYS finite element analysis software can be used to find the flux at specific nodes to be able to make the plots. The data obtained by using the methods found in the ASHRAE handbook will only give the average value of the flux. These values are plotted on the graph as straight lines. For the steel connector, the Zone Method had a value of 63.8 W/m/m. The Parallel Flow Method calculated the flux as 64.6 W/m/m, and the Isothermal Planes Method had a value of 67.0 W/m/m. All of these values are at the lower boundary of the curves. Similar fluxes were found for the CFRP ties. The fluxes for the GFRP connectors were roughly 64.5 W/m/m. This value is also close to the lower limits of the graphs.

Figures 5-25 and 5-26 contain the graphs from the sandwich wall panels with four W-shaped connectors. These graphs have two peaks. The largest peaks are located on the second line. The second line is located ¼ of the way from the edge and this is close to the location of two of the four connectors.

The steel tie model's large peak values are 105 W/m/m. This is an increase from the 90 W/m/m peak shown with only one connector. The proximity of the connectors caused the flux of both of the connectors to work together to create a larger flux. This shows why sandwich wall panels designed with connectors closely spaced together will diminish the thermal efficiency of the panel. The ASHRAE methods calculate fluxes that are approximately 85 W/m/m.

The GFRP model stays fairly constant throughout the three lines. The flux of these connectors is 67 W/m/m. This is a little higher than the 64.5 W/m/m calculated for one W-shaped tie. The graph also shows that the ASHRAE methods overestimated the flux of the panel by 5-10 W/m/m. The Parallel Flow method had the closest calculation with a value of 74.5 W/m/m.

5.3.2. Other Connectors

Figures 5-27 through 5-33 summarize the remaining connectors. These include one and four J-shaped, one and four Z-shaped, glass dowel, carbon bar, and carbon strip. They all tend to follow the flow summarized in the W-shaped connector section. When there is one connector, line 1 will have the dominant peak. When there are four connectors, line 2 will have the two maximum peaks. The maximum flux from the panel with four connectors is higher than the maximum flux from sandwich panels with one tie. For the most part, the ASHRAE methods calculate fluxes that are near the bottom of the curves. There are a few noteworthy selections from the figures.

The J-shaped and Z-shaped connectors have similar diameters. The only significant difference is the geometry of the ties. The maximum flux for the J-shaped connecter was found to be 105 W/m/m, whereas, the peak flux for the Z-shaped connector was only 95 W/m/m. This happened because during the modeling process, the J-shaped connector is longer than the Z-shaped connector. This would make one edge of the shape closer to the surface of the panel than the Z-shaped connectors. Since the J-shaped connector is closer to the surface, the steel is able to affect the surface more. This leads to an increased flux at this location.

The peak flux of a panel increases with the increase of the area of the connector. This is consistent with the fundamental concept of heat transfer. If the connector has a large diameter, then there is more material for the heat to transfer through and it will create a larger thermal bridge.

The current ASHRAE methods do not appear to be accurate for the GFRP models. When there is more material being used, i.e. four connectors or a large diameter, the methods overestimate the overall flux of the system. One reason for this is the GFRP thermal conductivity is not in the applied range meant for application of these methods. Another possible explanation is that these methods were not designed to calculate the flux of these connections. Some were originally meant to be used for metal frame structures.

5.3.3. Comparisons

Looking at the peak flux values is a good way to evaluate how a specific connector affects its surrounding area. This process has one flaw. It doesn't show

how the connector affects the entire panel. To evaluate this, the average flux was found over the surface of the sandwich panel. The R-value can be found by using the flux. Since the flux and R-values are average values, they can now be more easily compared to the ASHRAE methods.

Figure 5-34 shows the comparisons of sandwich wall panel with one or four W-shaped connectors. It can be seen that the flux and R-value of the steel and CFRP models are identical. It also shows that as the heat flux increases, the R-value of the panels decrease. When the heat flux increases, there is more heat is being transferred through the area of the panel. If more heat is being transferred, that signifies the wall has less resistance to the flow of heat energy, which leads to a decrease in the R-value.

Figures 5-35 and 5-36 compare the thermal efficiency of sandwich panels constructed with Z-shaped or J-shaped connectors. These graphs show the same characteristics as the W-shaped connectors. When the amount of connectors is quadrupled in the same amount of available area, the steel and CFRP panels are affected more than the GFRP panels.

Figure 5-37 compares the dowel geometry with the three material types. With such a large diameter connector being used, the difference between the R-values and fluxes is magnified. There is a significant difference between the GFRP models and the steel or CFRP models.

Figure 5-38 shows the material types being used in the bar and strip geometries. This figure shows the inaccuracy of ASHRAE methods. The ANSYS

finite element analysis flux is significantly higher than the calculated flux from the three numerical methods.

Figure 5.39 gives three bar graphs showing the accuracy of each method as it relates to the finite element analysis results. A value of 1 signifies the numerical model agrees 100 percent with the finite element analysis results. The single connector GFRP comparisons are the most accurate. They only differ by a few decimal points. The four connector GFRP comparisons are among the most inaccurate of the results. The methods become excessively conservative when more GFRP material is used.

5.4. Parametric Study

A parametric study was performed using the ANSYS finite element software program. The values found in ANSYS were cross checked using the three ASHRAE methods and the Revised Zone Method.

Spacing sizes used in the parametric study were 1 ft., 2 ft., 3 ft., and 4 ft. All four of these sizes were examined using the W-shaped connector. The largest and smallest spacing sizes (1ft. and 4ft.) were used for both the Z-shaped and the J-shaped connectors.

The notation used in the table is described by the following: Sandwich wall panel layer thicknesses are written using three numbers with dashes in between. A sandwich wall panel with a 3 in. layer of concrete, a 2 in. layer of insulation, and a 4 in. layer of concrete would be written as 3-2-4. The wythe thicknesses used for the parametric study are 2-4-2, 3-1-3, 3-4-3, 4-1-4, 4-4-4, 6-1-6, and 6-4-6.

The concrete and insulation thermal conductivities remained constant for the study. The thermal conductivity of the connecters was varied between steel, GFRP, and CFRP. A temperature of -30°C was applied to one side, while a temperature of 20°C was applied on the other.

The results of the parametric study are shown in Table 5-1 to 5-4 and additional graphs of the first set of data follows. The findings of the study showed that at small connector spacing, the effects of the steel on thick layers of insulation are noticeable. At 4 ft. spacing, the R-value of the 3-4-3 panel with GFRP connector is 1.69 m*m*K/W, whereas, the R-value of the steel connector panels is 1.65 m*m*K/W. GFRP is expected to have a greater resistance to heat transfer because of its superior thermal conductivity. GFRPs beneficial thermal efficiency is diminished with larger spacing between connectors.

At 1 ft. spacing, the R-value of panels with GFRP ties is 1.64 m*m*K/W, whereas, the value of the panel with steel is only 1.22 m*m*K/W. There thermal performance of the steel tie panels dropped roughly 26 percent, while the GFRP sandwich panel only dropped 3 percent. Steel has a larger thermal conductivity, so these connectors have a larger area affected by the flux. At 4 ft. spacing, this area appeared small. At 1 ft. spacing, the area of the flux was much relatively larger and caused the R-value to drop.

The thermal superiority of the GFRP sandwich panel is also diminished when thin layers of insulation are used. A 3-1-3 GFRP sandwich panel with 1 ft. spacing has an R-value of 0.58 m*m*K/W. The steel panel has a value of 0.56 m*m*K/W.

This signifies a 3.5 percent change between the two values. Adding more concrete cover with a smaller layer of insulation also makes the difference between the two values smaller. A 6-1-6 steel sandwich wall panel only had a 2.7 percent difference from the GFRP panel.

The accuracy of the methods has improved over the previous results. The Revised Zone Method proved to be very accurate. The ratio of the method to the finite element analysis solution remained within 2 or 3 hundredths of a point. There are instances where the method overestimated by a few more points. Those instances can be attributed to the complexity of the modeled connectors.

5.5. Large Scale Model

A large scale model was constructed using the ANSYS finite element software. A full scale sandwich wall panel is constructed with a height of 45 ft. and a width of 12 ft. Because of meshing limits, only a model with a height of 4 ft. and a width of 3 ft. was able to be meshed. A 4-4-4 sandwich panel with 1 ft. spacing was modeled. The flux values found were just under those found for the models with a single connector (Figure 5-58). For steel, GFRP, and CFRP, the model with the single connector found heat flux values of 29.54, 27.69, and 29.66 W/m/m. While the large scale model found values of 29.39, 27.67, and 29.40 W/m/m for steel, GFRP, and CFRP. These values are close enough to signify that the results from the smaller scale analysis can be applied to a large scale model with minimal error.

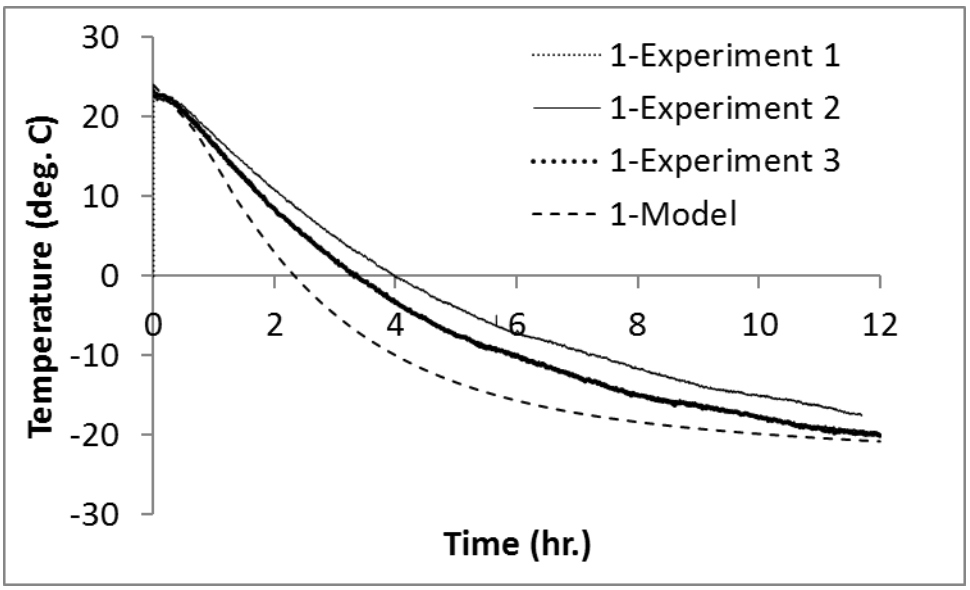

Figure 5-1: One W-Shaped Connector at Position 1

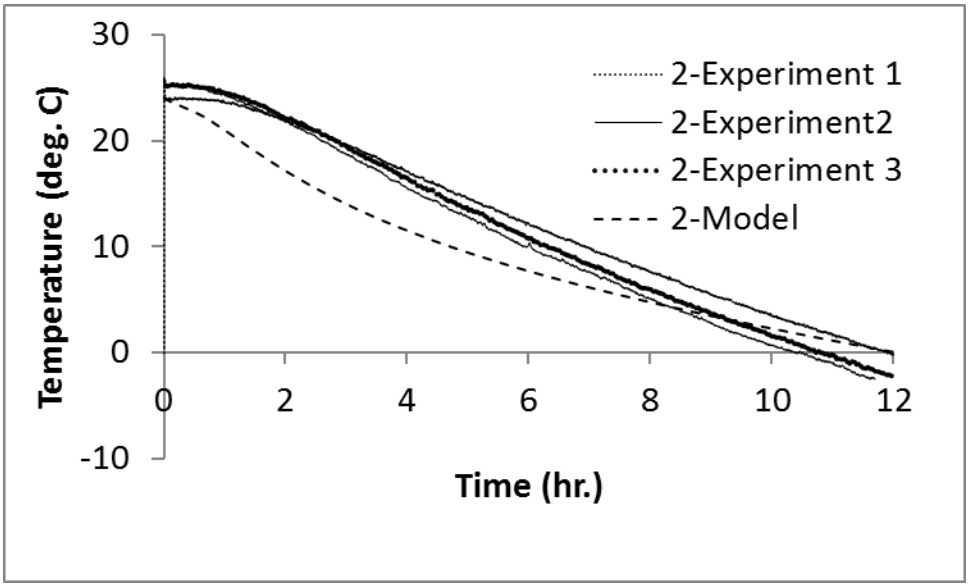

Figure 5-2: One W-Shaped Connector at Position 2

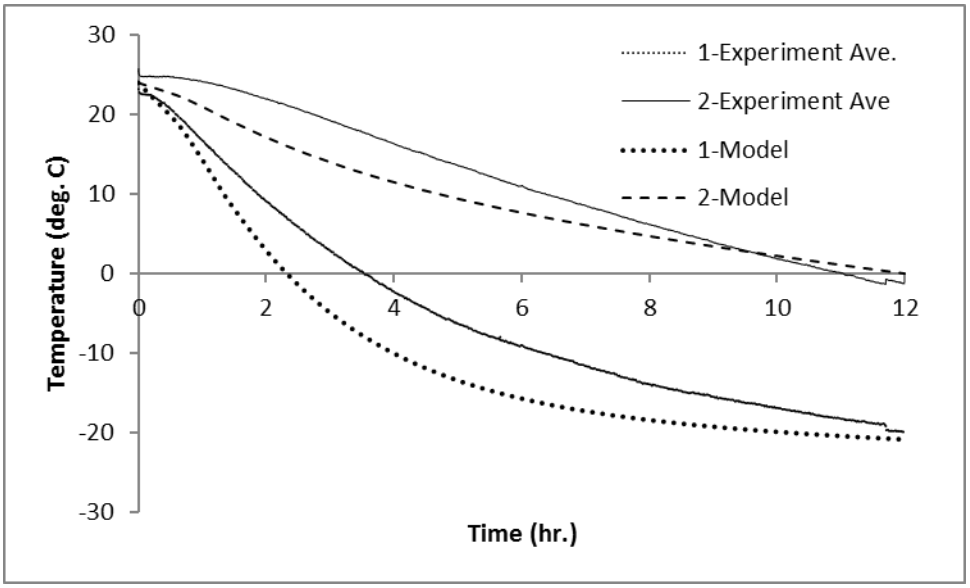

Figure 5-3: One W-Shaped Connector Comparison

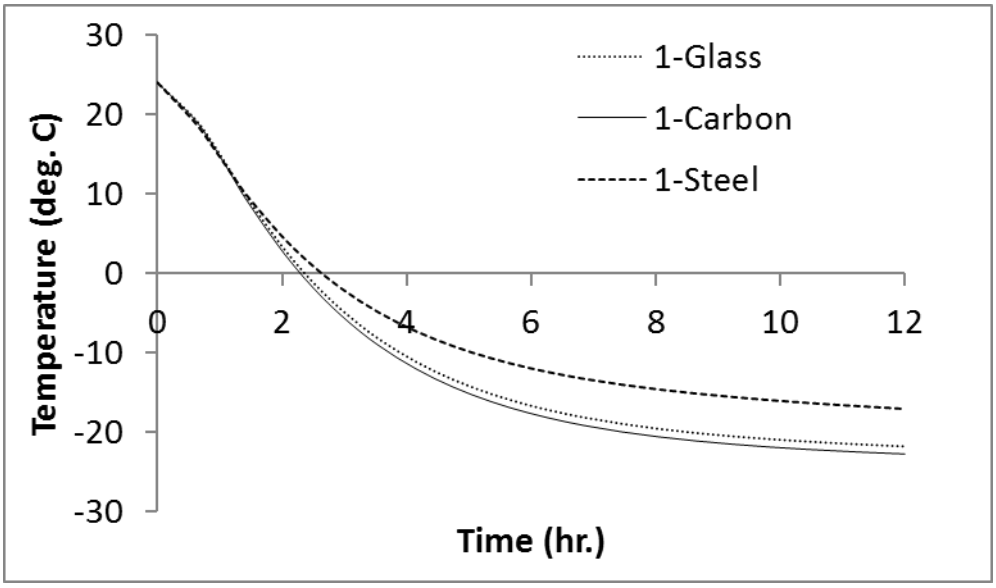

Figure 5-4: One W-Shaped Connector at Position One

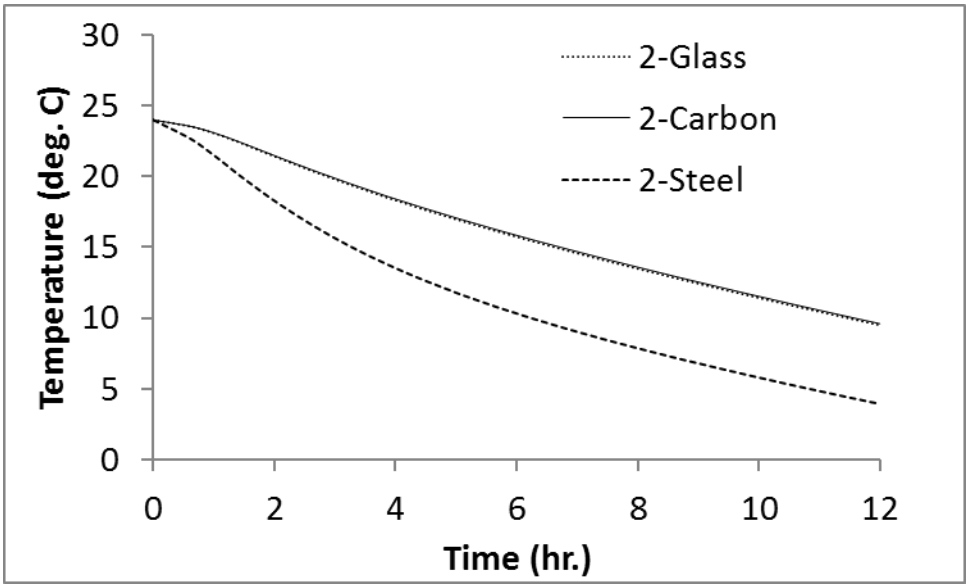

Figure 5-5: One W-Shaped Connector at Position 2

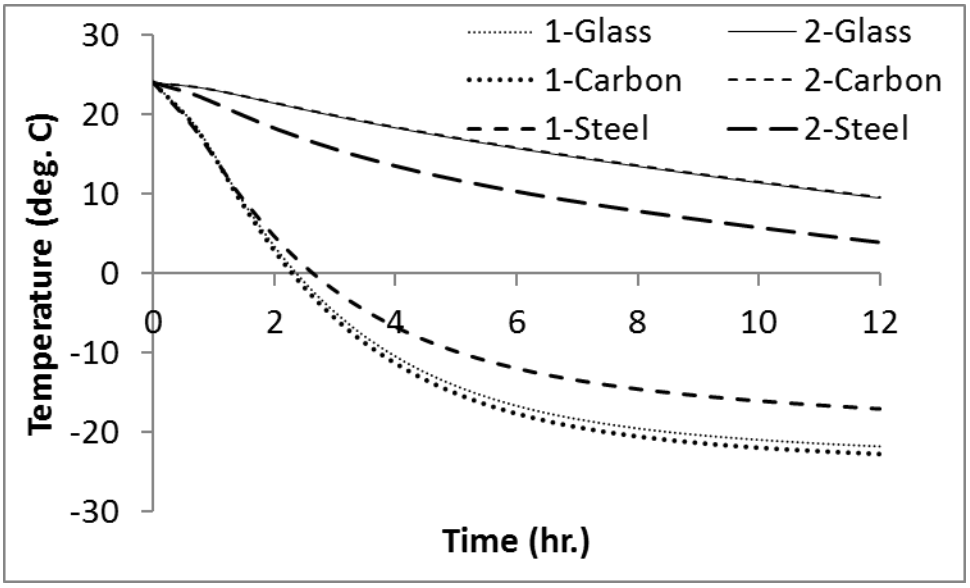

Figure 5-6: One W-Shaped Connector Comparison

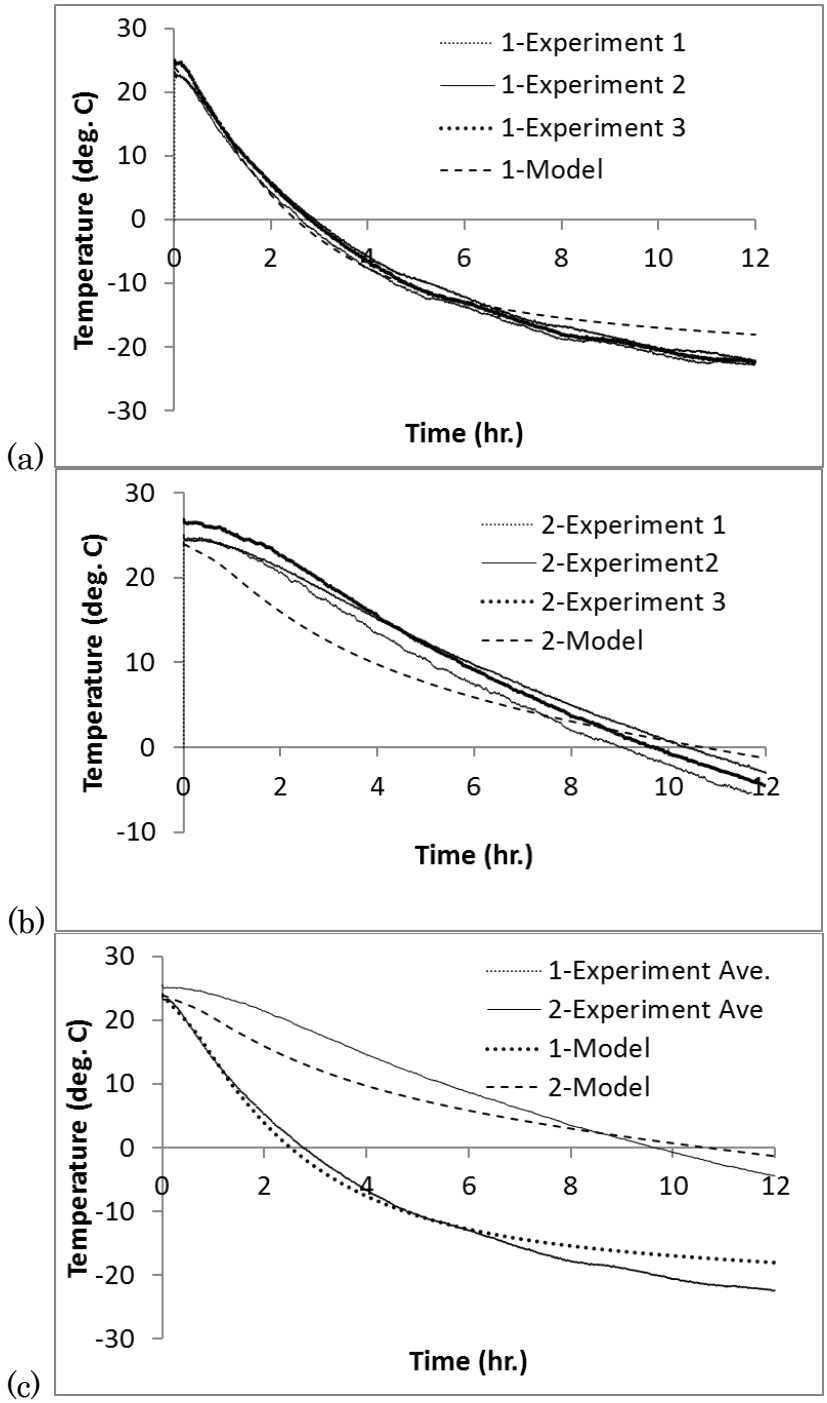

Figure 5-7: Four W-Shaped Connectors; a: Position one, b: Position two, c: Comparison

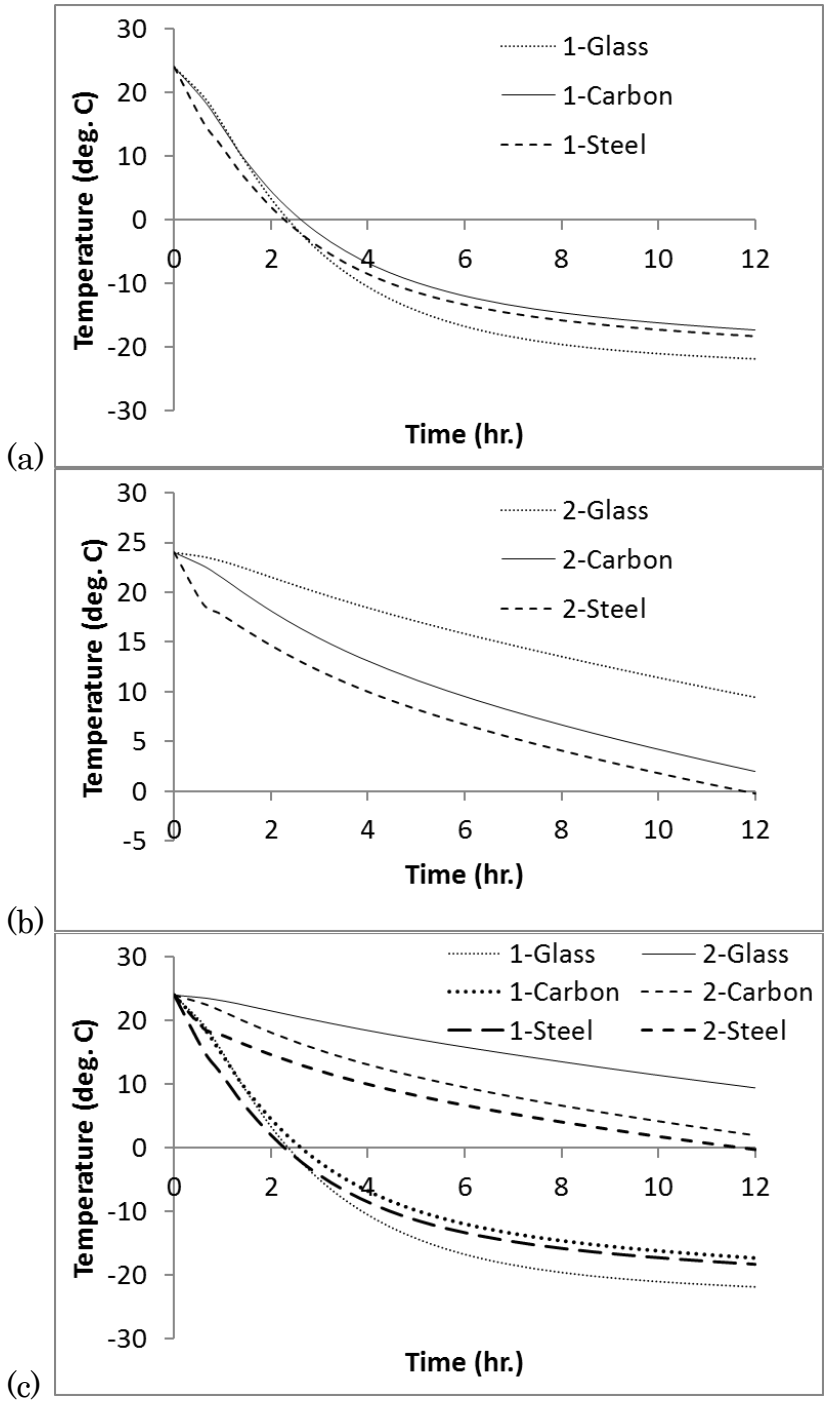

Figure 5-8: Four W-Shaped Connectors; a: Position one, b: Position two, c: Comparison

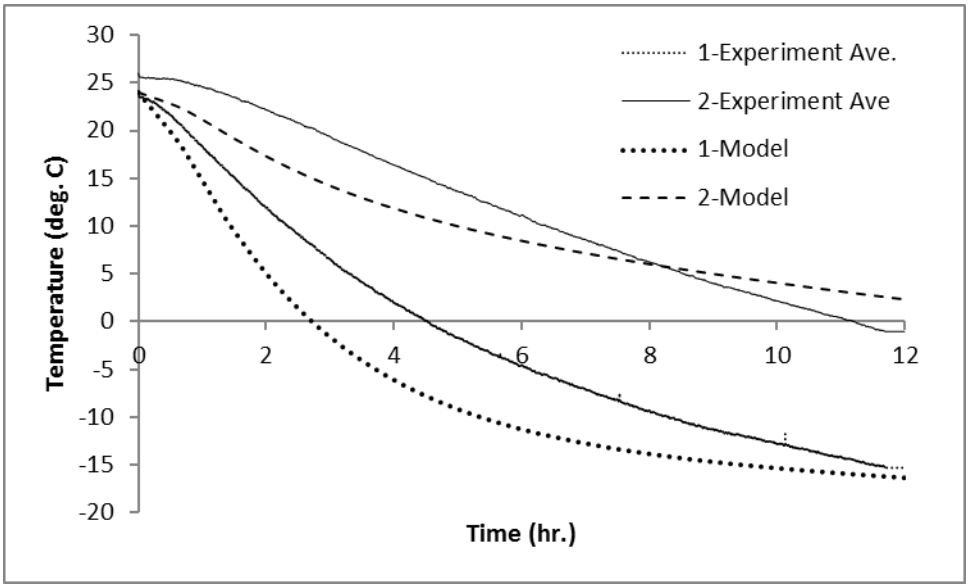

Figure 5-9: One Z-Shaped Connector Comparison

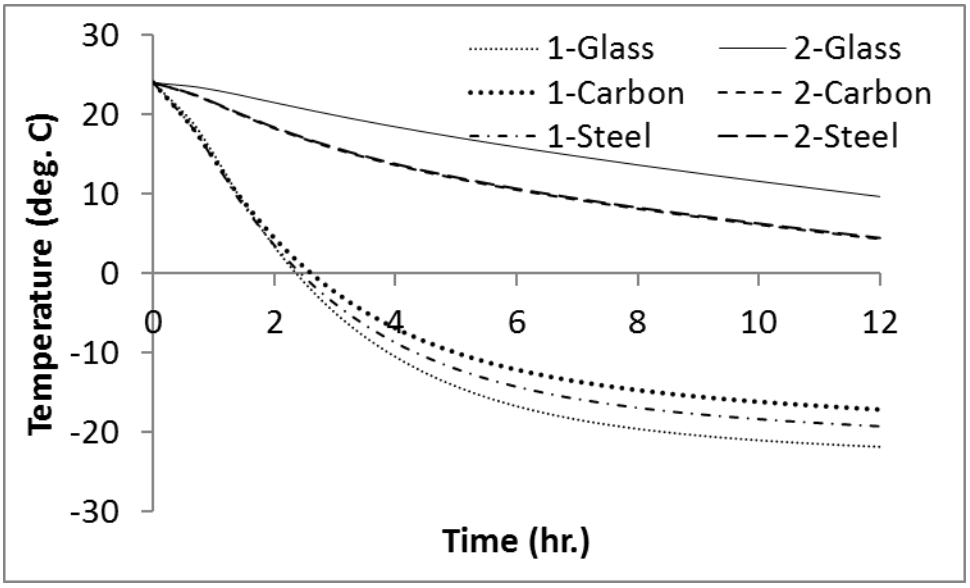

Figure 5-10: One Z-Shape Connector Comparison

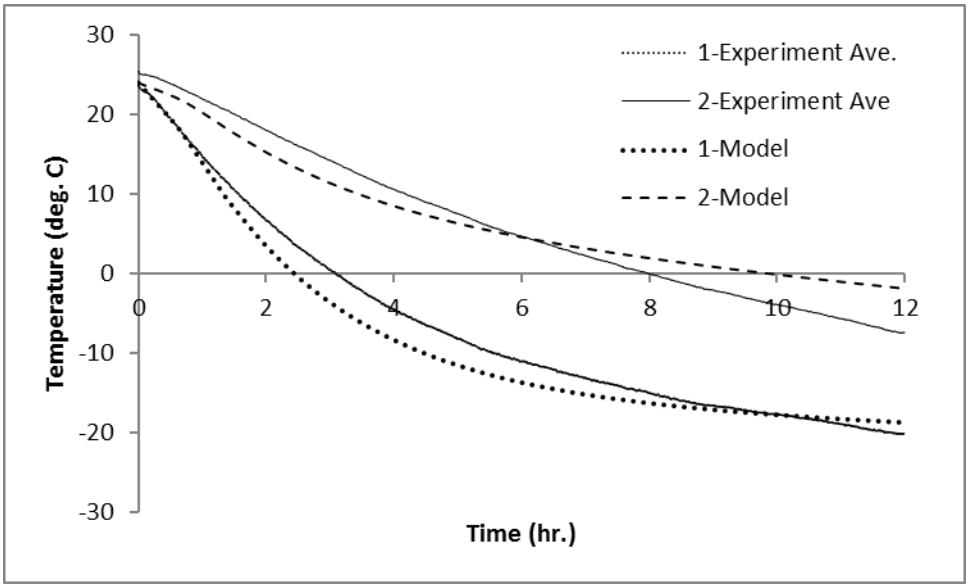

Figure 5-11: Four Z-Shape Connector Comparison

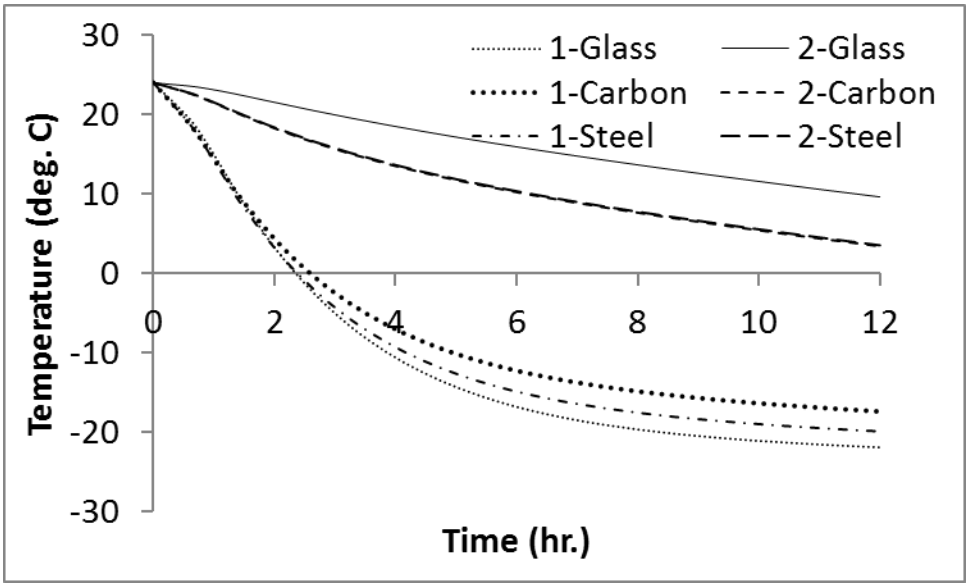

Figure 5-12: Four Z-Shape Connector Comparison

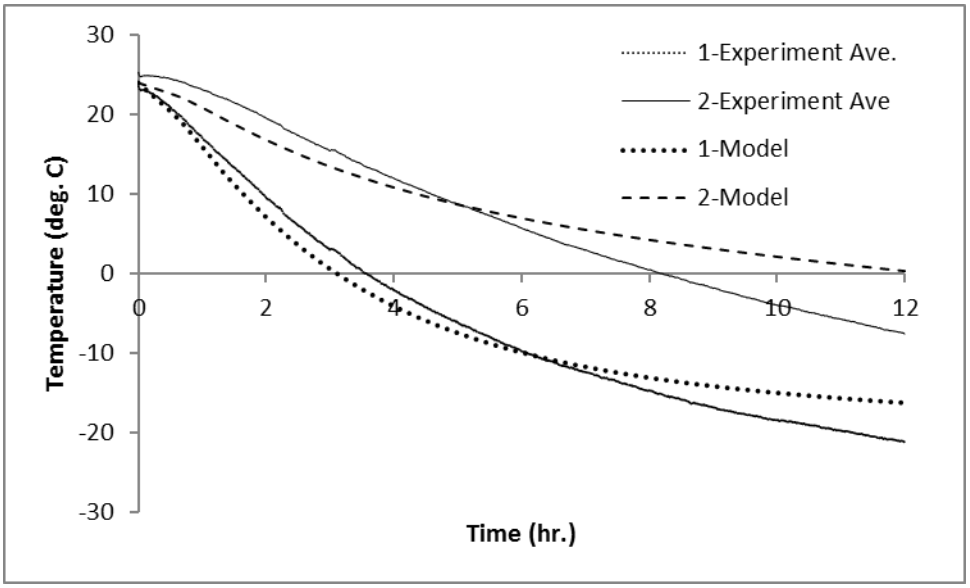

Figure 5-13: One J-Shaped Connector Comparison

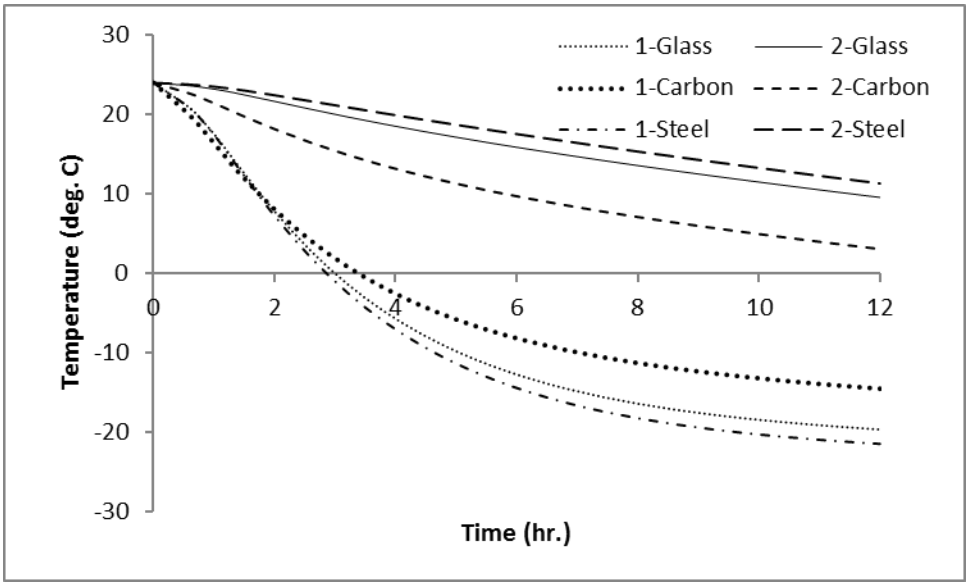

Figure 5-14: One J-Shaped Connector Comparison

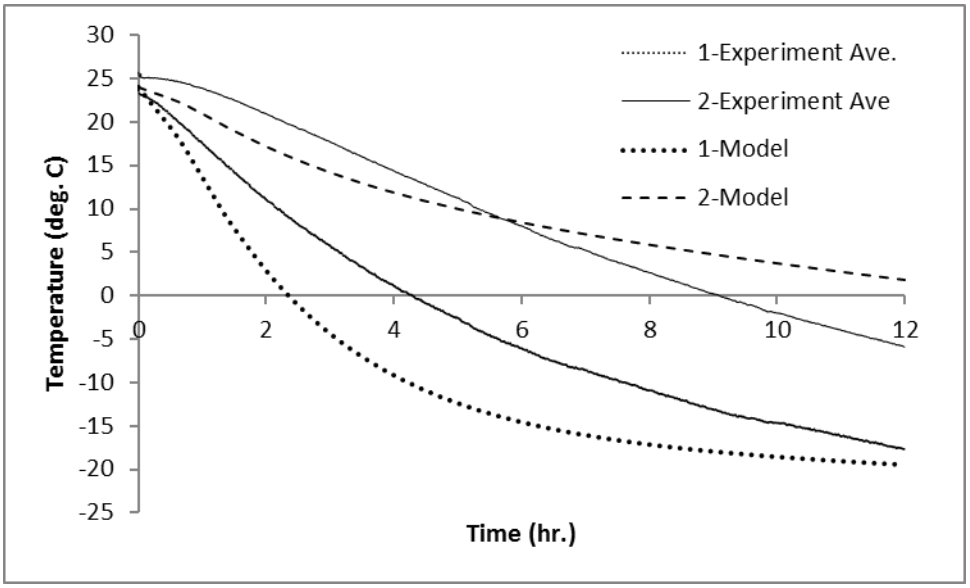

Figure 5-15: Four J-Shaped Connectors Comparison

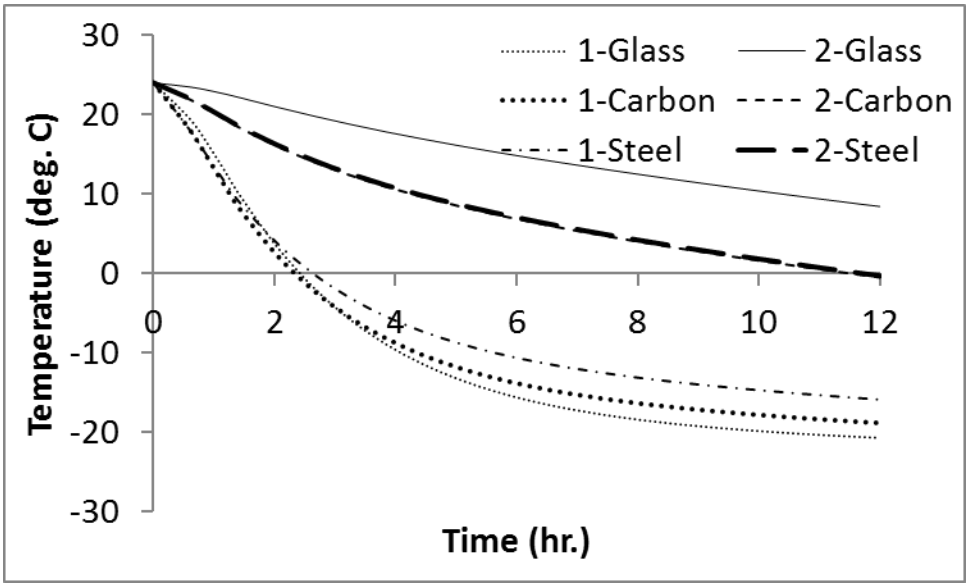

Figure 5-16: One J-Shaped Connector Comparison

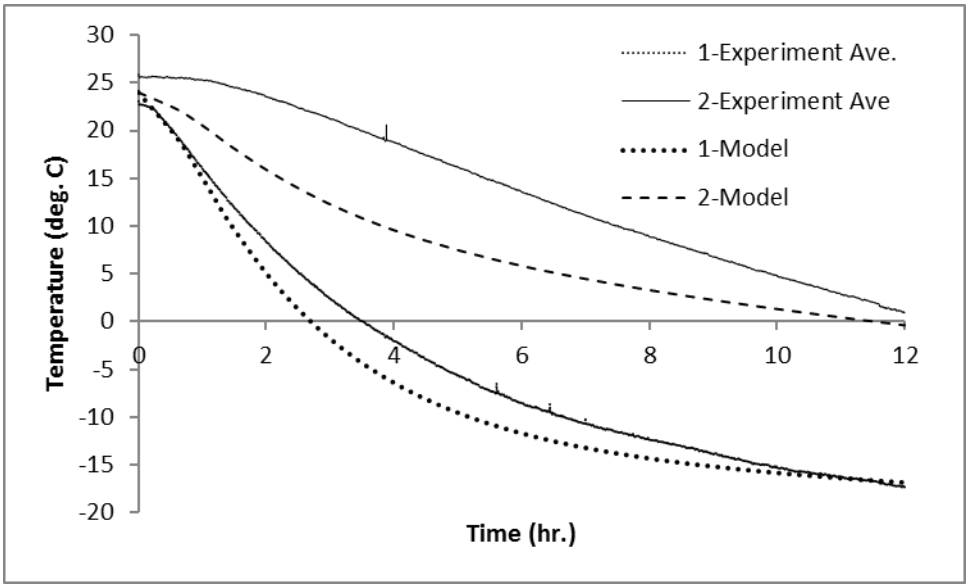

Figure 5-17: Glass Dowel Connector Comparison

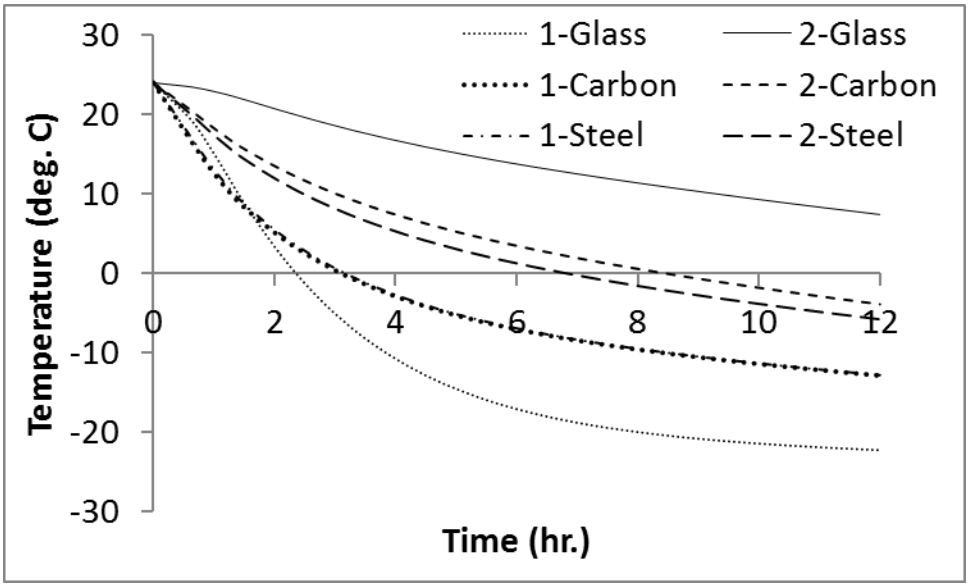

Figure 5-18: Glass Dowel Connector Comparison

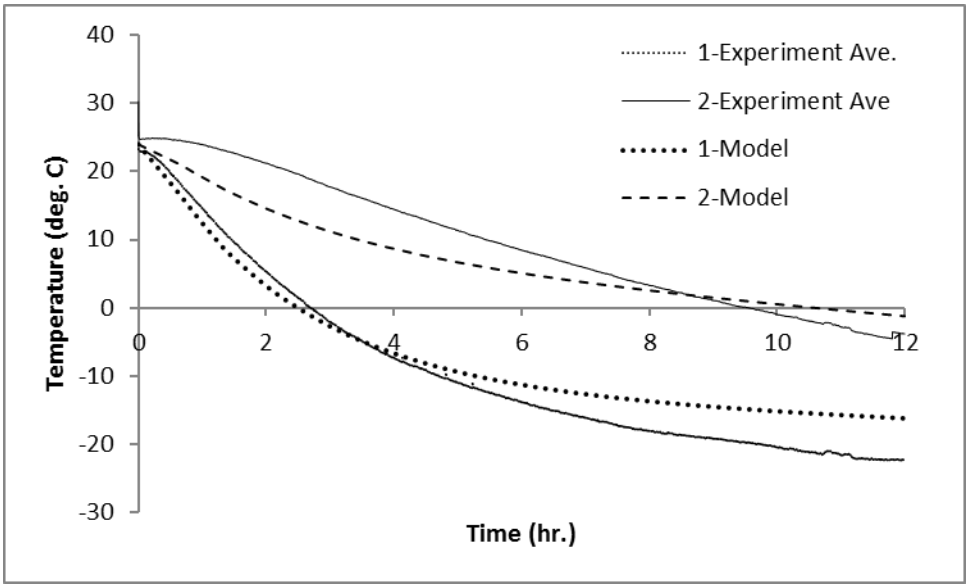

Figure 5-19: Carbon Bar Connector Comparison

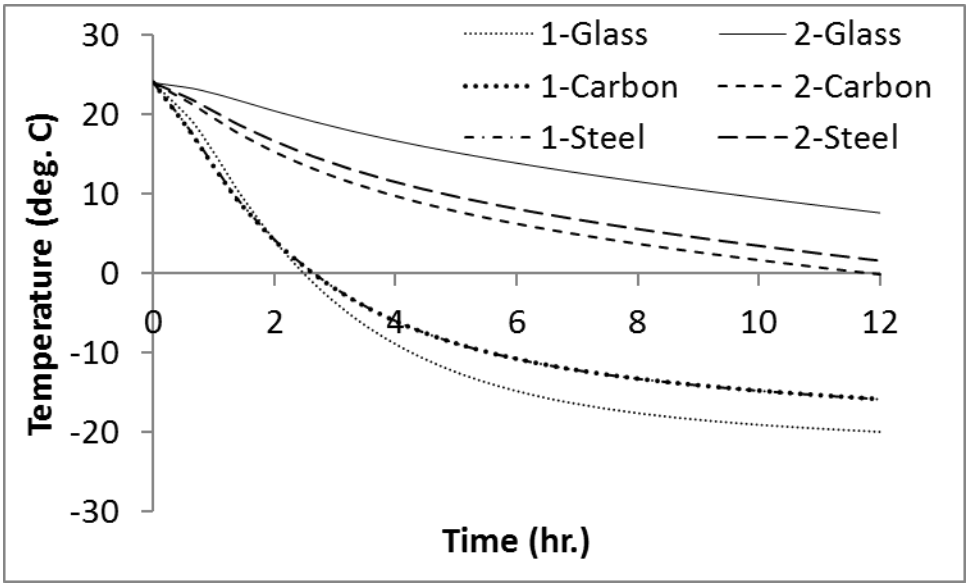

Figure 5-20: Carbon Rod Connector Comparison

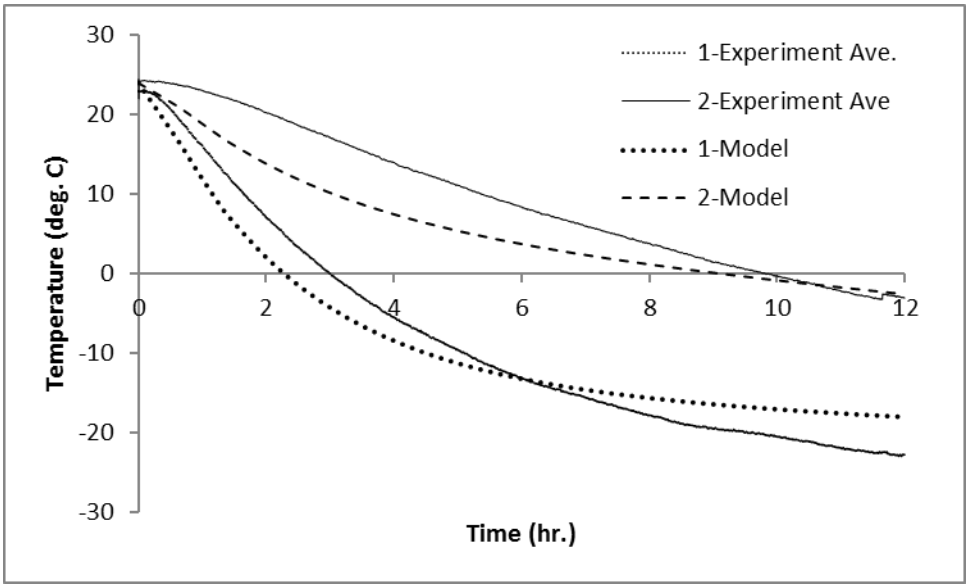

Figure 5-21: Carbon Strip Connector Comparison

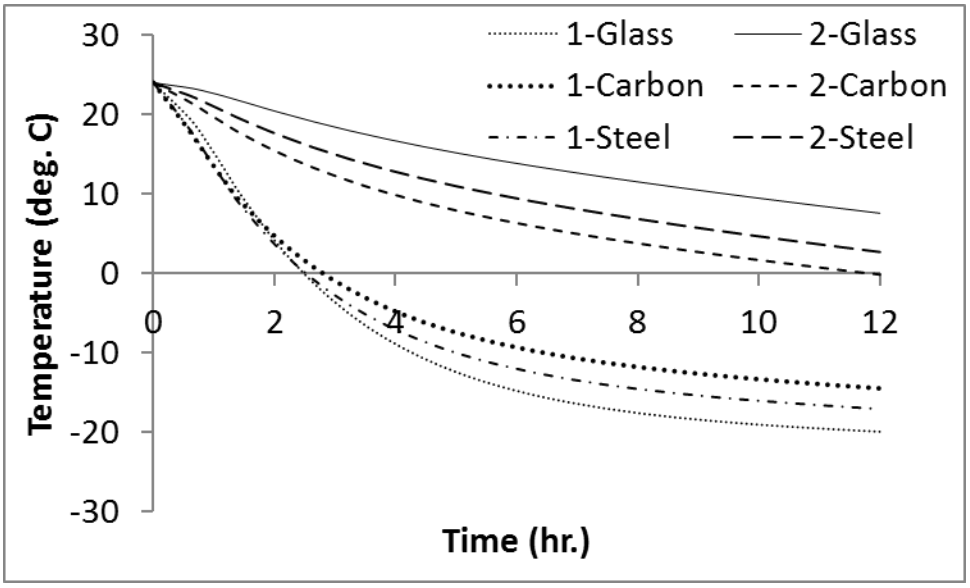

Figure 5-22: Carbon Strip Connector Comparison

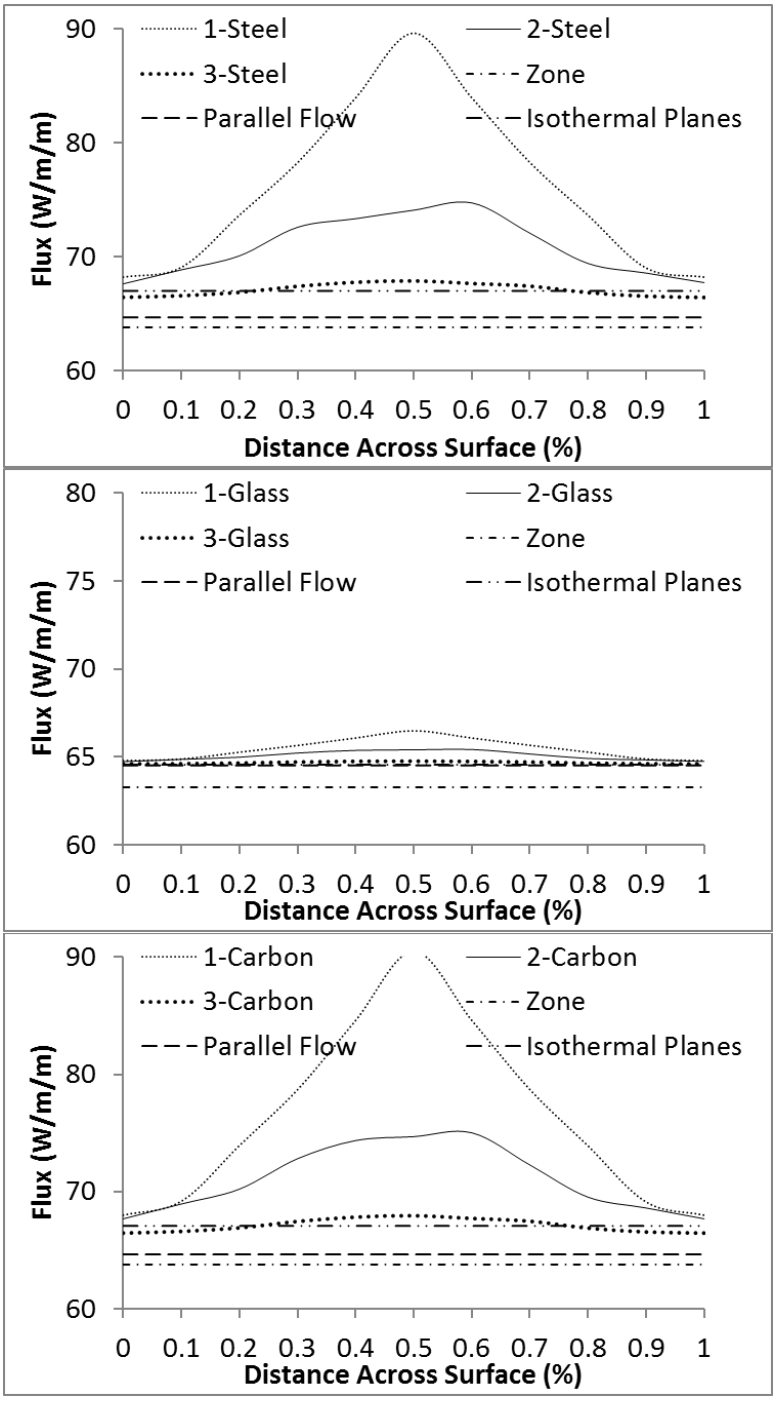

Figure 5-23: One W-Shaped Connector Flux Comparison; a: Steel, b: GFRP, c:CFRP

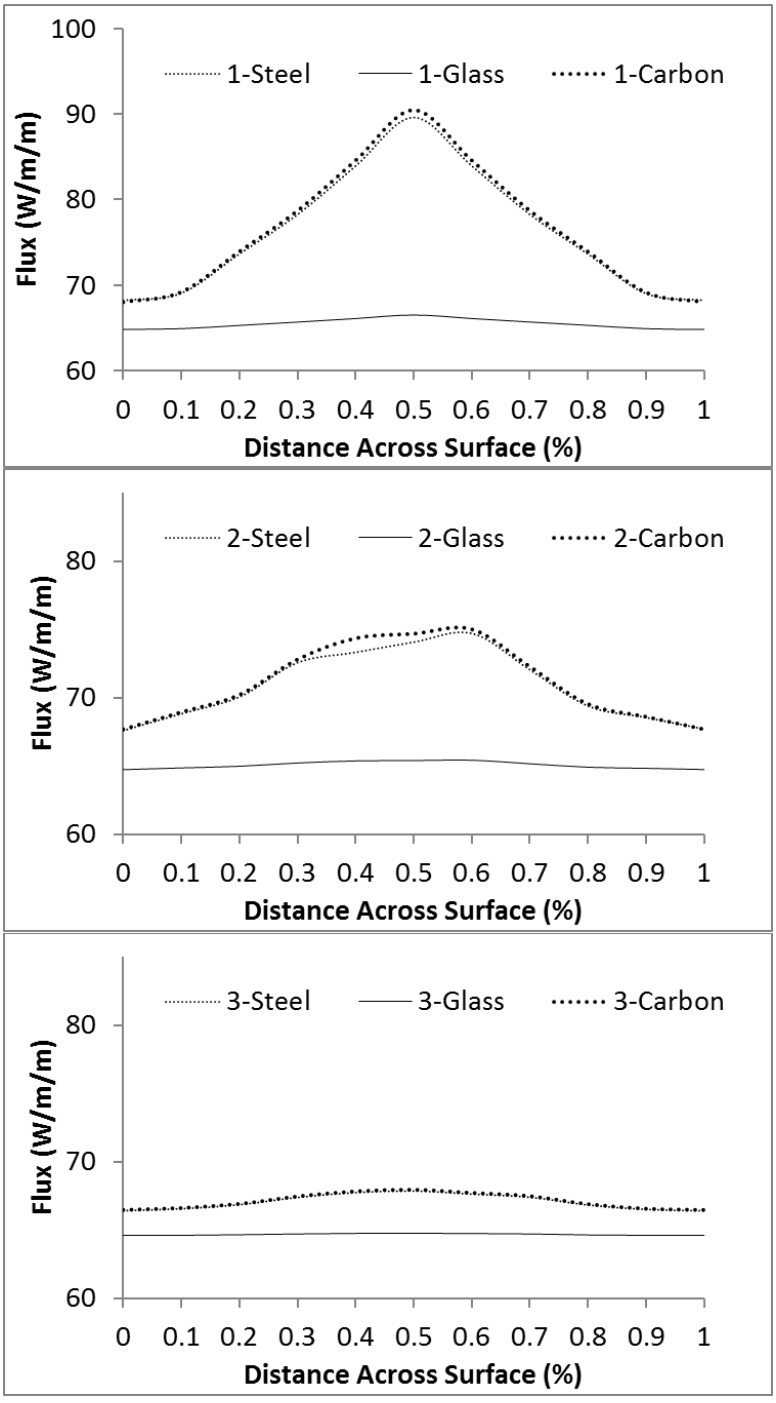

Figure 5-24: One W-Shaped Connector Flux Comparison; a: Line 1, b: Line 2, c: Line 3

a)

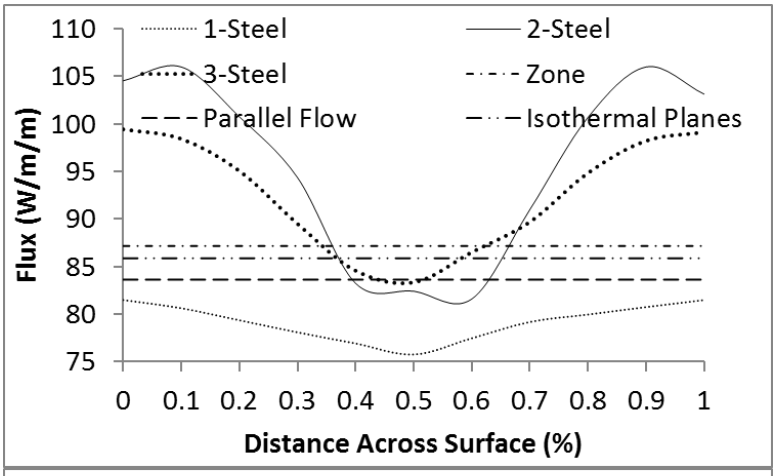

b)

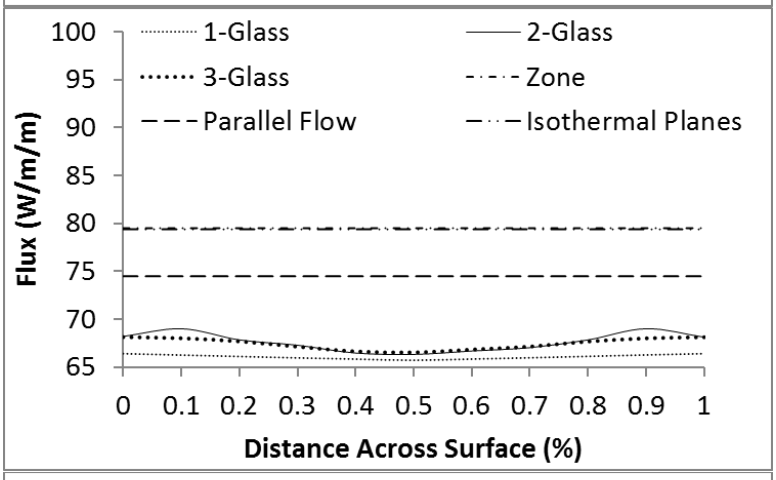

c)

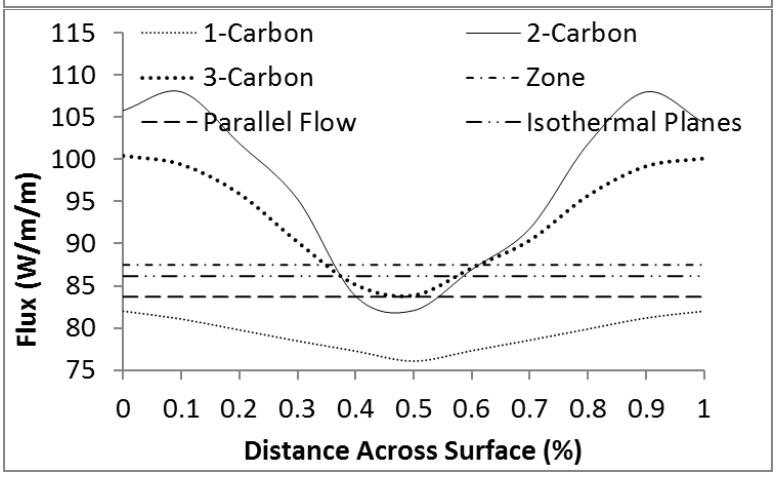

Figure 5-25: Four W-Shaped Connector Flux Comparison; a: Steel, b: GFRP, c: CFRP

a)

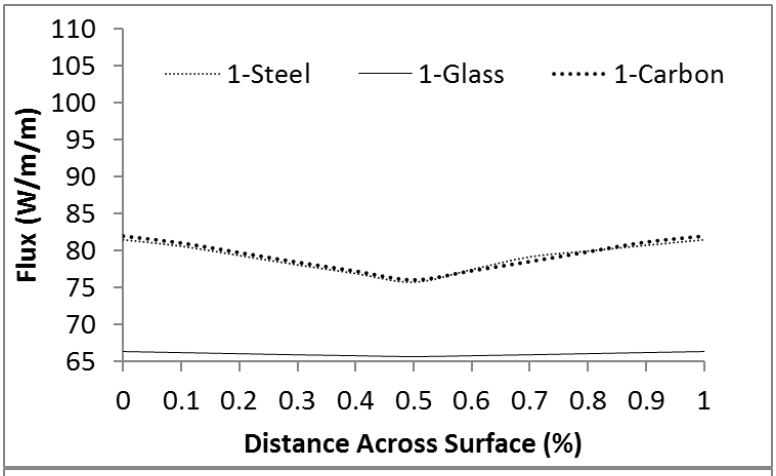

b)

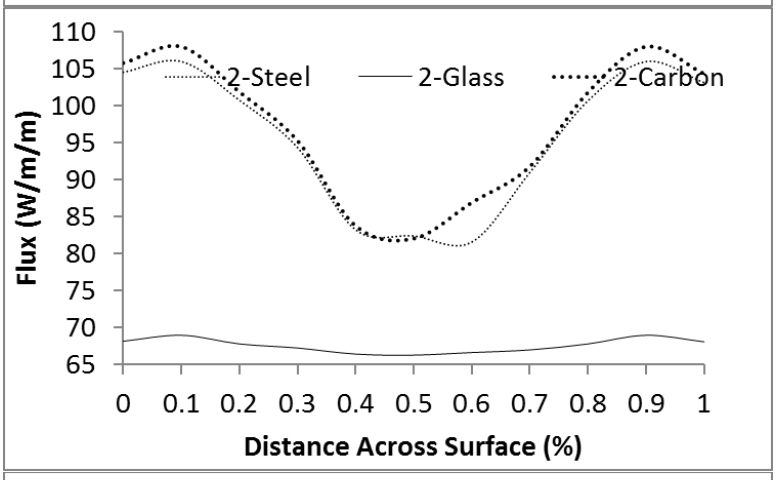

c)

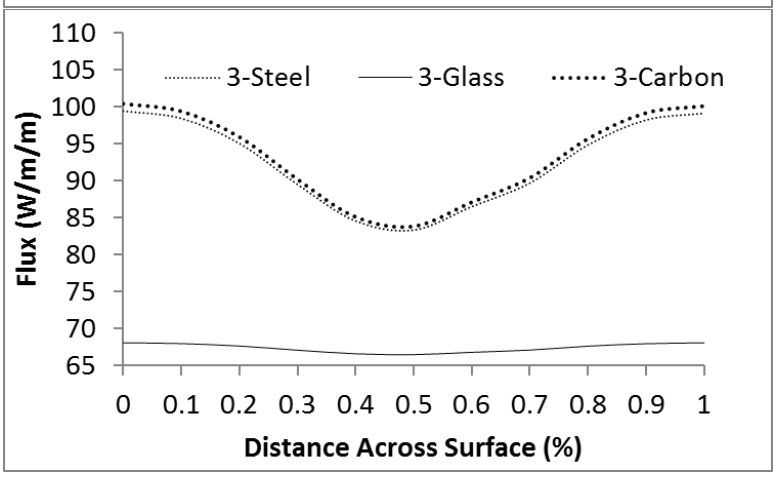

Figure 5-26: Four W-Shaped Connector Flux Comparison; a: Line 1, b: Line 2, c: Line 3

a)

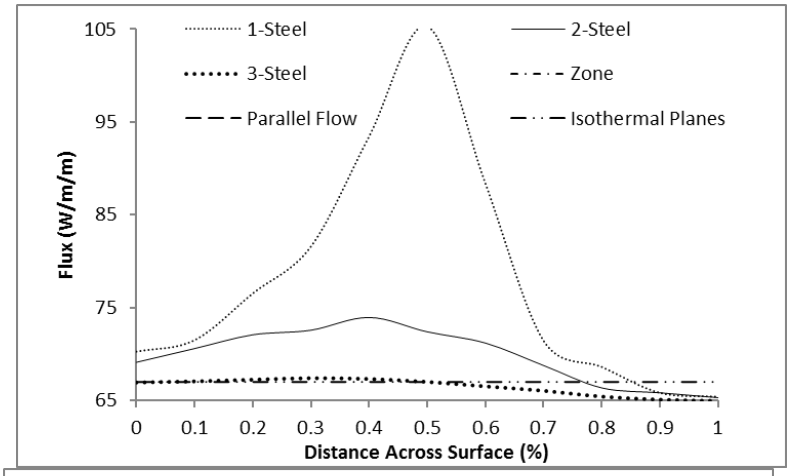

b)

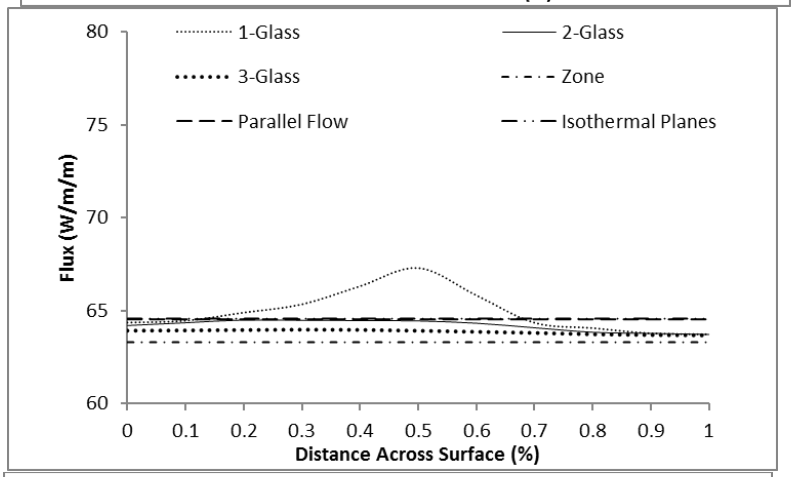

c)

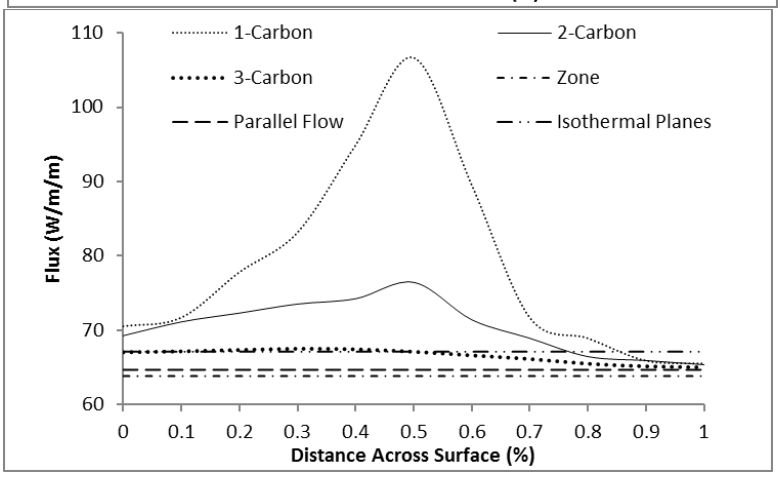

Figure 5-27: One J-Shaped Connector Flux Comparison; a: Steel, b: GFRP, c: CFRP

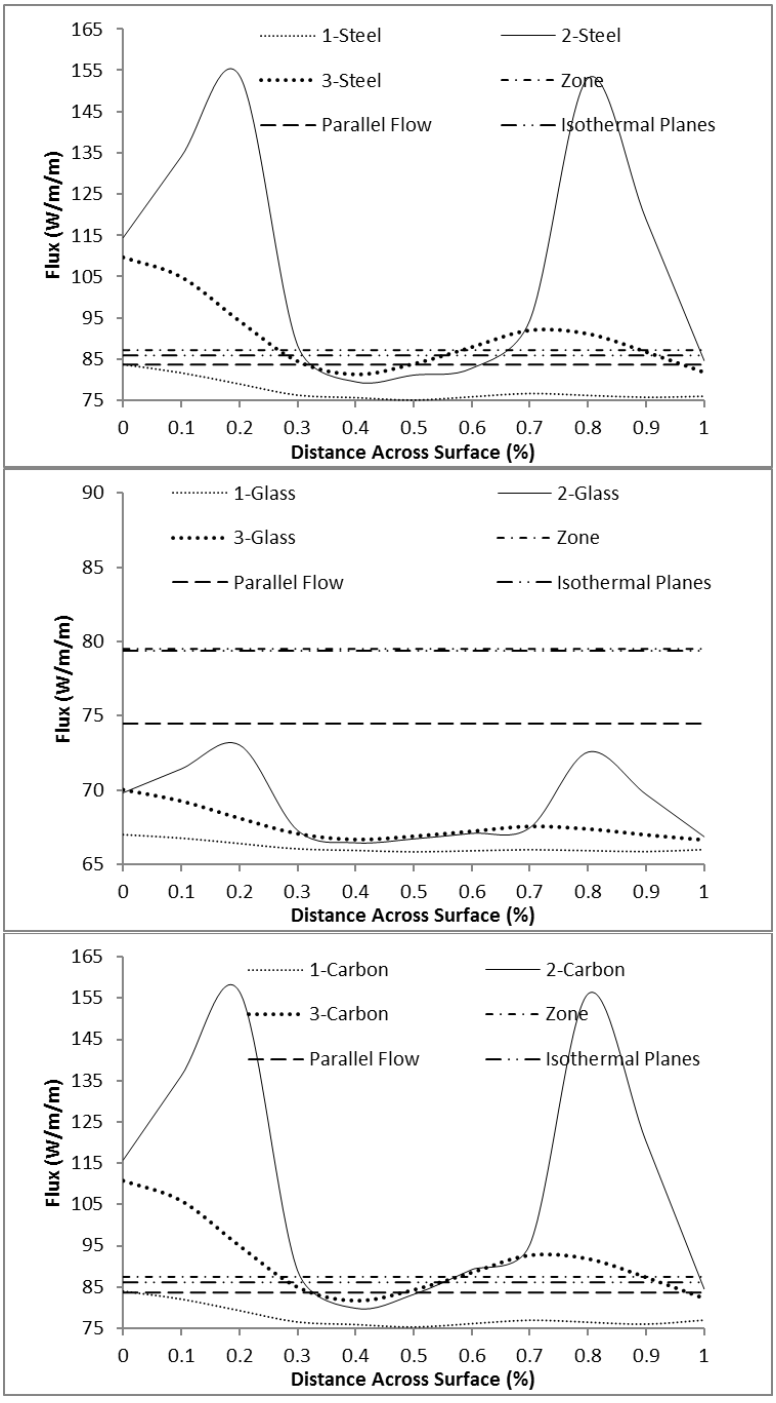

Figure 5-28: Four J-Shaped Connector Flux Comparison; a: Steel, b: GFRP, c: CFRP

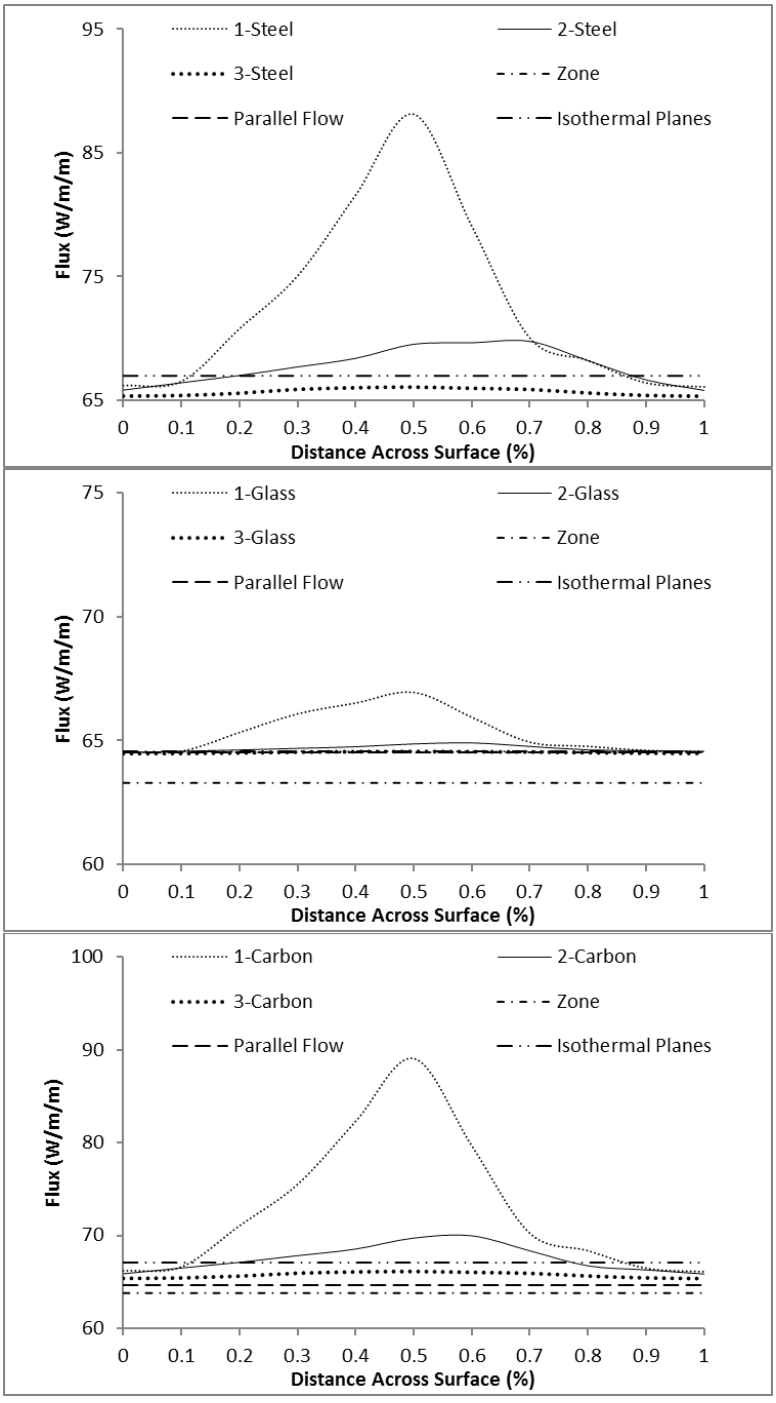

Figure 5-29: One Z-Shaped Connector Flux Comparison; a: Steel, b: GFRP, c: CFRP

a)

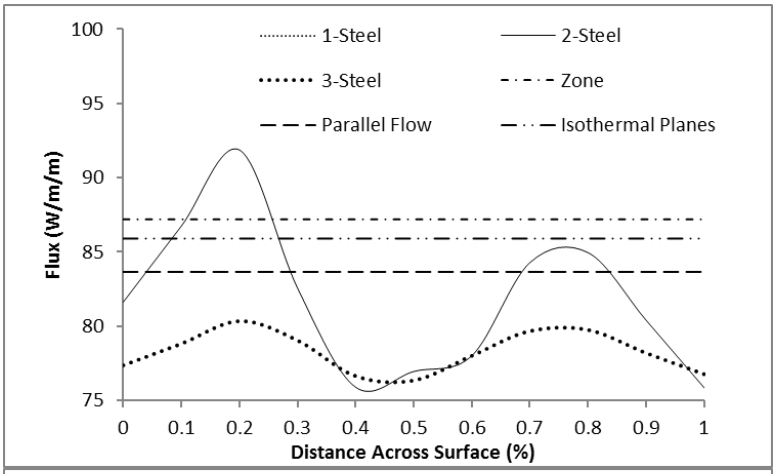

b)

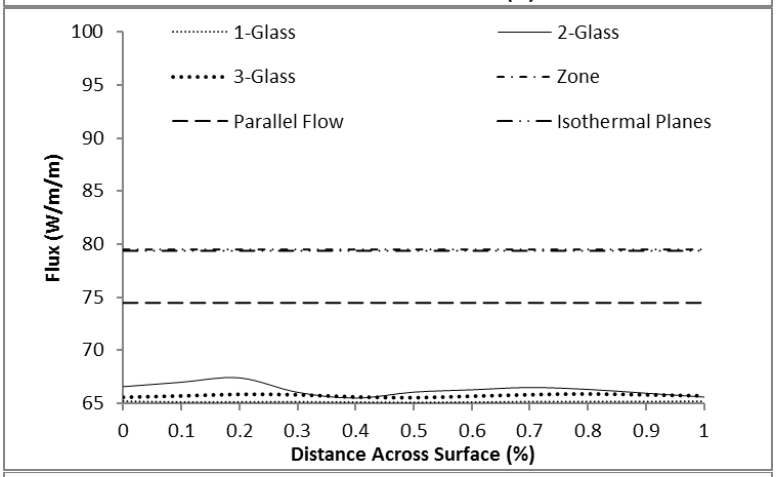

c)

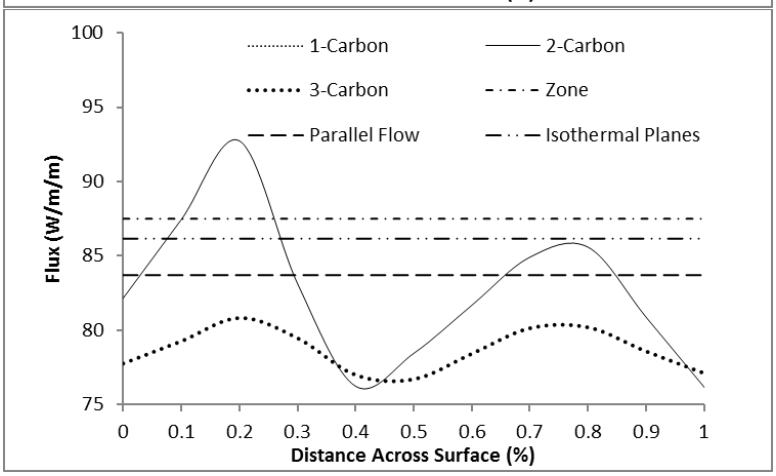

Figure 5-30: Four Z-Shaped Connector Flux Comparison; a: Steel, b: GFRP, c: CFRP

a)

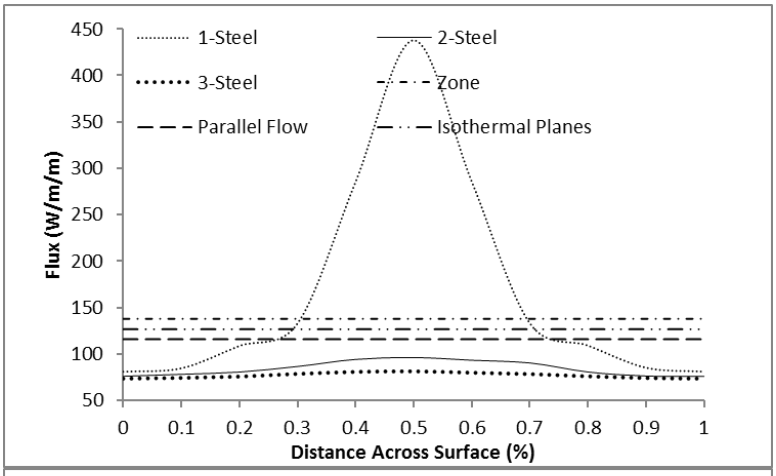

b)

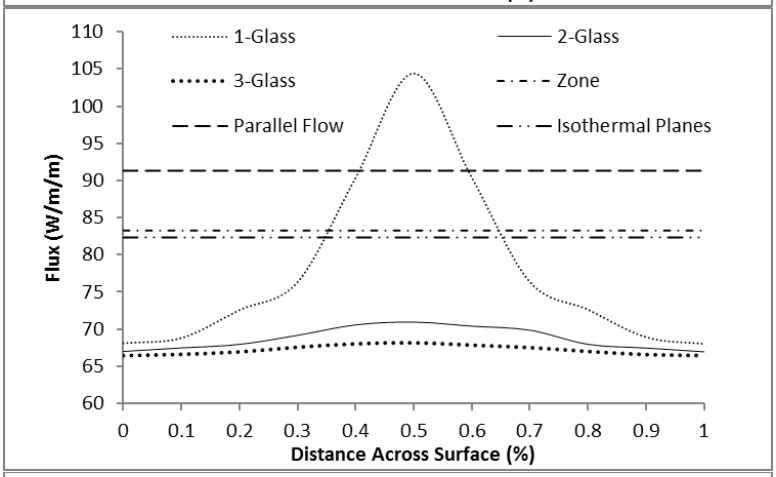

c)

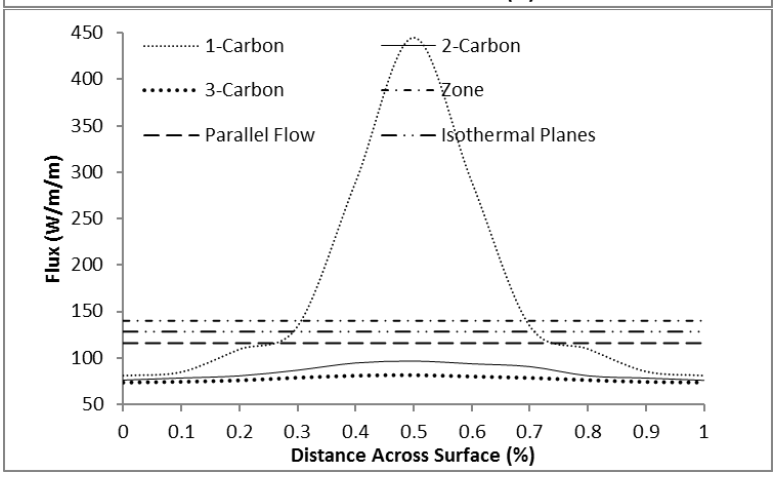

Figure 5-31: Glass Dowel Connector Flux Comparison; a: Steel, b: GFRP, c: CFRP

a)

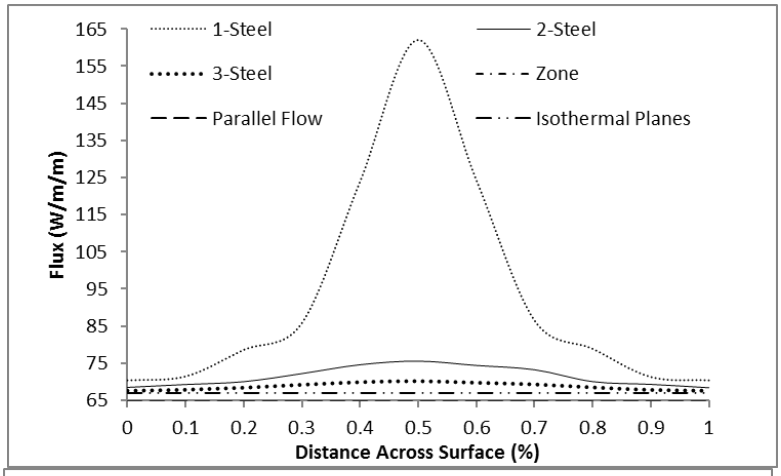

b)

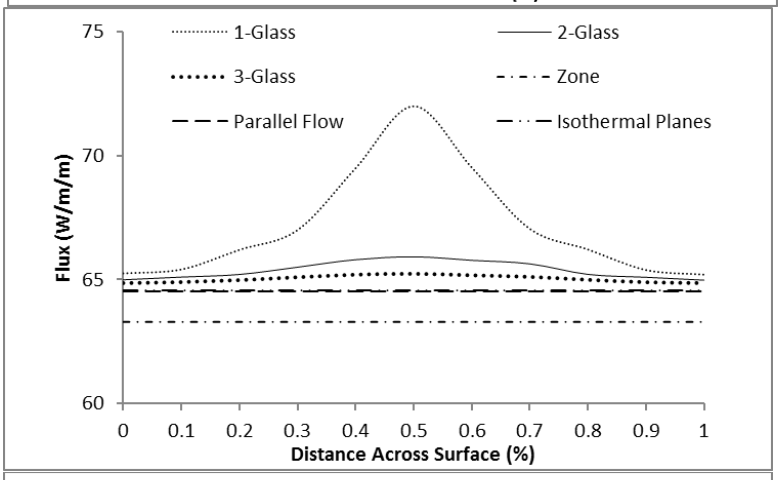

c)

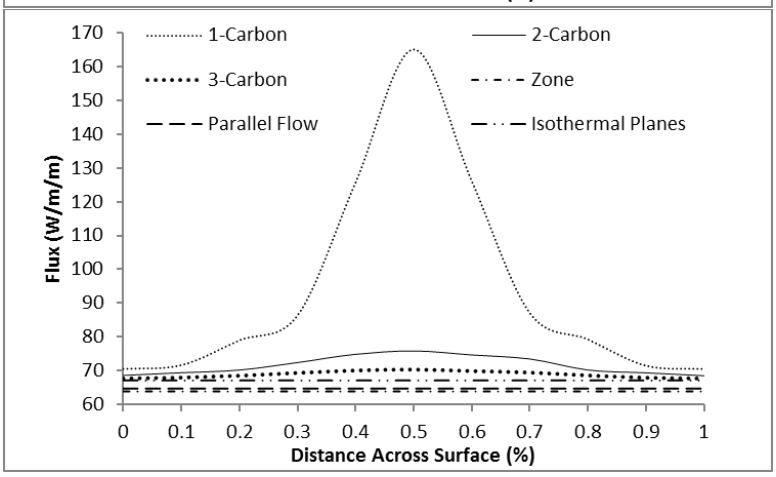

Figure 5-32: Carbon Bar Connector Flux Comparison; a: Steel, b: GFRP, c: CFRP

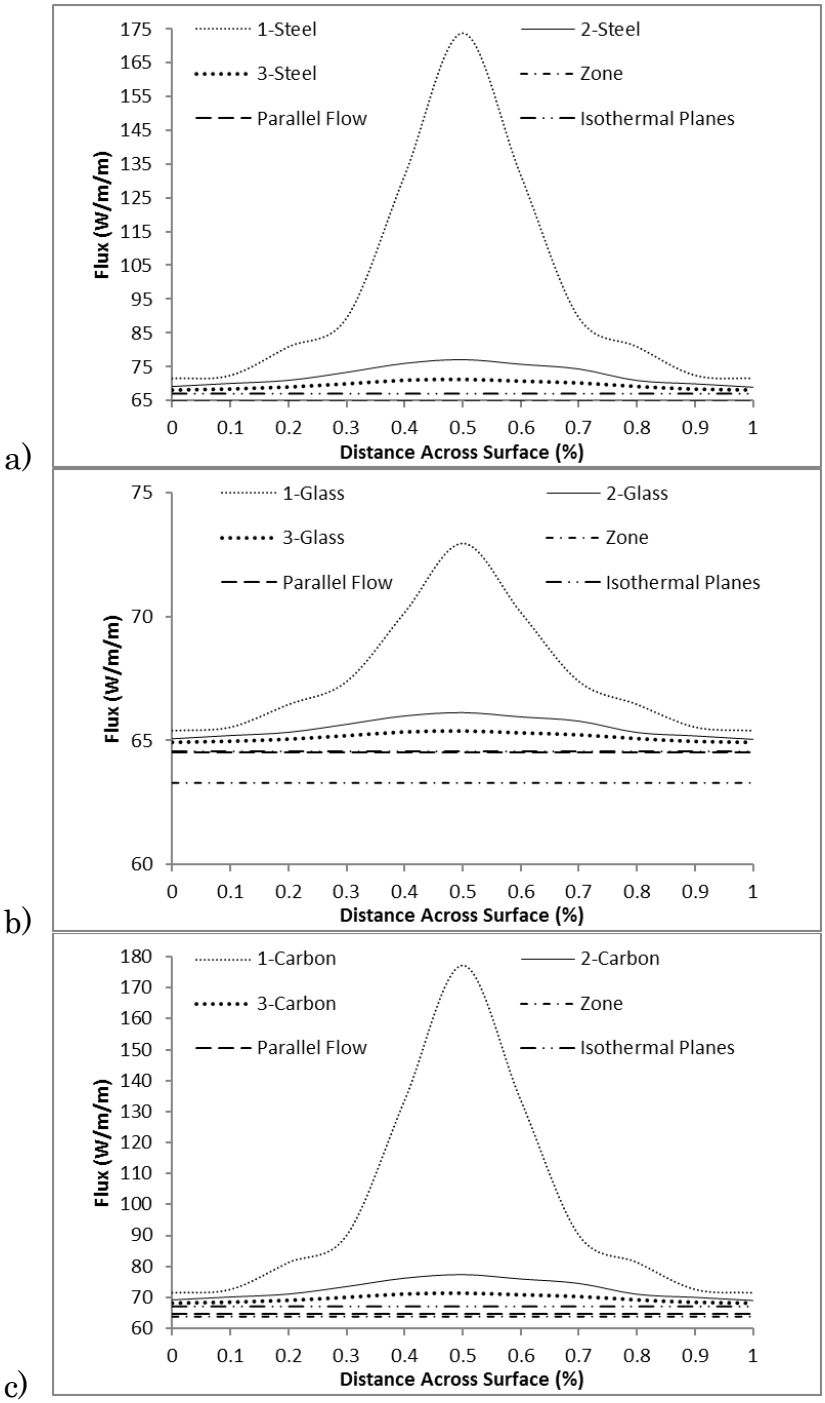

Figure 5-33: Carbon Strip Connector Flux Comparison; a: Steel, b: GFRP, c: CFRP

a)

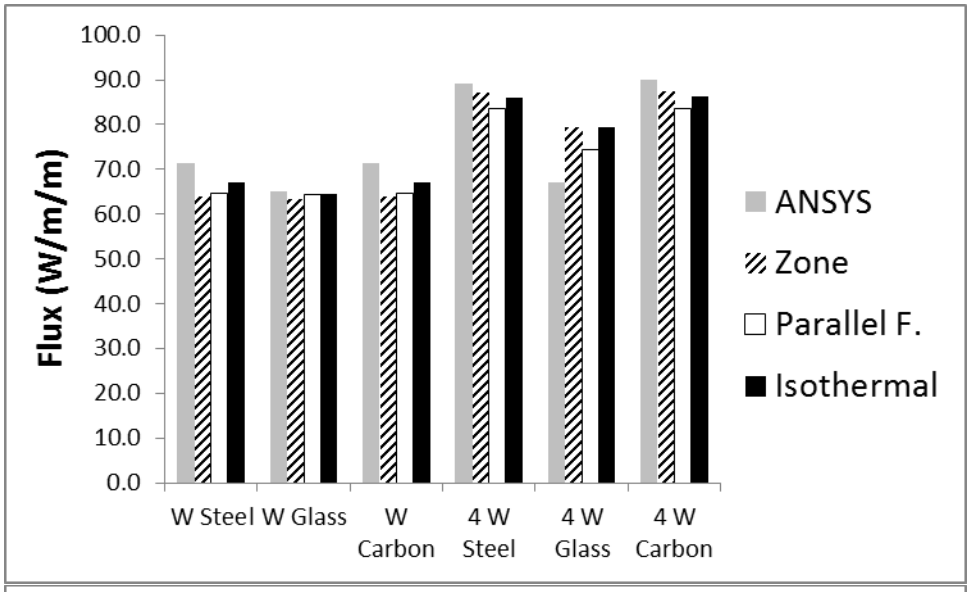

b)

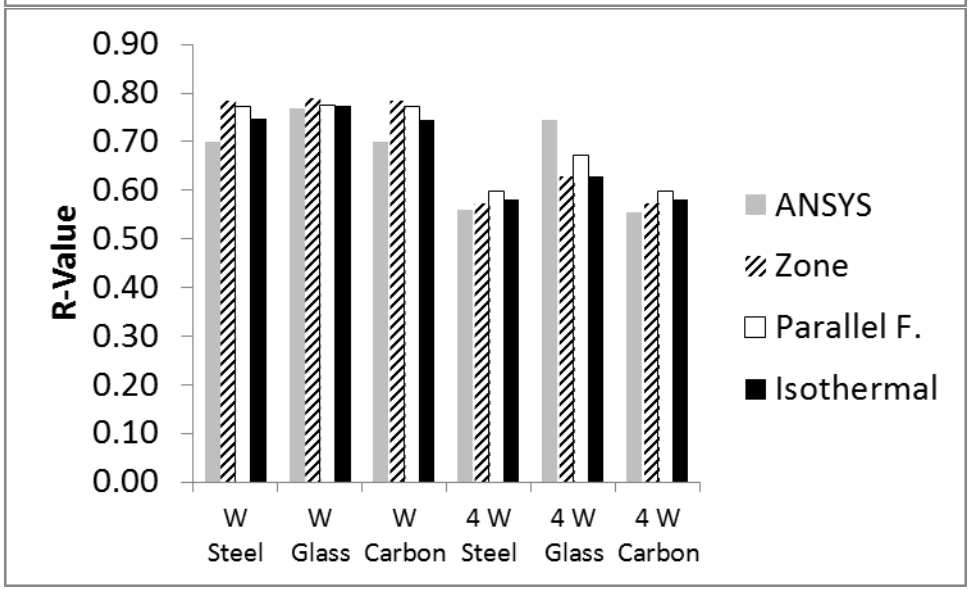

Figure 5-34: Comparison of W-Shaped Connectors; a: Flux, b: R-Value

a)

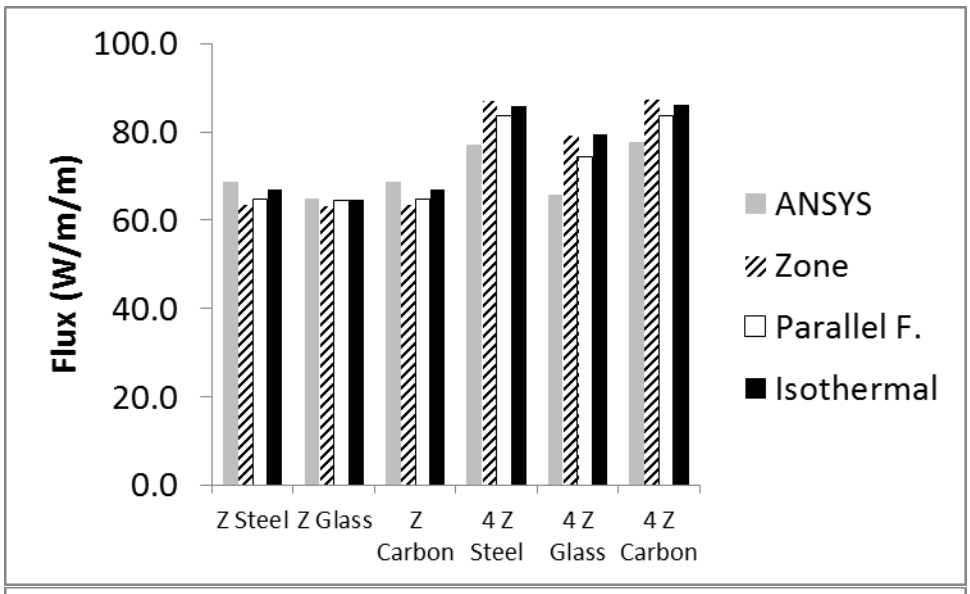

b)

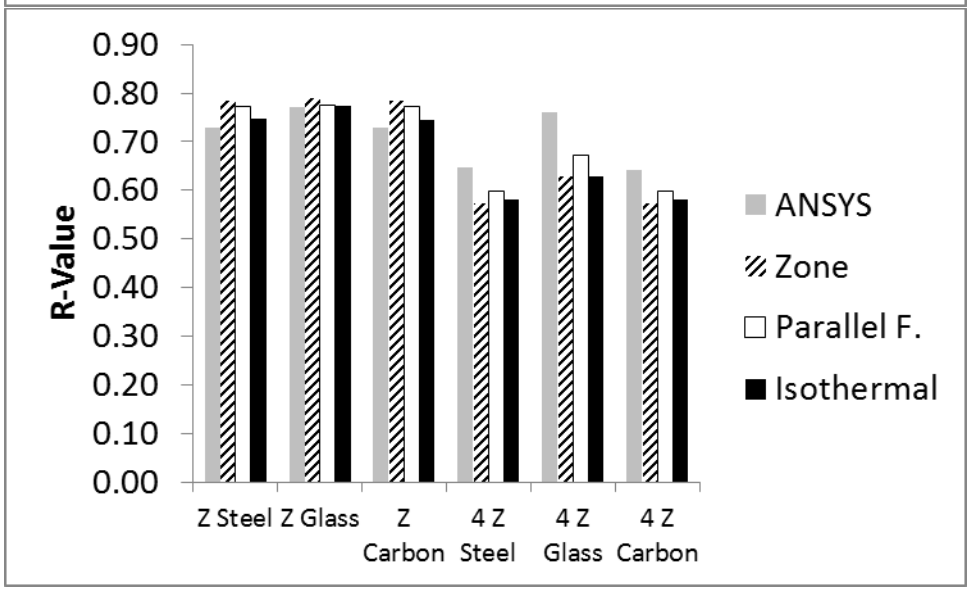

Figure 5-35: Comparison of Z-Shaped Connectors; a: Flux, b: R-Value

a)

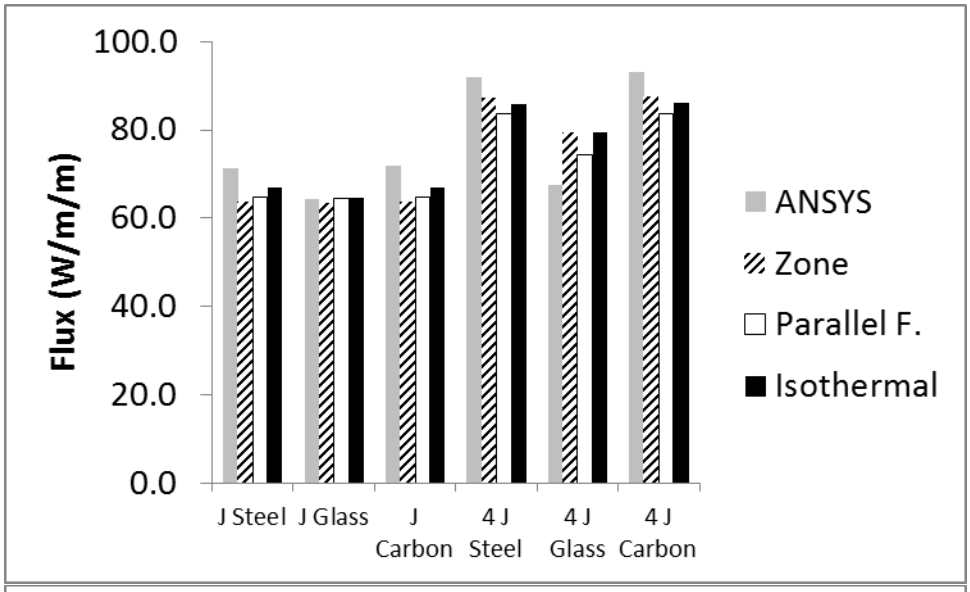

b)

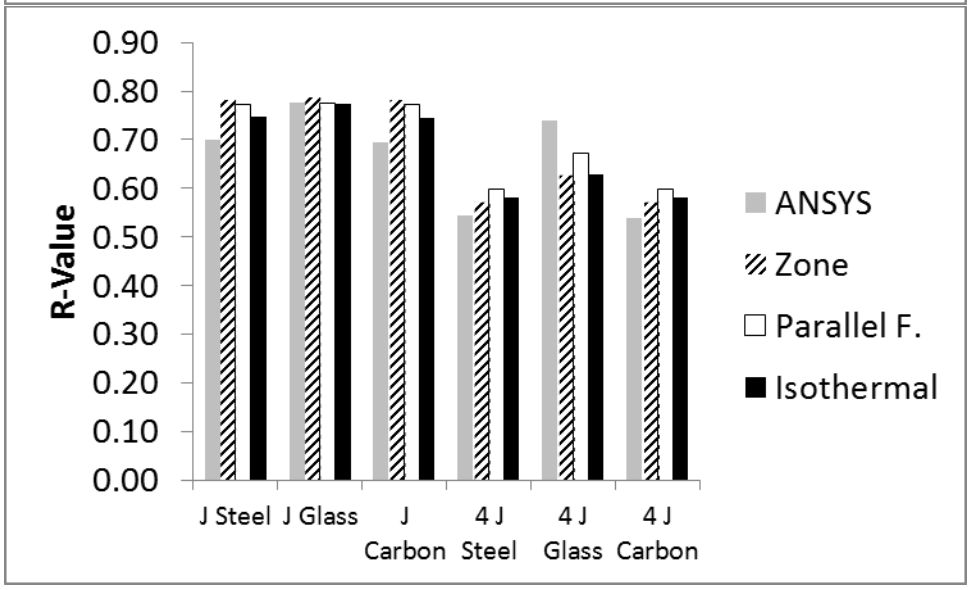

Figure 5-36: Comparison of J-Shaped Connectors; a: Flux, b: R-Value

a)

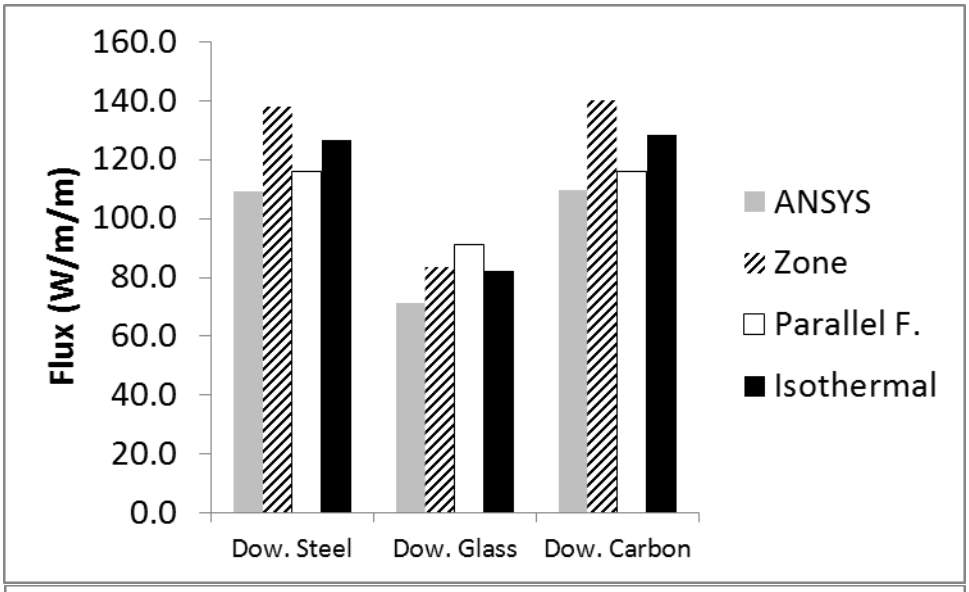

b)

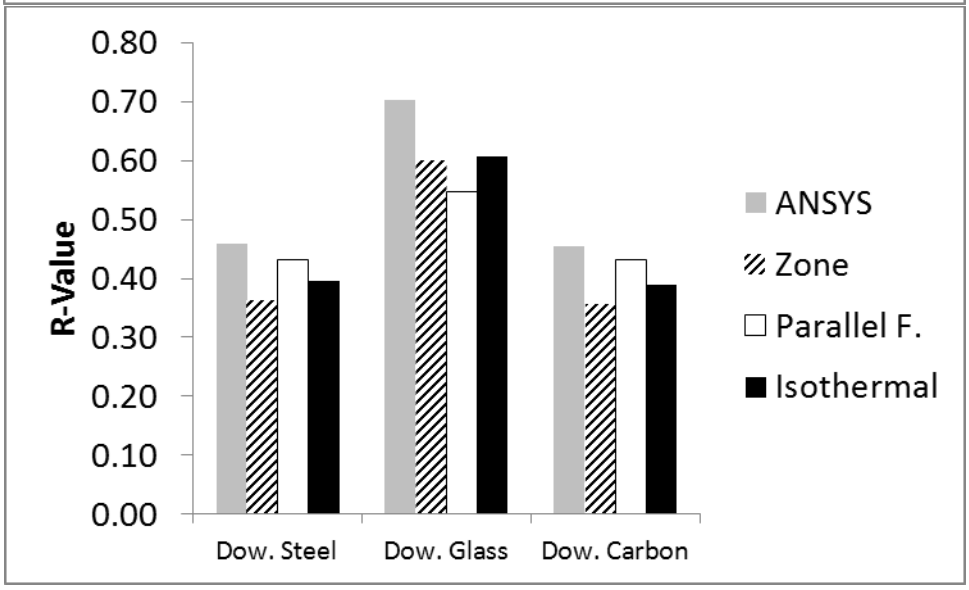

Figure 5-37: Comparison of Dowel Connectors; a: Flux, b: R-Value

a)

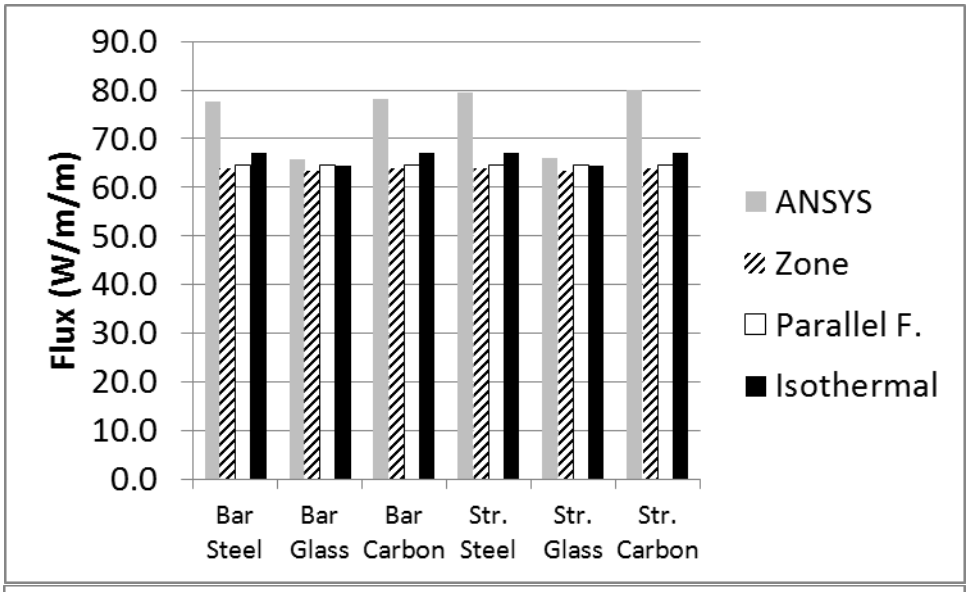

b)

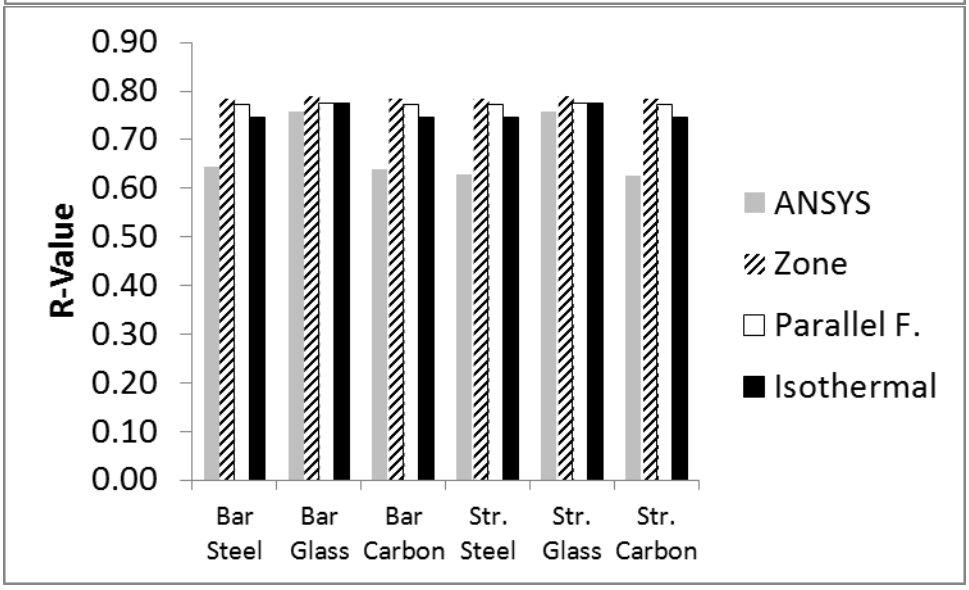

Figure 5-38: Comparison of Bar and Strip Connectors; a: Flux, b: R-Value

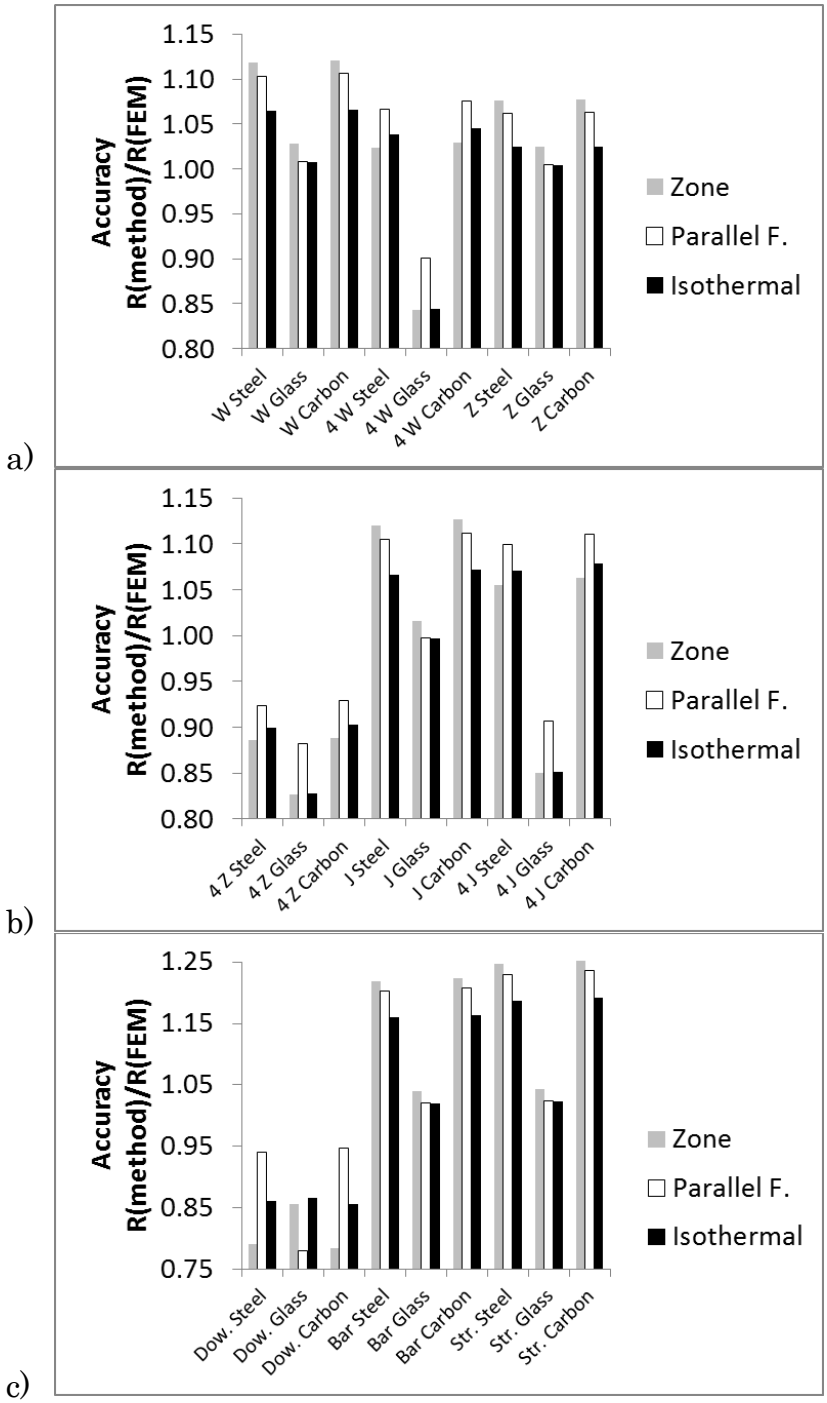

Figure 5-39: Comparison of the Accuracy of the Methods; a: W, 4W, Z, b: 4Z, J, 4J, c: Dowel, Bar, Strip

Table 5-1: Parametric Study

	Space	Size	Mat.	Ansys Flux	Ansys R-val.	Zone	R_{Zone}/R_{FEM}	PF	R_{PF}/R_{FEM}	IP	R_{IP}/R_{FEM}	R. Zone	$R_{R.Zone}/R_{FEM}$
W	1 ft.	2-4-2	Steel	31.90	1.57	1.19	0.76	1.23	0.78	1.50	0.96	1.60	1.02
			GFRP	29.80	1.68	1.58	0.94	1.38	0.82	1.61	0.96	1.67	1.00
			CFRP	32.28	1.55	1.18	0.76	1.23	0.79	1.49	0.96	1.60	1.03
		3-1-3	Steel	89.80	0.56	0.38	0.68	0.47	0.84	0.41	0.74	0.56	1.01
			GFRP	86.41	0.58	0.41	0.71	0.52	0.90	0.42	0.73	0.57	0.99
			CFRP	89.91	0.56	0.38	0.68	0.46	0.83	0.41	0.74	0.56	1.01
		3-4-3	Steel	30.69	1.63	1.22	0.75	1.47	0.90	1.56	0.96	1.70	1.04
			GFRP	28.70	1.74	1.64	0.94	1.53	0.88	1.68	0.96	1.74	1.00
			CFRP	30.81	1.62	1.21	0.75	1.47	0.91	1.56	0.96	1.70	1.05
		4-1-4	Steel	80.48	0.62	0.43	0.69	0.59	0.95	0.47	0.76	0.63	1.01
			GFRP	77.86	0.64	0.48	0.75	0.61	0.95	0.48	0.75	0.64	1.00
			CFRP	80.56	0.62	0.43	0.69	0.59	0.95	0.47	0.76	0.63	1.02
		4-4-4	Steel	29.54	1.69	1.25	0.74	1.61	0.95	1.62	0.96	1.79	1.06
			GFRP	27.69	1.81	1.70	0.94	1.64	0.91	1.74	0.96	1.80	1.00
			CFRP	29.66	1.69	1.24	0.74	1.61	0.96	1.62	0.96	1.79	1.06
		6-1-6	Steel	66.73	0.75	0.53	0.71	0.74	0.99	0.60	0.80	0.76	1.01
			GFRP	64.99	0.77	0.60	0.78	0.75	0.97	0.61	0.79	0.77	1.00
			CFRP	66.79	0.75	0.53	0.71	0.74	0.99	0.60	0.80	0.76	1.02
		6-4-6	Steel	27.46	1.82	1.32	0.72	1.80	0.99	1.75	0.96	1.93	1.06
			GFRP	25.87	1.93	1.82	0.94	1.82	0.94	1.87	0.97	1.94	1.00
			CFRP	27.51	1.82	1.30	0.72	1.80	0.99	1.75	0.96	1.93	1.06
W	2 ft.	2-4-2	Steel	30.26	1.65	1.49	0.90	1.42	0.86	1.59	0.96	1.66	1.00
			GFRP	29.64	1.69	1.61	0.95	1.51	0.90	1.62	0.96	1.68	1.00
			CFRP	30.47	1.64	1.48	0.90	1.42	0.87	1.59	0.97	1.66	1.01
		3-1-3	Steel	87.25	0.57	0.41	0.72	0.52	0.91	0.42	0.73	0.57	0.99
			GFRP	86.13	0.58	0.42	0.72	0.55	0.95	0.42	0.72	0.58	1.00
			CFRP	87.29	0.57	0.41	0.72	0.52	0.91	0.42	0.73	0.57	1.00
		3-4-3	Steel	28.76	1.74	1.54	0.89	1.60	0.92	1.65	0.95	1.74	1.00
			GFRP	28.56	1.75	1.67	0.95	1.63	0.93	1.68	0.96	1.75	1.00
			CFRP	28.80	1.74	1.53	0.88	1.60	0.92	1.65	0.95	1.74	1.00
		4-1-4	Steel	78.39	0.64	0.47	0.74	0.61	0.96	0.48	0.75	0.64	1.00
			GFRP	77.63	0.64	0.48	0.75	0.62	0.96	0.48	0.75	0.64	0.99
			CFRP	78.42	0.64	0.47	0.74	0.61	0.96	0.48	0.75	0.64	1.00
		4-4-4	Steel	27.60	1.81	1.59	0.88	1.70	0.94	1.72	0.95	1.81	1.00
			GFRP	27.55	1.81	1.74	0.96	1.72	0.95	1.75	0.96	1.81	1.00
			CFRP	28.09	1.78	1.59	0.89	1.70	0.96	1.71	0.96	1.81	1.02
		6-1-6	Steel	65.29	0.77	0.59	0.77	0.75	0.98	0.61	0.80	0.77	1.01
			GFRP	64.83	0.77	0.61	0.79	0.76	0.99	0.61	0.79	0.77	1.00
			CFRP	65.31	0.77	0.59	0.77	0.75	0.98	0.61	0.80	0.77	1.01
		6-4-6	Steel	26.18	1.91	1.70	0.89	1.87	0.98	1.84	0.96	1.94	1.02
			GFRP	25.75	1.94	1.86	0.96	1.88	0.97	1.87	0.96	1.94	1.00
			CFRP	26.14	1.91	1.69	0.88	1.87	0.98	1.84	0.96	1.94	1.01

Table 5-2: Parametric Study

	Space	Size	Mat.	Ansys Flux	Ansys R-val.	Zone	R_{Zone}/R_{FEM}	PF	R_{FF}/R_{FEM}	IP	R_{IP}/R_{FEM}	R. Zone	$R_{R.Zone}/R_{FEM}$
W	3 ft.	2-4-2	Steel	30.07	1.66	1.56	0.94	1.50	0.90	1.61	0.97	1.68	1.01
			GFRP	29.61	1.69	1.62	0.96	1.57	0.93	1.62	0.96	1.68	0.99
			CFRP	30.00	1.67	1.56	0.94	1.50	0.90	1.61	0.97	1.68	1.01
		3-1-3	Steel	86.62	0.58	0.41	0.71	0.53	0.92	0.42	0.73	0.57	0.99
			GFRP	86.08	0.58	0.42	0.72	0.56	0.96	0.42	0.72	0.58	1.00
			CFRP	86.76	0.58	0.41	0.71	0.54	0.94	0.42	0.73	0.57	0.99
		3-4-3	Steel	28.85	1.73	1.62	0.93	1.64	0.95	1.67	0.96	1.74	1.00
			GFRP	28.54	1.75	1.68	0.96	1.67	0.95	1.68	0.96	1.75	1.00
			CFRP	28.89	1.73	1.61	0.93	1.64	0.95	1.67	0.96	1.74	1.01
		4-1-4	Steel	78.02	0.64	0.48	0.75	0.62	0.97	0.48	0.75	0.64	1.00
			GFRP	77.58	0.64	0.48	0.74	0.53	0.82	0.48	0.74	0.64	0.99
			CFRP	78.03	0.64	0.48	0.75	0.62	0.97	0.48	0.75	0.64	1.00
		4-4-4	Steel	27.79	1.80	1.68	0.93	1.74	0.97	1.73	0.96	1.81	1.01
			GFRP	27.53	1.82	1.74	0.96	1.75	0.96	1.75	0.96	1.81	1.00
			CFRP	27.81	1.80	1.67	0.93	1.74	0.97	1.73	0.96	1.81	1.01
		6-1-6	Steel	65.04	0.77	0.60	0.78	0.76	0.99	0.61	0.79	0.77	1.00
			GFRP	64.80	0.77	0.61	0.79	0.76	0.98	0.61	0.79	0.77	1.00
			CFRP	65.04	0.77	0.60	0.78	0.76	0.99	0.61	0.79	0.77	1.00
		6-4-6	Steel	25.93	1.93	1.79	0.93	1.89	0.98	1.86	0.96	1.94	1.01
			GFRP	25.30	1.98	1.87	0.95	1.90	0.96	1.87	0.95	1.94	0.98
			CFRP	25.94	1.93	1.79	0.93	1.89	0.98	1.86	0.96	1.94	1.01
W	4 ft.	2-4-2	Steel	29.89	1.67	1.59	0.95	1.54	0.92	1.61	0.96	1.68	1.00
			GFRP	29.61	1.69	1.62	0.96	1.60	0.95	1.62	0.96	1.69	1.00
			CFRP	29.94	1.67	1.58	0.95	1.54	0.92	1.61	0.96	1.68	1.01
		3-1-3	Steel	86.36	0.58	0.42	0.73	0.55	0.95	0.42	0.73	0.58	1.00
			GFRP	86.04	0.58	0.42	0.72	0.56	0.96	0.42	0.72	0.58	1.00
			CFRP	86.37	0.58	0.42	0.73	0.54	0.93	0.42	0.73	0.58	1.00
		3-4-3	Steel	28.70	1.74	1.65	0.95	1.67	0.96	1.68	0.96	1.75	1.00
			GFRP	28.52	1.75	1.69	0.96	1.69	0.96	1.68	0.96	1.75	1.00
			CFRP	28.71	1.74	1.65	0.95	1.67	0.96	1.68	0.96	1.75	1.00
		4-1-4	Steel	77.75	0.64	0.48	0.75	0.63	0.98	0.48	0.75	0.64	1.00
			GFRP	77.56	0.64	0.48	0.74	0.63	0.98	0.48	0.74	0.64	0.99
			CFRP	77.75	0.64	0.48	0.75	0.63	0.98	0.48	0.75	0.64	1.00
		4-4-4	Steel	27.72	1.80	1.71	0.95	1.76	0.98	1.74	0.96	1.81	1.00
			GFRP	27.50	1.82	1.75	0.96	1.77	0.97	1.75	0.96	1.81	1.00
			CFRP	27.73	1.80	1.71	0.95	1.76	0.98	1.74	0.97	1.81	1.00
		6-1-6	Steel	64.89	0.77	0.60	0.78	0.76	0.99	0.61	0.79	0.77	1.00
			GFRP	64.79	0.77	0.61	0.79	0.76	0.98	0.61	0.79	0.77	1.00
			CFRP	64.90	0.77	0.60	0.78	0.76	0.99	0.61	0.79	0.77	1.00
		6-4-6	Steel	25.84	1.93	1.83	0.95	1.90	0.98	1.87	0.97	1.94	1.00
			GFRP	25.72	1.94	1.87	0.96	1.91	0.98	1.87	0.96	1.94	1.00
			CFRP	25.85	1.93	1.83	0.95	1.90	0.98	1.87	0.97	1.94	1.00

Table 5-3: Parametric Study

	Space	Size	Mat.	Ansys Flux	Ansys R-val.	Zone	R_{Zone}/R_{FEM}	PF	R_{FF}/R_{FEM}	IP	R_{IP}/R_{FEM}	R. Zone	$R_{R.Zone}/R_{FEM}$
Z	1 ft.	2-4-2	Steel	31.02	1.61	1.19	0.74	1.23	0.76	1.50	0.93	1.60	0.99
			GFRP	29.70	1.68	1.58	0.94	1.38	0.82	1.61	0.96	1.67	0.99
			CFRP	31.09	1.61	1.18	0.73	1.23	0.76	1.49	0.93	1.60	0.99
		3-1-3	Steel	88.22	0.57	0.38	0.67	0.47	0.83	0.41	0.72	0.56	0.99
			GFRP	86.26	0.58	0.41	0.71	0.52	0.90	0.42	0.72	0.57	0.98
			CFRP	88.28	0.57	0.38	0.67	0.46	0.81	0.41	0.72	0.56	0.99
		3-4-3	Steel	29.66	1.69	1.22	0.72	1.47	0.87	1.56	0.93	1.70	1.01
			GFRP	28.60	1.75	1.64	0.94	1.53	0.88	1.68	0.96	1.74	1.00
			CFRP	29.72	1.68	1.21	0.72	1.47	0.87	1.56	0.93	1.70	1.01
		4-1-4	Steel	79.10	0.63	0.43	0.68	0.59	0.93	0.47	0.74	0.63	1.00
			GFRP	77.73	0.64	0.48	0.75	0.61	0.95	0.48	0.75	0.64	0.99
			CFRP	79.11	0.63	0.43	0.68	0.59	0.93	0.47	0.74	0.63	1.00
		4-4-4	Steel	28.55	1.75	1.25	0.71	1.61	0.92	1.62	0.93	1.79	1.02
			GFRP	27.59	1.81	1.70	0.94	1.64	0.90	1.74	0.96	1.80	0.99
			CFRP	28.59	1.75	1.24	0.71	1.61	0.92	1.62	0.93	1.79	1.02
		6-1-6	Steel	65.79	0.76	0.53	0.70	0.74	0.97	0.60	0.79	0.76	1.00
			GFRP	64.89	0.77	0.60	0.78	0.75	0.97	0.61	0.79	0.77	1.00
			CFRP	64.89	0.77	0.53	0.69	0.74	0.96	0.60	0.78	0.76	0.99
		6-4-6	Steel	26.61	1.88	1.32	0.70	1.80	0.96	1.75	0.93	1.93	1.03
			GFRP	25.80	1.94	1.82	0.94	1.82	0.94	1.87	0.96	1.94	1.00
			CFRP	26.64	1.88	1.30	0.69	1.80	0.96	1.75	0.93	1.93	1.03
Z	4 ft.	2-4-2	Steel	29.71	1.68	1.59	0.94	1.54	0.92	1.61	0.96	1.68	1.00
			GFRP	29.59	1.69	1.62	0.96	1.60	0.95	1.62	0.96	1.69	1.00
			CFRP	29.72	1.68	1.58	0.94	1.54	0.92	1.61	0.96	1.68	1.00
		3-1-3	Steel	86.26	0.58	0.42	0.72	0.55	0.95	0.42	0.72	0.58	1.00
			GFRP	86.03	0.58	0.42	0.72	0.56	0.96	0.42	0.72	0.58	1.00
			CFRP	86.29	0.58	0.42	0.72	0.54	0.93	0.42	0.72	0.58	1.00
		3-4-3	Steel	28.60	1.75	1.65	0.94	1.67	0.96	1.68	0.96	1.75	1.00
			GFRP	28.51	1.75	1.69	0.96	1.69	0.96	1.68	0.96	1.75	1.00
			CFRP	28.60	1.75	1.65	0.94	1.67	0.96	1.68	0.96	1.75	1.00
		4-1-4	Steel	77.63	0.64	0.48	0.75	0.63	0.98	0.48	0.75	0.64	0.99
			GFRP	77.55	0.64	0.48	0.74	0.63	0.98	0.48	0.74	0.64	0.99
			CFRP	77.63	0.64	0.48	0.75	0.63	0.98	0.48	0.75	0.64	0.99
		4-4-4	Steel	27.58	1.81	1.71	0.94	1.76	0.97	1.74	0.96	1.81	1.00
			GFRP	27.51	1.82	1.75	0.96	1.77	0.97	1.75	0.96	1.81	1.00
			CFRP	27.59	1.81	1.71	0.94	1.76	0.97	1.74	0.96	1.81	1.00
		6-1-6	Steel	64.83	0.77	0.60	0.78	0.76	0.99	0.61	0.79	0.77	1.00
			GFRP	64.78	0.77	0.61	0.79	0.76	0.98	0.61	0.79	0.77	1.00
			CFRP	64.84	0.77	0.60	0.78	0.76	0.99	0.61	0.79	0.77	1.00
		6-4-6	Steel	25.76	1.94	1.83	0.94	1.90	0.98	1.87	0.96	1.94	1.00
			GFRP	25.71	1.94	1.87	0.96	1.91	0.98	1.87	0.96	1.94	1.00
			CFRP	25.76	1.94	1.83	0.94	1.90	0.98	1.87	0.96	1.94	1.00

Table 5-4: Parametric Study

	Space	Size	Mat.	Ansys Flux	Ansys R-val.	Zone	R_{Zone}/R_{FEM}	PF	R_{FF}/R_{FEM}	IP	R_{IP}/R_{FEM}	R. Zone	$R_{R.Zone}/R_{FEM}$
J	1 ft.	2-4-2	Steel	33.23	1.50	1.19	0.79	1.23	0.82	1.50	1.00	1.60	1.06
			GFRP	29.86	1.67	1.58	0.94	1.38	0.82	1.61	0.96	1.67	1.00
			CFRP	33.16	1.51	1.18	0.78	1.23	0.82	1.49	0.99	1.60	1.06
		3-1-3	Steel										
			GFRP										
			CFRP										
		3-4-3	Steel	31.13	1.61	1.22	0.76	1.47	0.92	1.56	0.97	1.70	1.06
			GFRP	28.74	1.74	1.64	0.94	1.53	0.88	1.68	0.97	1.74	1.00
			CFRP	31.21	1.60	1.21	0.76	1.47	0.92	1.56	0.97	1.70	1.06
		4-1-4	Steel	81.01	0.62	0.43	0.70	0.59	0.96	0.47	0.76	0.63	1.02
			GFRP	76.62	0.65	0.48	0.74	0.61	0.93	0.48	0.74	0.64	0.98
			CFRP	81.10	0.62	0.43	0.70	0.59	0.96	0.47	0.76	0.63	1.02
		4-4-4	Steel	29.83	1.68	1.25	0.75	1.61	0.96	1.62	0.97	1.79	1.07
			GFRP	27.72	1.80	1.70	0.94	1.64	0.91	1.74	0.96	1.80	1.00
			CFRP	29.90	1.67	1.24	0.74	1.61	0.96	1.62	0.97	1.79	1.07
		6-1-6	Steel	66.90	0.75	0.53	0.71	0.74	0.99	0.60	0.80	0.76	1.02
			GFRP	65.01	0.77	0.60	0.78	0.75	0.98	0.61	0.79	0.77	1.00
			CFRP	66.92	0.75	0.53	0.71	0.74	0.99	0.60	0.80	0.76	1.02
		6-4-6	Steel	27.67	1.81	1.32	0.73	1.80	1.00	1.75	0.97	1.93	1.07
			GFRP	25.89	1.93	1.82	0.94	1.82	0.94	1.87	0.97	1.94	1.00
			CFRP	27.75	1.80	1.30	0.72	1.80	1.00	1.75	0.97	1.93	1.07
J	4 ft.	2-4-2	Steel	29.80	1.68	1.59	0.95	1.54	0.92	1.61	0.96	1.68	1.00
			GFRP	29.60	1.69	1.62	0.96	1.60	0.95	1.62	0.96	1.69	1.00
			CFRP	29.81	1.68	1.58	0.94	1.54	0.92	1.61	0.96	1.68	1.00
		3-1-3	Steel										
			GFRP										
			CFRP										
		3-4-3	Steel	28.71	1.74	1.65	0.95	1.67	0.96	1.68	0.96	1.75	1.00
			GFRP	28.52	1.75	1.69	0.96	1.69	0.96	1.68	0.96	1.75	1.00
			CFRP	28.73	1.74	1.65	0.95	1.67	0.96	1.68	0.97	1.75	1.01
		4-1-4	Steel	77.75	0.64	0.48	0.75	0.63	0.98	0.48	0.75	0.64	1.00
			GFRP	77.56	0.64	0.48	0.74	0.63	0.98	0.48	0.74	0.64	0.99
			CFRP	77.75	0.64	0.48	0.75	0.63	0.98	0.48	0.75	0.64	1.00
		4-4-4	Steel	27.69	1.81	1.71	0.95	1.76	0.97	1.74	0.96	1.81	1.00
			GFRP	27.52	1.82	1.75	0.96	1.77	0.97	1.75	0.96	1.81	1.00
			CFRP	27.70	1.81	1.71	0.95	1.76	0.98	1.74	0.96	1.81	1.00
		6-1-6	Steel	64.90	0.77	0.60	0.78	0.76	0.99	0.61	0.79	0.77	1.00
			GFRP	64.79	0.77	0.61	0.79	0.76	0.98	0.61	0.79	0.77	1.00
			CFRP	64.91	0.77	0.60	0.78	0.76	0.99	0.61	0.79	0.77	1.00
		6-4-6	Steel	25.83	1.94	1.83	0.95	1.90	0.98	1.87	0.97	1.94	1.00
			GFRP	25.72	1.94	1.87	0.96	1.91	0.98	1.87	0.96	1.94	1.00
			CFRP	25.84	1.93	1.83	0.95	1.90	0.98	1.87	0.97	1.94	1.00

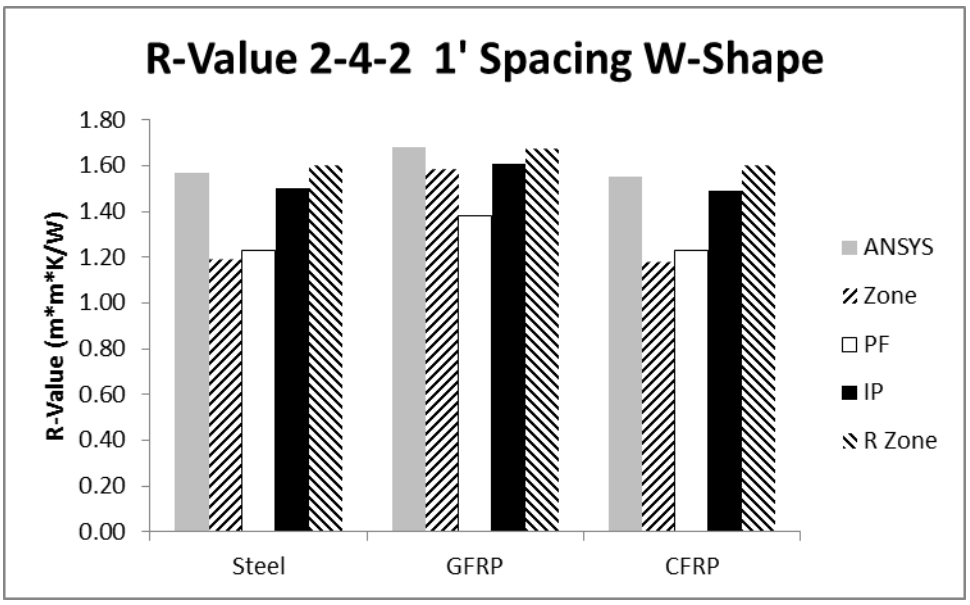

Figure 5-40: Parametric Study

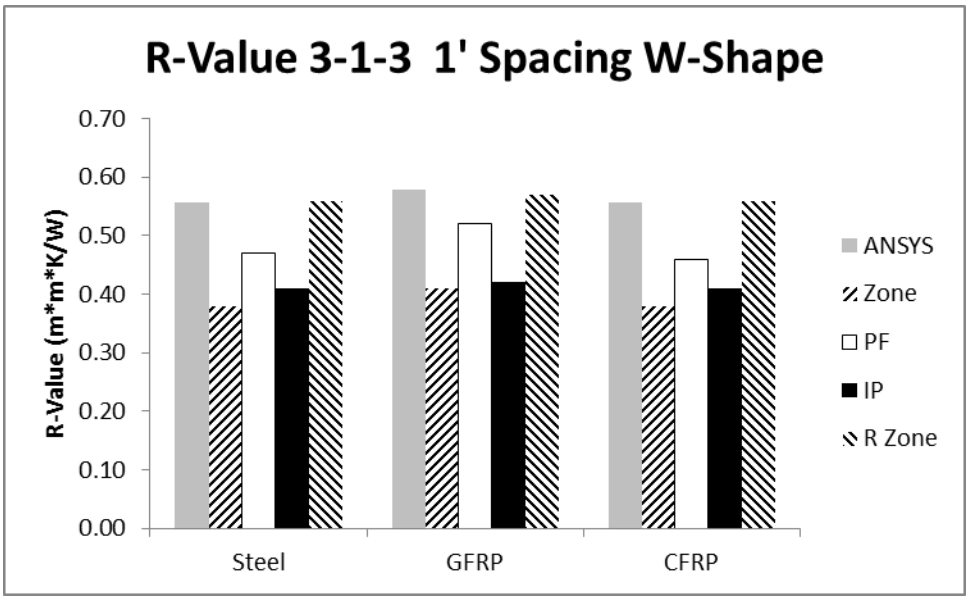

Figure 5-41: Parametric Study

a)

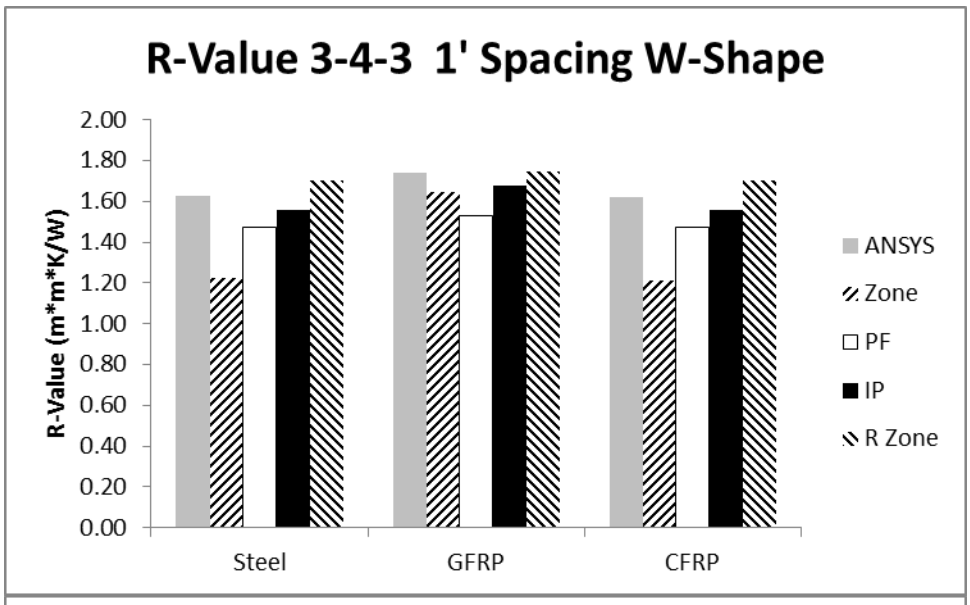

b)

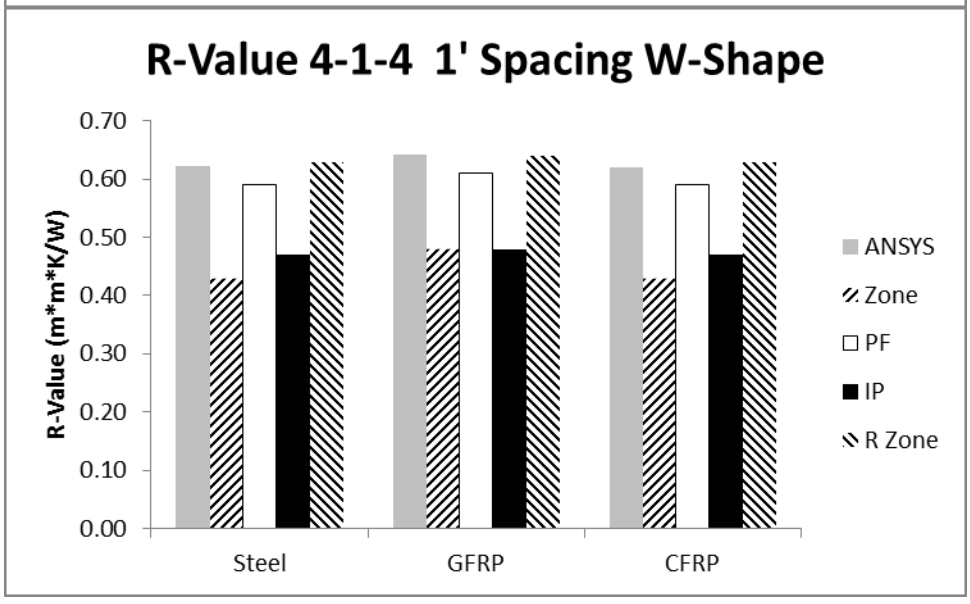

Figure 5-42: Parametric Study

a)

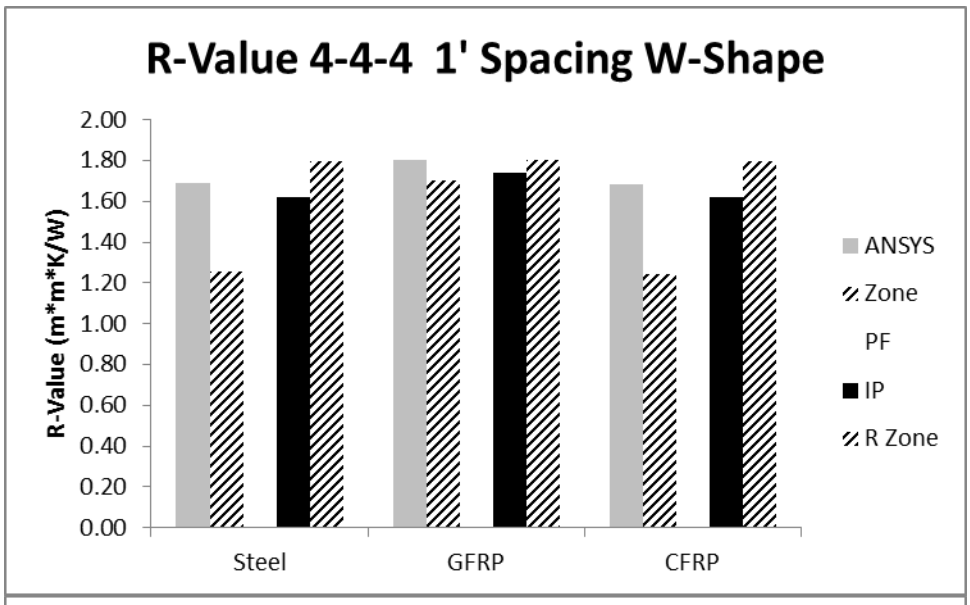

b)

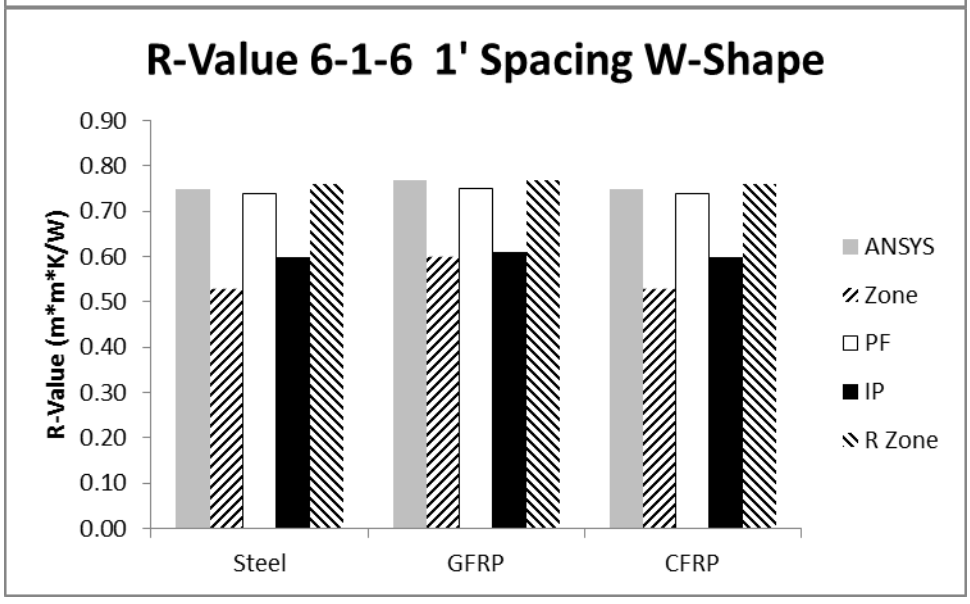

Figure 5-53: Parametric Study

a)

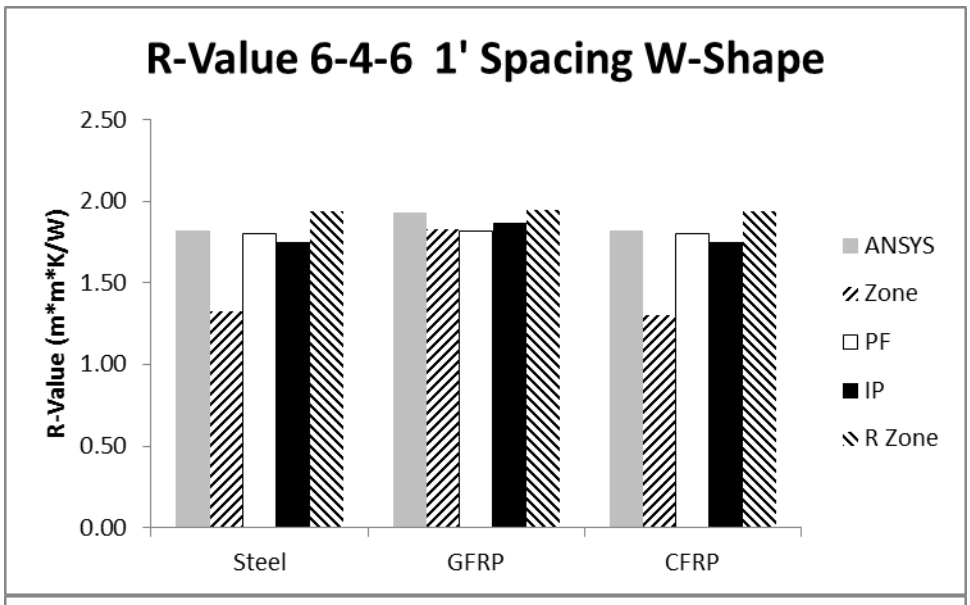

b)

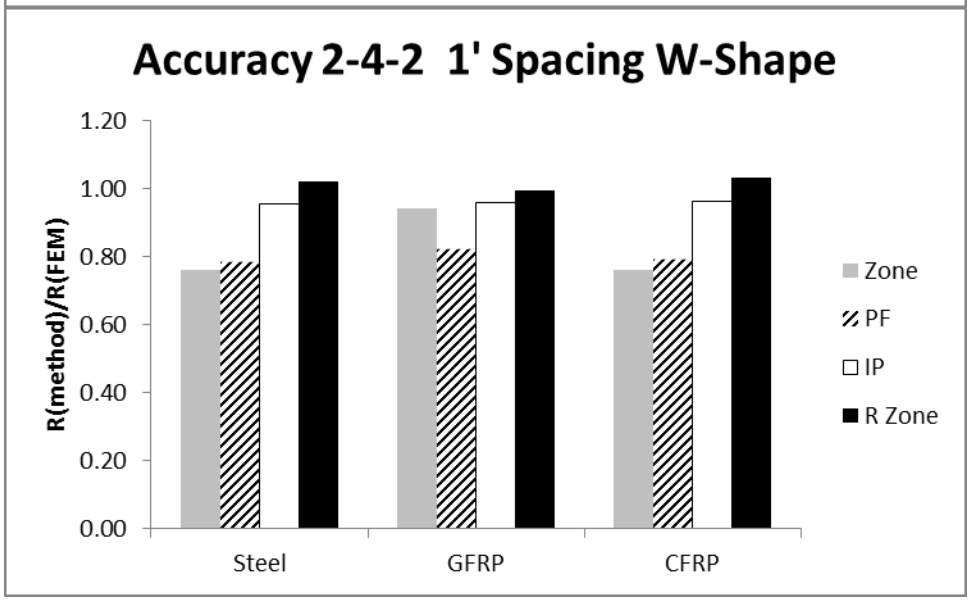

Figure 5-54: Parametric Study

a)

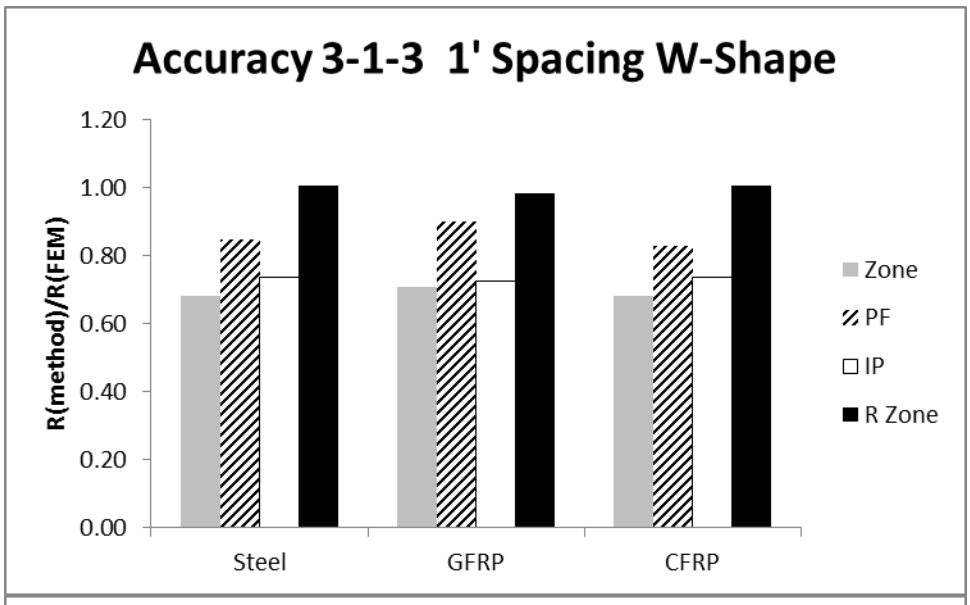

b)

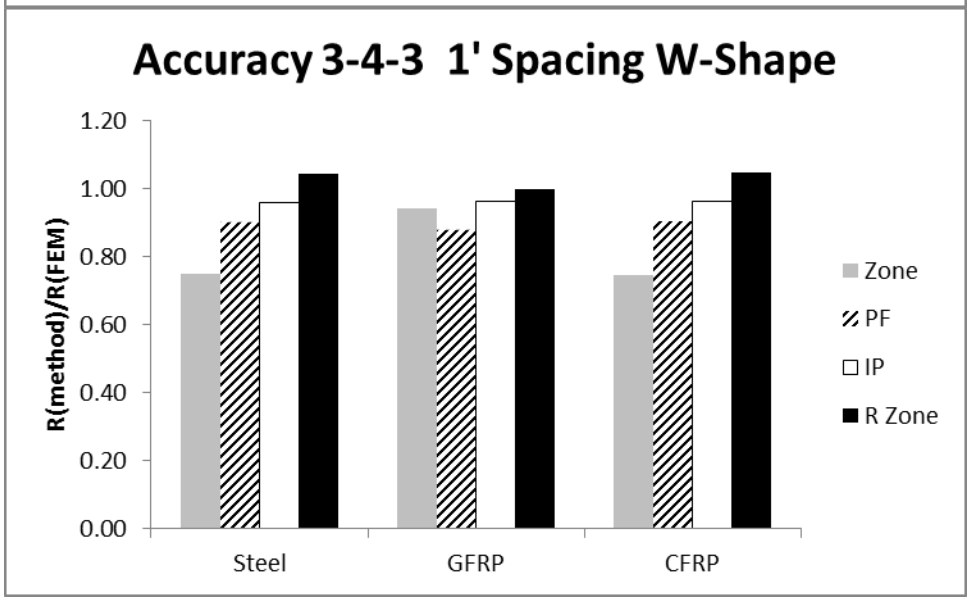

Figure 5-55: Parametric Study

a)

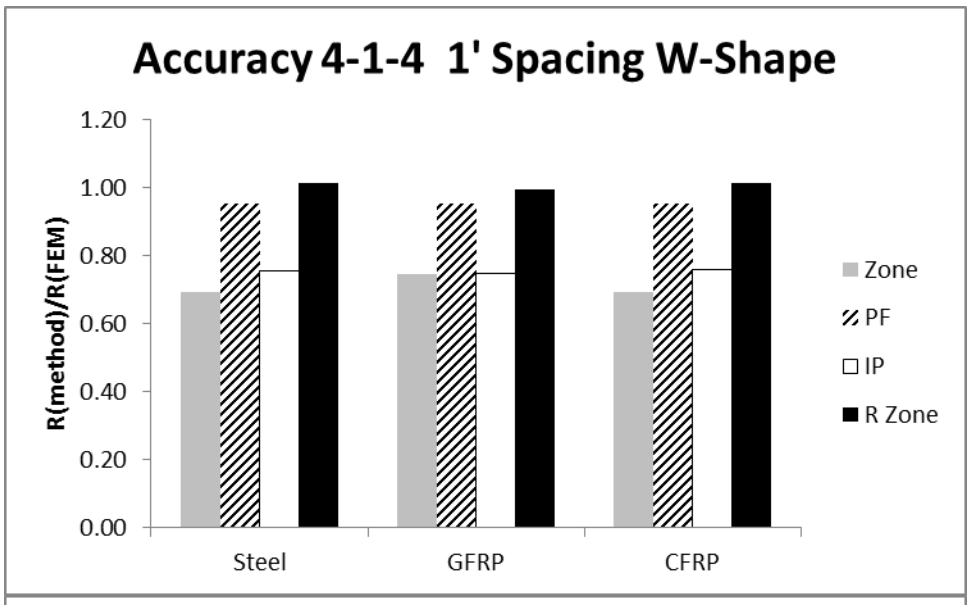

b)

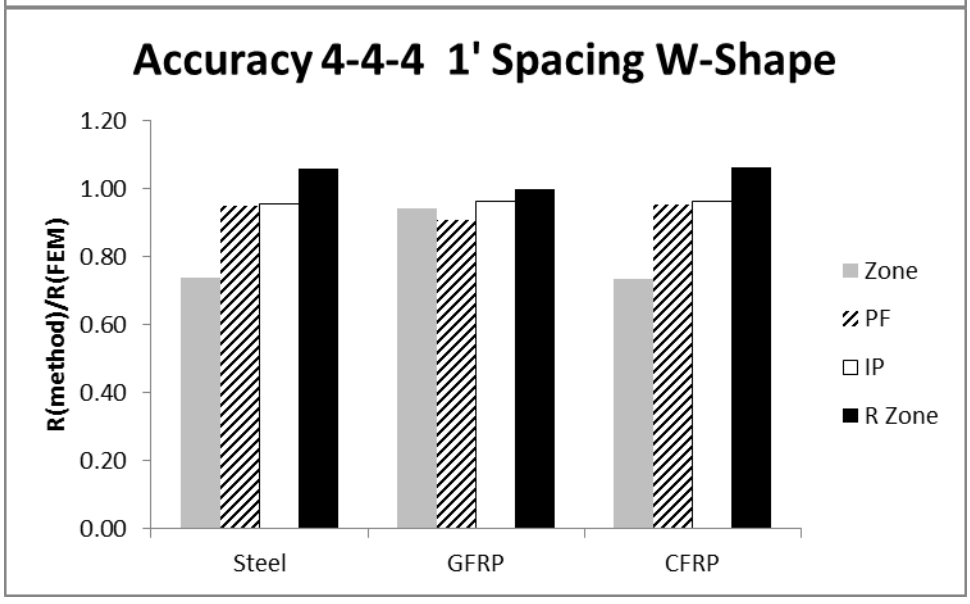

Figure 5-56: Parametric Study

a)

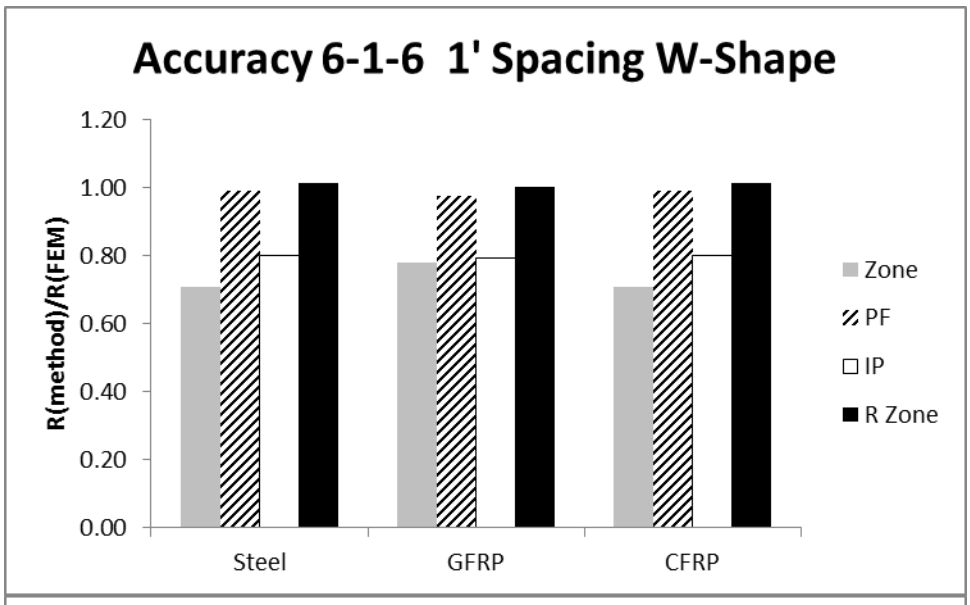

b)

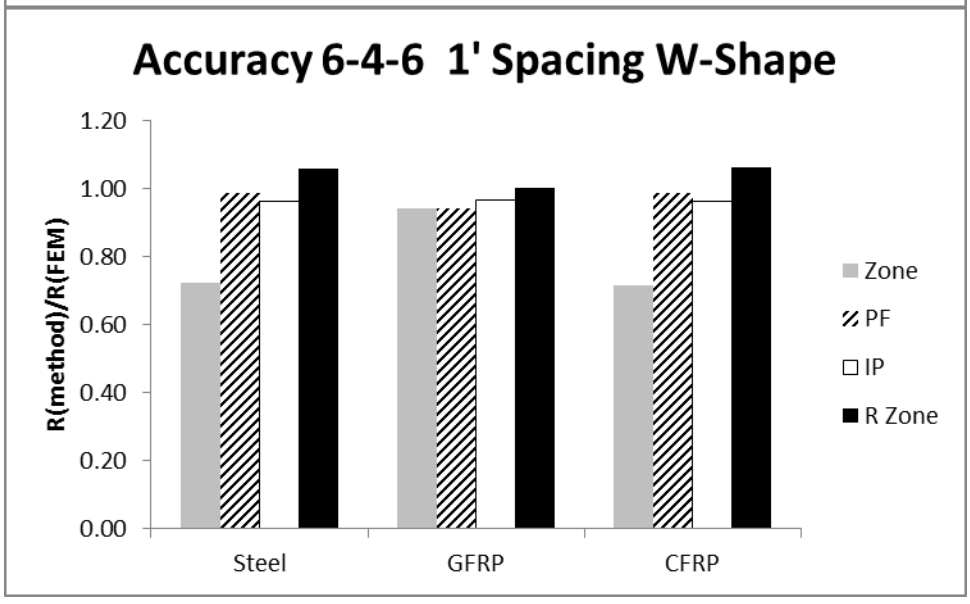

Figure 5-57: Parametric Study

a)

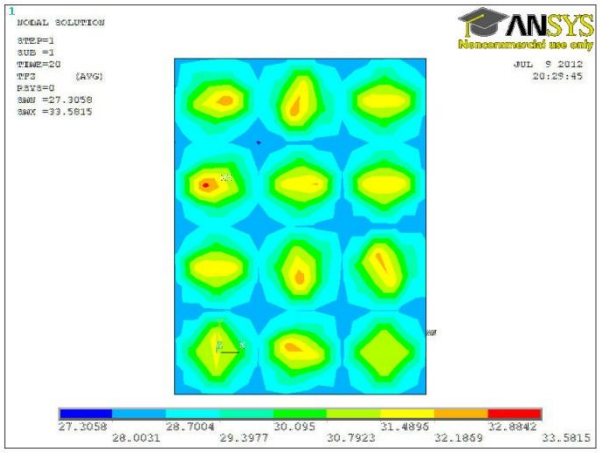

b)

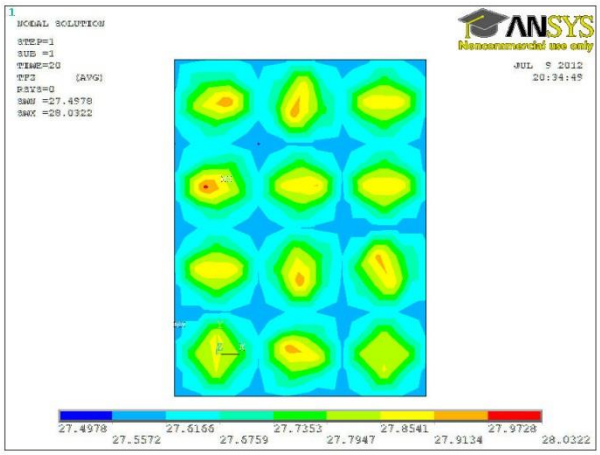

c)

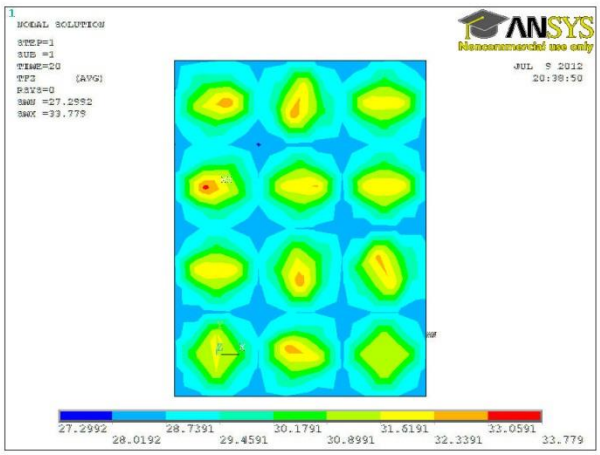

Figure 5-58: Large Scale Model; a: Steel, b: GFRP, c: CFRP

CHAPTER 6. SUMMARY AND CONCLUSION

6.1. Summary

The thermal performance of a sandwich wall panel was examined. Sandwich panels are designed to be structurally and thermally efficient. Conventional sandwich wall panels use steel to connect two wythes of concrete and a layer of insulation. The steel connectors penetrate through the insulation layer. This causes heat to be transferred through the steel as opposed to being resisted by the insulation. This creates a thermal bridge, and can degrade the thermal efficiency of the sandwich panel. GFRP, unlike steel, has a low thermal conductivity value. This makes GFRP an ideal material to be used in a sandwich wall panel when thermal performance is a key issue, such as cold region applications.

A small scale sandwich wall panel was constructed using three different types of steel connectors, a GFRP dowel, CFRP bar, and CFRP strip. The size of the panel included a 9 in. x 9 in. cross sectional area. A 3-1.5-3 sandwich panel was used for the experiments. The variation of temperature with time was recorded through the center of the panel. This data was used to compare with data obtained from a finite element software package.

The finite element software was also used to compare the heat flux value with numerical methods that are used to find the R-value of a sandwich panel. These numerical methods are found in the American Society of Heating, Refrigeration, and Air-Conditioning Engineers handbook. The methods that are

commonly used to estimate the R-value for a designed sandwich wall panel include the Zone, Parallel Flow, and Isothermal Planes Methods.

With the knowledge gained from the experiment, finite element analysis program, and the numerical modeling, a parametric study was conducted using the ANSYS finite element computer software to determine the thermal performance of a GFRP sandwich wall panel.

6.2. Conclusions

The following conclusions were made from the experimental analysis and the finite element analysis that accompanied the results:

1) GFRP is an ideal material for a sandwich wall panel because of its low thermal conductivity and an advantageous specific heat and density.
2) The experiment/computational analysis found that GFRP can adequately be used to prevent thermal bridging. Computational panels constructed with GFRP instead of steel or CFRP kept the inside of a sandwich panel warmer.
3) Sandwich wall panels constructed with GFRP connectors show a sharper decrease in temperature on the side of the insulation that is closer to the applied cold temperature than the samples constructed with CFRP or steel.
4) According to the predicted results, the sandwich wall panels with GFRP ties showed more resistance against the heat transfer through the

insulation than the steel or CFRP ties. These panels remained warmer on the side of the insulation that was farther away from applied cold air.

5) When the finite element analysis model was compared to the experimental data, the comparison varied by less than 4 degrees Celsius for a majority of the geometry types.

6) The computer program can adequately determine the change of temperature with time on the connectors of a sandwich wall panel with various geometries and material properties.

The following conclusions were made from the analytical analysis and the finite element analysis that accompanied the results:

1) The Zone Method, Parallel Flow Method, and Isothermal Planes method did a reasonable job at predicting the R-value of the sandwich wall panels. The ratio of the resistances stayed within the range of 0.9 to 1.1 for a majority of the sample analyzed.

2) The single connector glass fiber reinforced polymer connector panels were the most accurately predicted model, because GFRP has a low thermal conductivity and the spacing is close to the values that the equations were designed for. The low thermal conductivity gives the panel a resistance that is close to the value of a panel without connectors. The ratio of the R-values stayed close to one for five (W-shaped, J-shaped, Z-shaped, Bar, Strip) geometries. These findings were consistent for the three methods.

3) The prediction of the four GFRP connector sandwich panels was the most inaccurate compared with that of other panels. The Zone and Isothermal Planes Methods had comparison ratios of less than 0.85. The Parallel Flow Method was slightly better with almost an R_{Method}/R_{FEM} ratio of 0.9. The three methods overestimated the R-value for the panels with four GFRP connectors. This inaccuracy could be the result of using 4.5 in spacing for the calculations.
4) The remaining connectors underestimated the R-values and had ratios that were within the 1.05 to 1.1 range.
5) The Isothermal Planes was the most accurate of the three methods. The comparison ratios were off by an average of 0.09. The ratios of the Zone and Parallel Path Methods were off by an average of 0.12 and 0.1, respectively.

The following conclusions were made from the parametric study using the finite element software:

1) GFRP provides better thermal performance for panels that are spaced closely and have a thicker layer of insulation.
2) For the diameter of the connector used, if the spacing is greater than 3 ft., then steel would provide an efficient design. If the insulation thickness is 1 in., then steel would also be acceptable. In these situations, GFRP provides more resistance to heat transfer, but the difference may not be great enough to warrant a change from steel.

3) Increasing the insulation from 1 in. to 4 in. nearly tripled the resistance of the sandwich panel for the various concrete sizes and material properties used in the analysis.
4) Increasing the connector spacing from 1 ft. to 2 ft. decreased the difference between the R-values of the GFRP, CFRP, and steel connector sandwich panels.
5) The Revised Zone method is the most accurate current method that can be used to design sandwich wall panels. The average amount that the ratio of the R-values was off by was 0.01. The parallel flow method had the next best accuracy and was off by 0.06. The Zone and Isothermal Planes Methods were off by 0.17 and 0.12.

6.3. Recommendations

The following contains recommendations for future work that can be done related to this research.

1) Use GFRP and CFRP connectors that will or have been used in field application during the experiments.
2) Conduct a Guarded Hot Box experiment using the GFRP, CFRP, and steel connector sandwich panels with various geometries to determine the heat flux or R-value. This will ensure accuracy in the finite element software.
3) Conduct a more comprehensive parametric study to ensure the revised zone method can be used for GFRP sandwich wall panel design with a variety of geometries and panel configurations.

REFERENCES

Ashby, M. F. 2009. Materials and the Environment: Eco-Informed Material Choice. Elseveir Inc.

ASHRAE Committee. 2001. ASHRAE Handbook: Fundamentals. American Society of Heating, Refrigerating and Air-Conditioning Engineers, Inc.

Chen, B., Salmon, D., Hancock, E., and Detloff, H. Measurement of Energy Efficiency of Building Envelopes. Passive Solar Research Group.

Chowdhury, E. U., Green, M. F., Bisby, L. A., Benichou, N., and Kodur, V. K. R. 2007. Thermal and Mechanical Characterizations of Fibre Reinforced Polymers, Concrete, Steel, and Insulation Materials for Use in Numerical Fire Endurance Modeling. National Research Council. (August).

Designer's Notebook. High Performance Precast Insulated Sandwich Wall Panels. *Designer's Notebook*. pp. 52-64.

Desjarlais, A. O., and McGowan, A. G. 1997. Comparison of Experimental and Analytical Methods to Evaluate Thermal Bridges in Wall Systems. *Insulation Materials: Testing and Applications*. (May).

Einea, A. E., Salmon, D. C., Tadros, M. K., and Culp, T. 1994. A New Structurally and Thermally Efficient Precast Sandwich Panel System. *PCI Journal.* (July-August): pp. 90-101.

Frankl, B. A., Lucier, G. W., Hassan, T. K., and Rizkalla, S. H., 2011. Behavior of Precast, Prestressed Concrete Sandwich Wall Panels Reinforced with GFRP Shear Grid. *PCI Journal*, (Spring); pp. 42-54.

Guy, A. G., and Nixon, J. A., 1987. A Detailed Verification Procedure for a Guarded Hot Box. *Thermal Insulation: Materials and Systems*. pp. 297-309.

Holmes, W. W., Kusolthamarat, D., and Tadros, M. K. 2005. NU Precast Concrete House Provides Spacious and Energy Efficient Solution for Residential Construction. *PCI Journal*. (May-June): pp. 16-25.

Incropera, F. P., Dewitt, D. P., Bergman, T. L., and Lavine, A. S. 2006. Fundamentals of Heat and Mass Transfer. *John Wiley & Sons*. 6th ed.

Lee, B. J., and Pessiki, S. 2008. Revised Zone Method R-value Calculation for Precast Concrete Sandwich Panels Containing Metal Wythe Connectors. *PCI Journal*. (September-October): pp. 86-100.

Lee, B. J., and Pessiki, S., 2006. Thermal Performance Evaluation of Precast Concrete Three-Wythe Sandwich Wall Panels. *Energy and Buildings*. pp. 1006-1014.

Maximos, H. N., Pong, W. A., and Tadros, M. K. 2007. Behavior and Design of Composite Precast Prestressed Concrete Sandwich Panels with NU-Tie. *University of Nebraska Lincoln*. (March).

Morcous, G., Tadros, M. K., Lafferty, M., and Gremel, D. 2010. Optimized NU Sandwich Panel System for Energy, Composite Action and Production Efficiency. *3rd fib International Congress*.

Naito, C., Beacraft, M., Hoeman, J. M., and Bewick, B. T., Performance and Characterization of Shear Ties for Use in Insulated Precast Concrete Sandwich Wall Panels. *Air Force Research Laboratory*. (November).

Pardini, L. C., and Gregori, M. L. 2010. Modeling Elastic and Thermal Properties of 2.5D Carbon Fiber and Carbon/SiC Hybrid Matrix Composites by Homogenization Method. *Journal of Aerospace Technology Management*. (May-August): pp. 183-194.

PCI Committee on Precast Sandwich Wall Panels. 1997. State-of-the-Art of Precast/Prestressed Sandwich Wall Panels. *PCI Journal*. (March-April): pp. 1-61.

PCI Committee on Precast Sandwich Wall Panels. 2011. State-of-the-Art of Precast/Prestressed Concrete Sandwich Wall Panels. *PCI Journal*. (Spring): pp. 131-176.

Salmon, D. C., Einea, A., Tadros, M. K., and Culp, T. D. 1997. Full Scale Testing of Precast Concrete Sandwich Panels. *ACI Structural Journal*. (July-August): pp. 354-362.

Shawkat, W., Honickman, H., and Fam, A. 2008. Investigation of a Novel Composite Cladding Wall Panel in Flexure. *Journal of Composite Materials*. (Vol. 42, No. 3): pp. 315-330.

Straube, J. 2007. Thermal Metrics for High Performance Enclosure Walls: The Limitations of R-Value. *Building Science Press*.

APPENDIX

a)

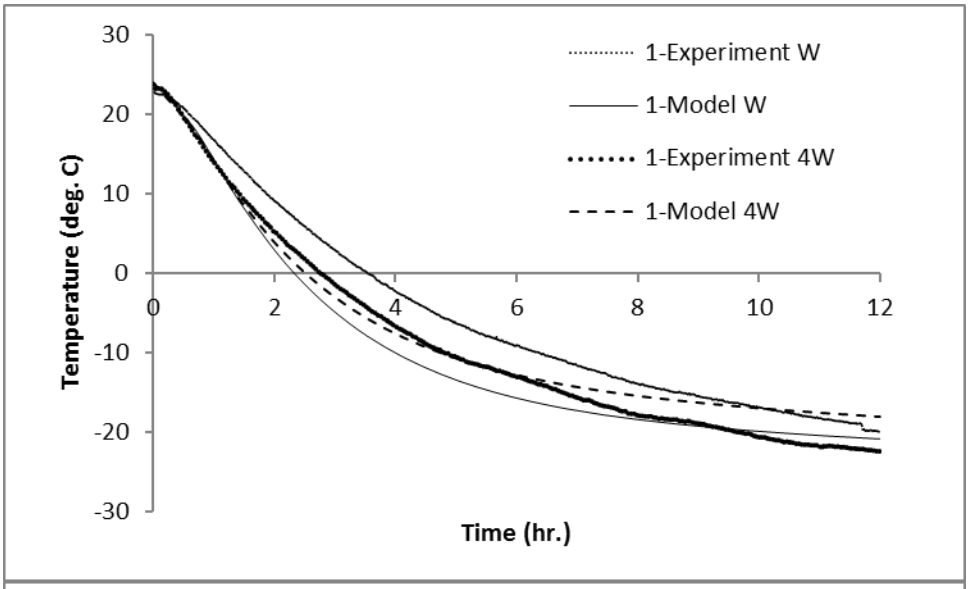

b)

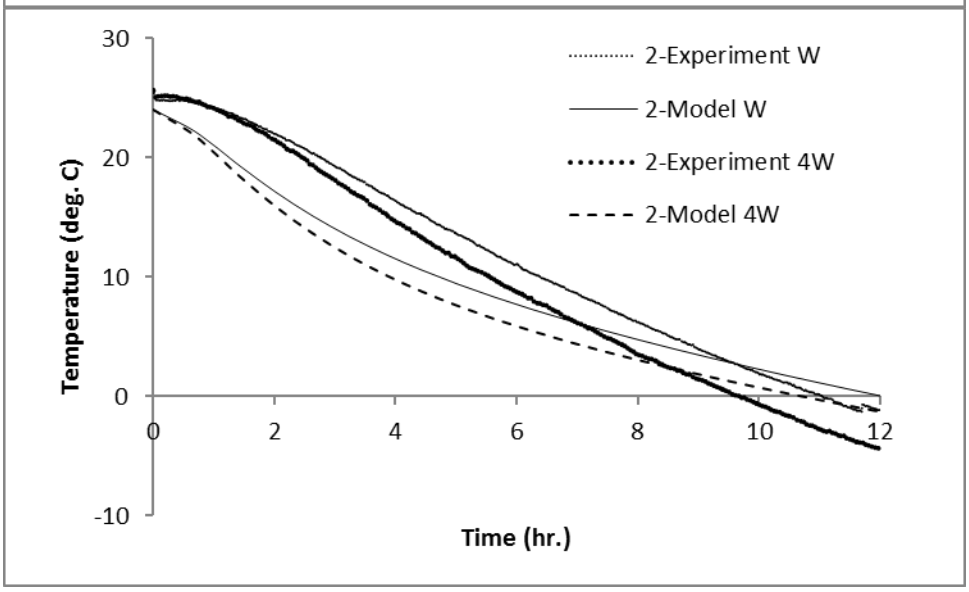

Figure A-1: W-Shaped Connector Comparison; a: Position One, b: Position Two

a)

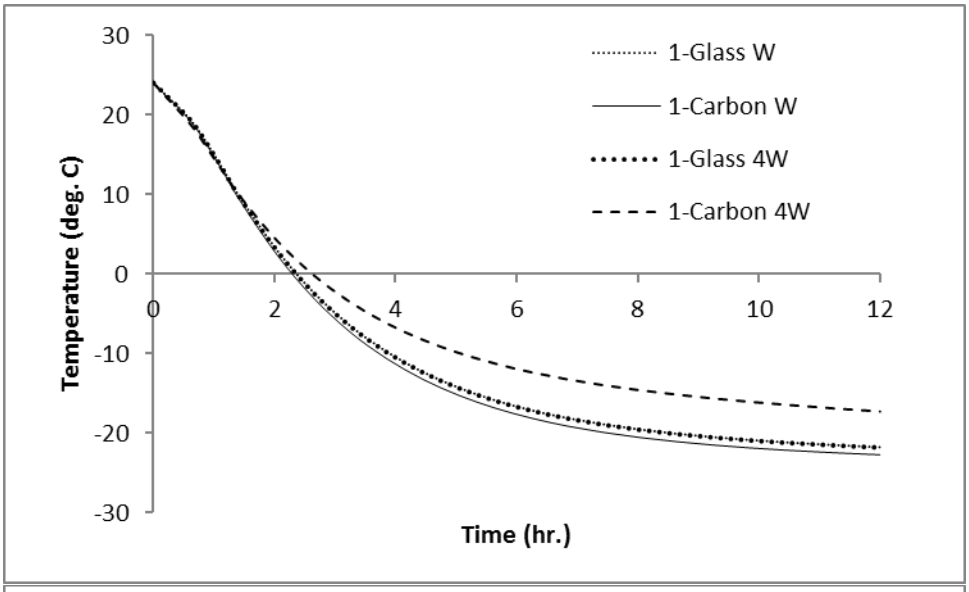

b)

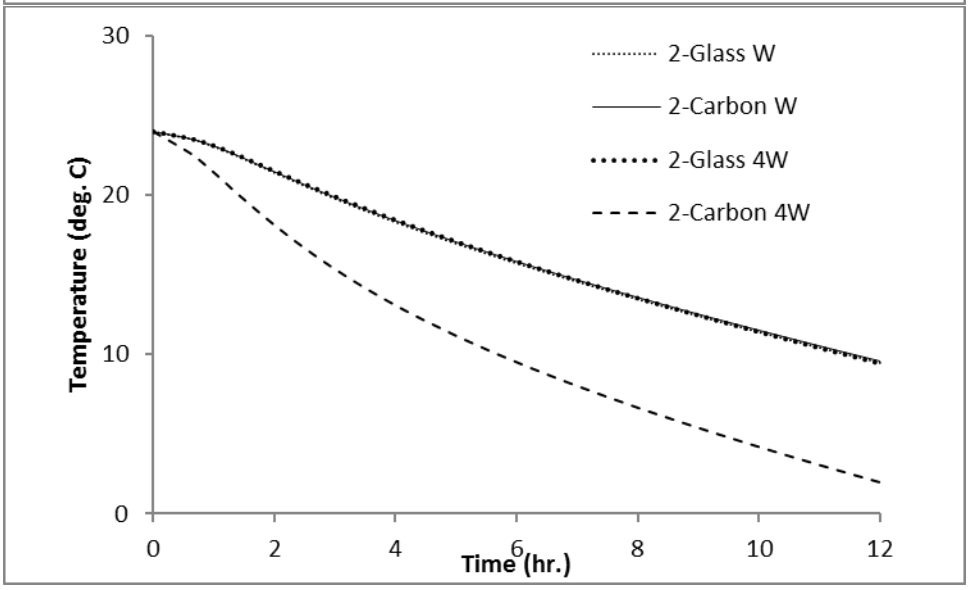

Figure A-2: W-Shaped Connector Comparison; a: Position One, b: Position Two

a)

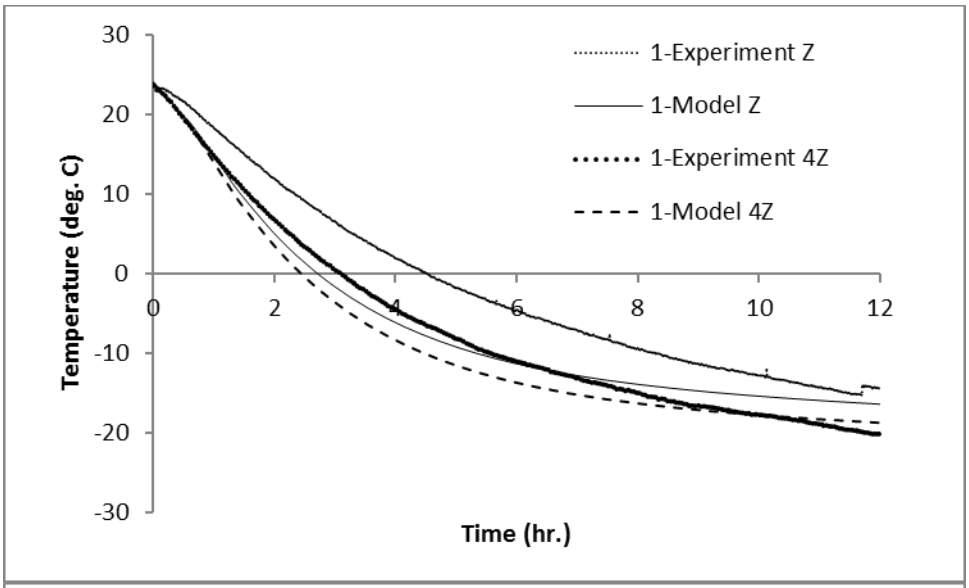

b)

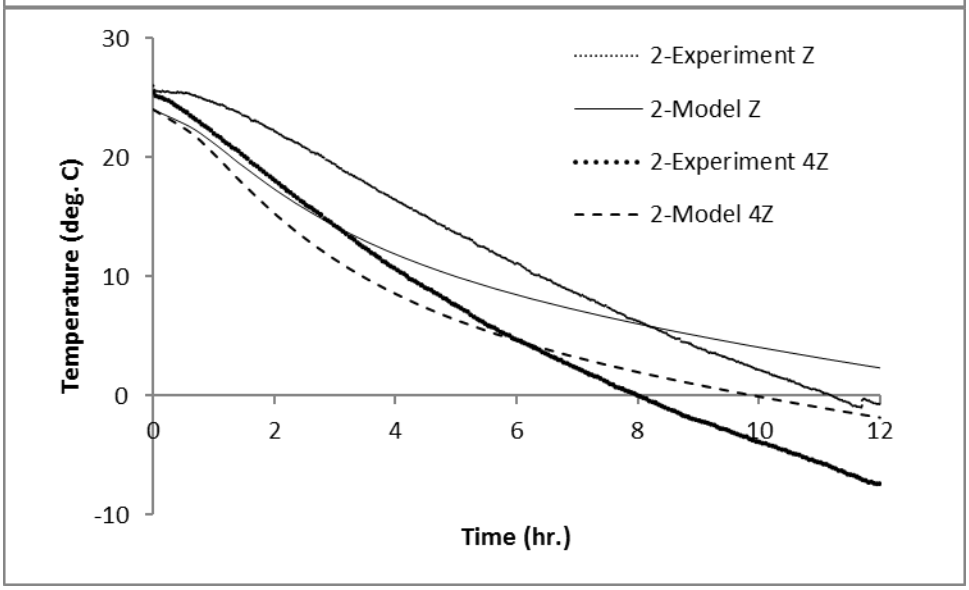

Figure A-3: Z-Shaped Connector Comparison; a: Position One, b: Position Two

a)

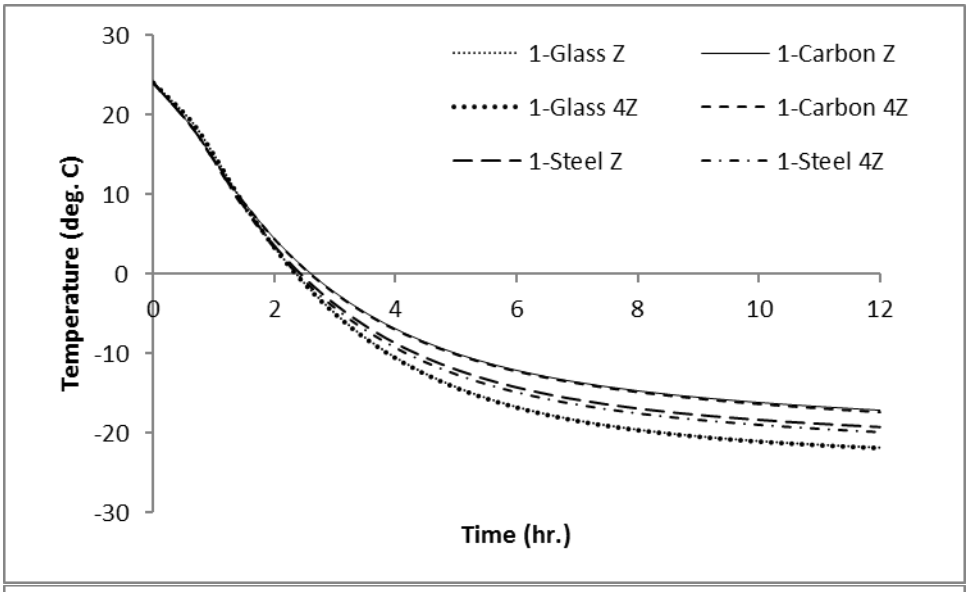

b)

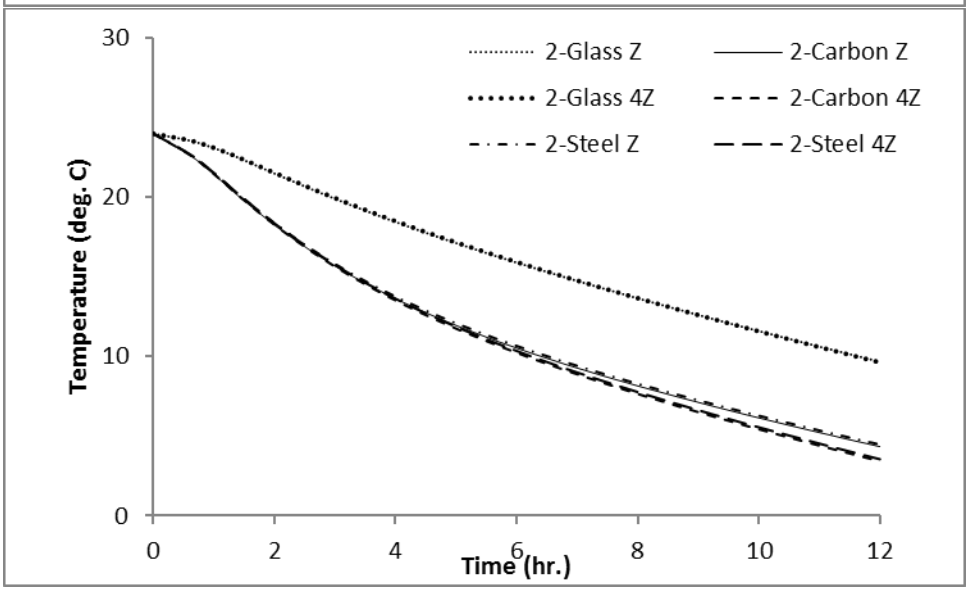

Figure A-4: Z-Shaped Connector Comparison; a: Position One, b: Position Two

a)

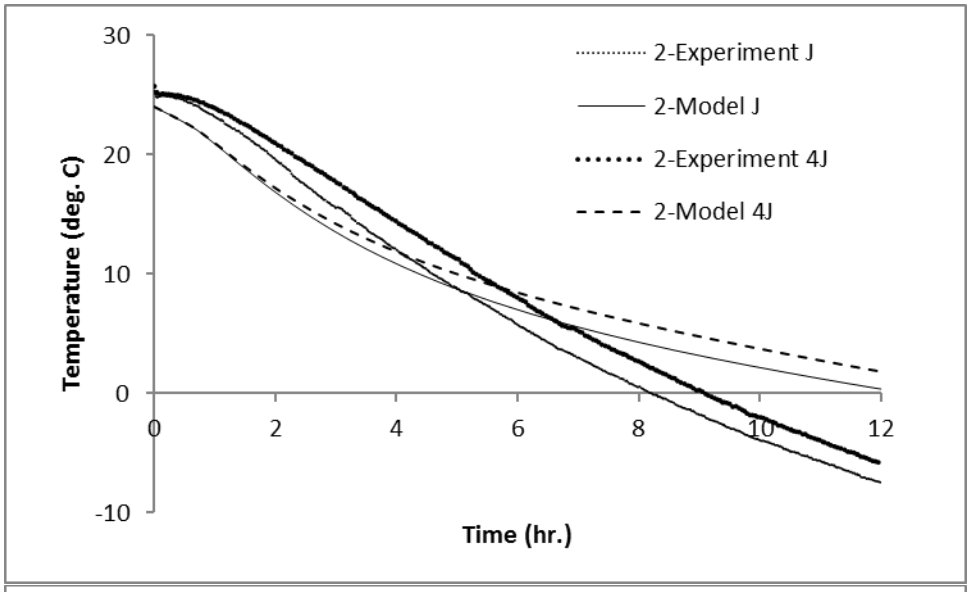

b)

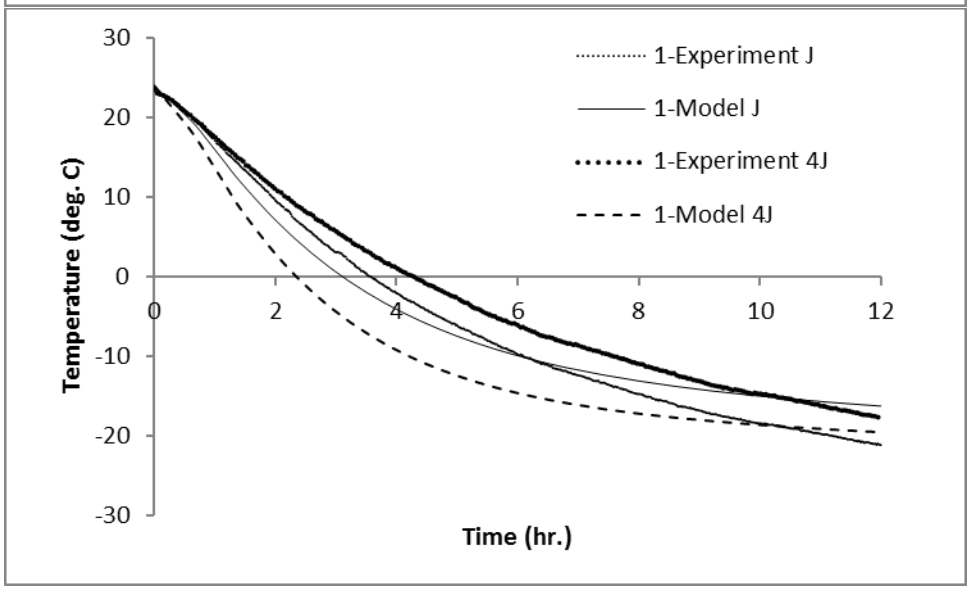

Figure A-5: J-Shaped Connector Comparison; a: Position One, b: Position Two

a)

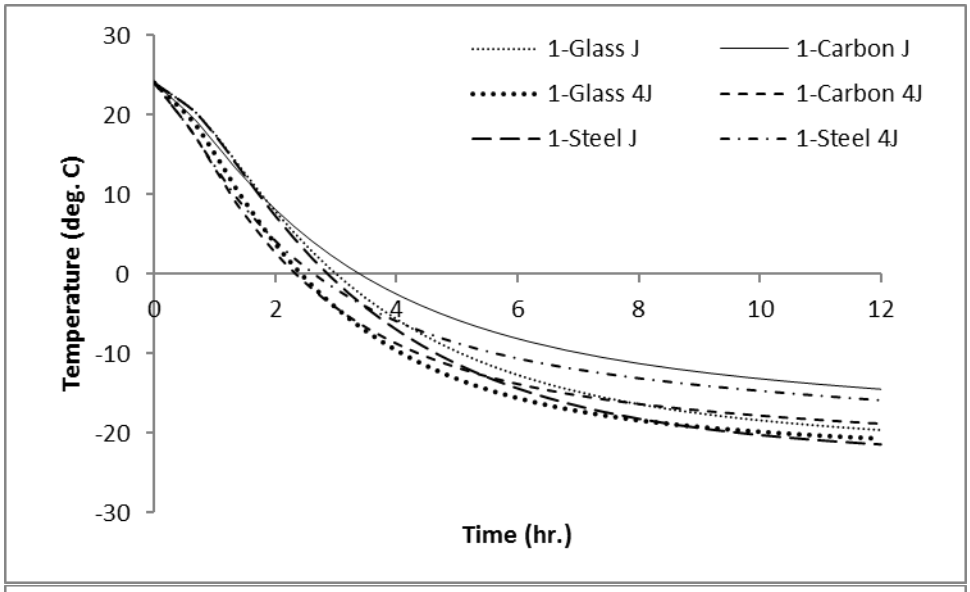

b)

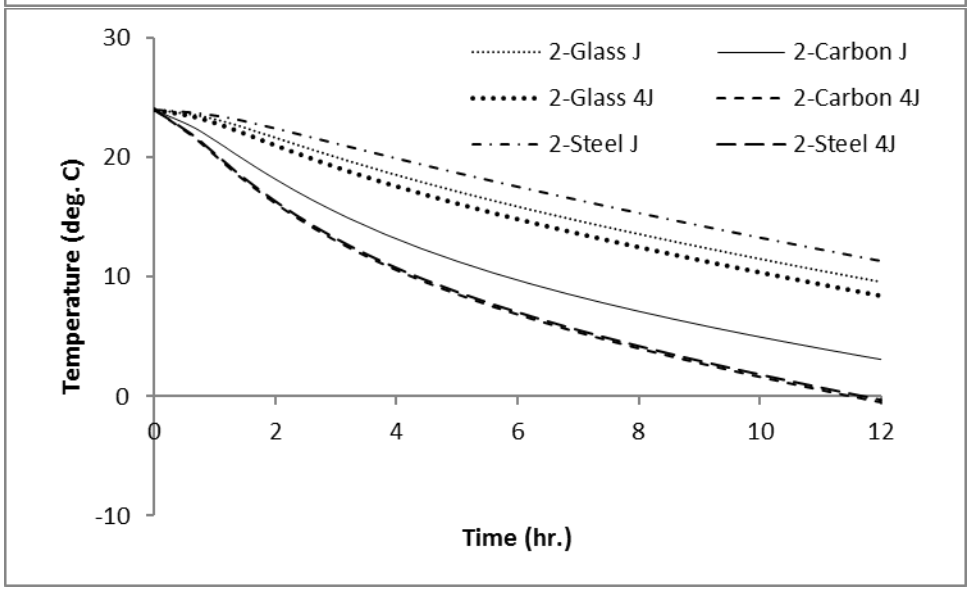

Figure A-6: J-Shaped Connector Comparison; a: Position One, b: Position Two

a)

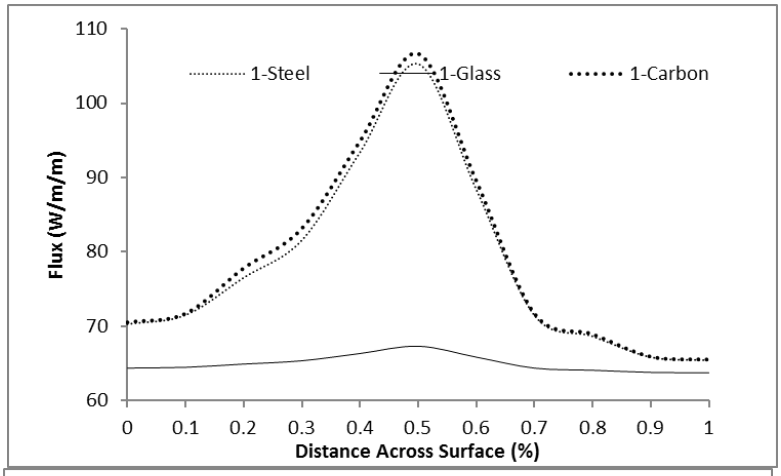

b)

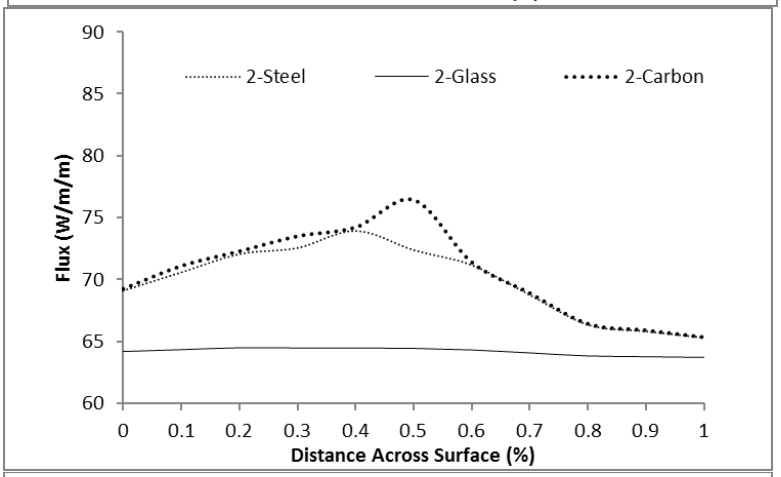

c)

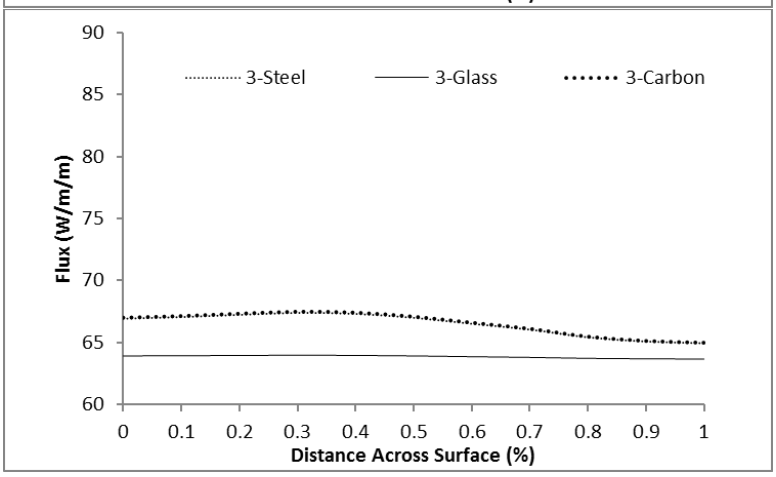

Figure A-7: One J-Shaped Connector Flux Comparison; a: Line 1, b: Line 2, c: Line 3

a)

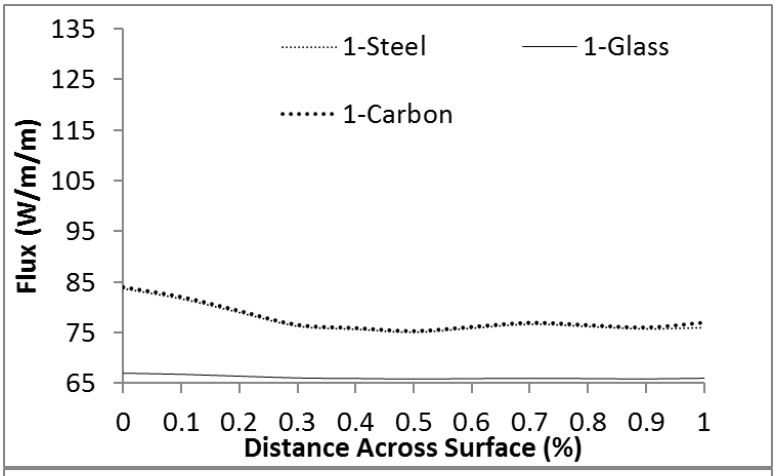

b)

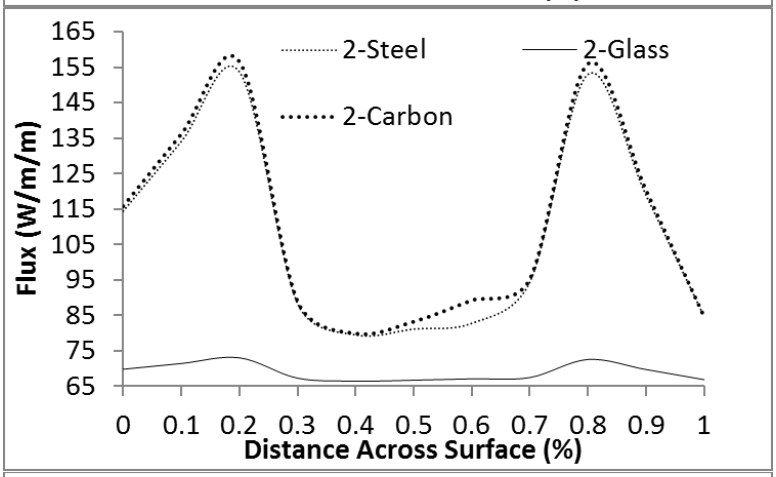

c)

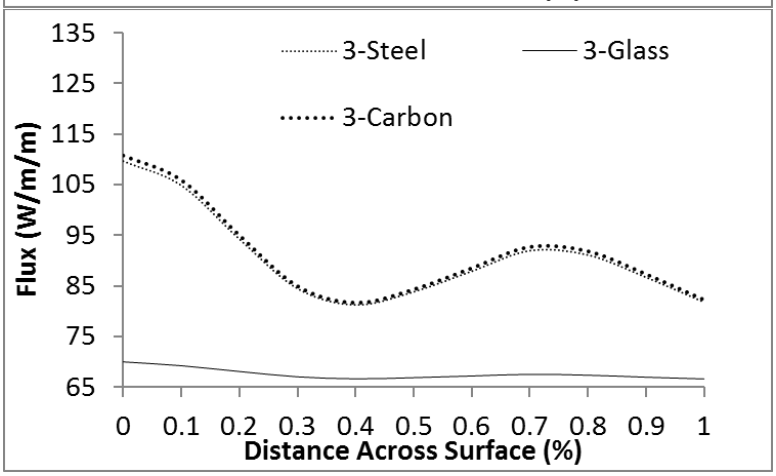

Figure A-8: Four J-Shaped Connector Flux Comparison; a: Line 1, b: Line 2, c: Line 3

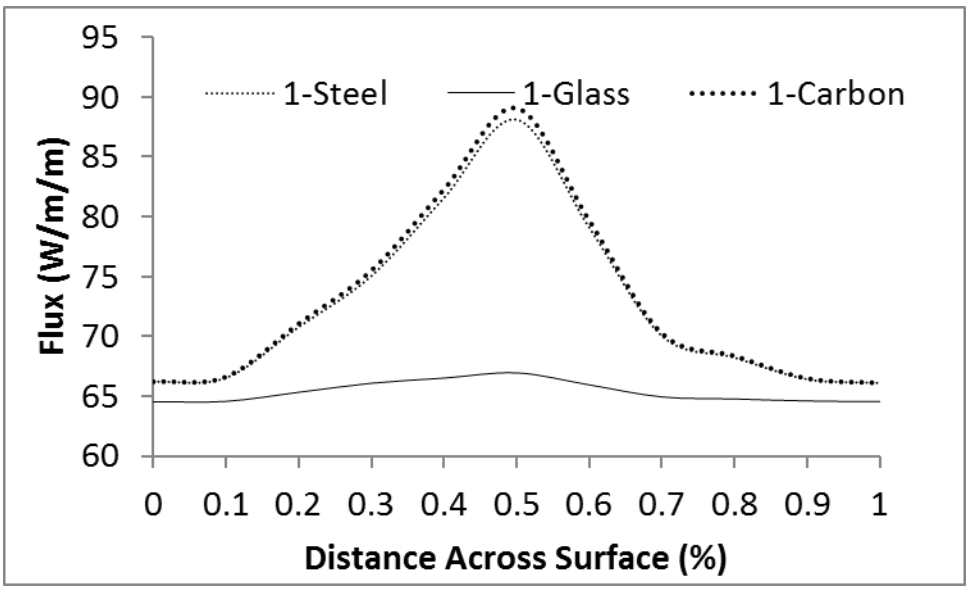

Figure A-9: One Z-Shaped Connector Flux Comparison

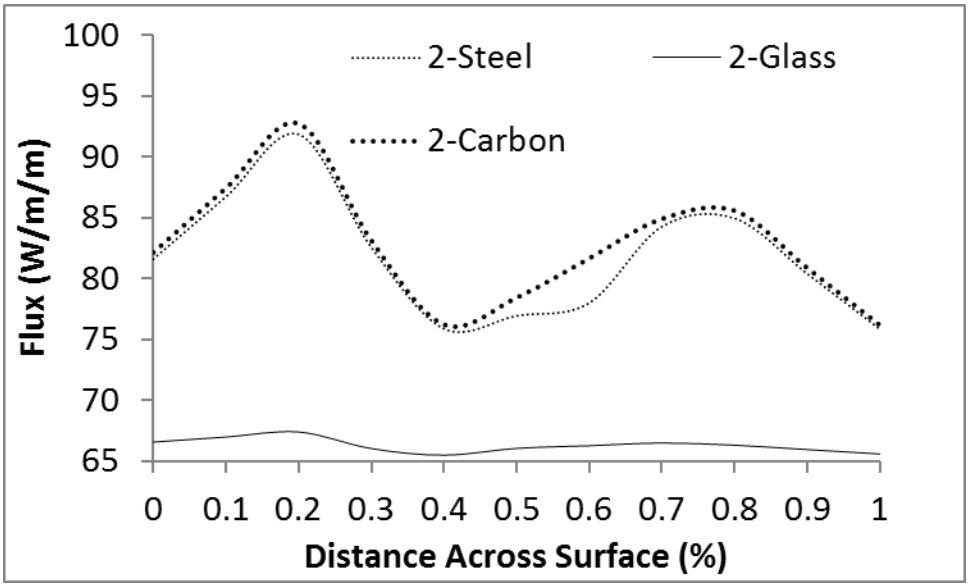

Figure A-10: Four Z-Shaped Connector Flux Comparison

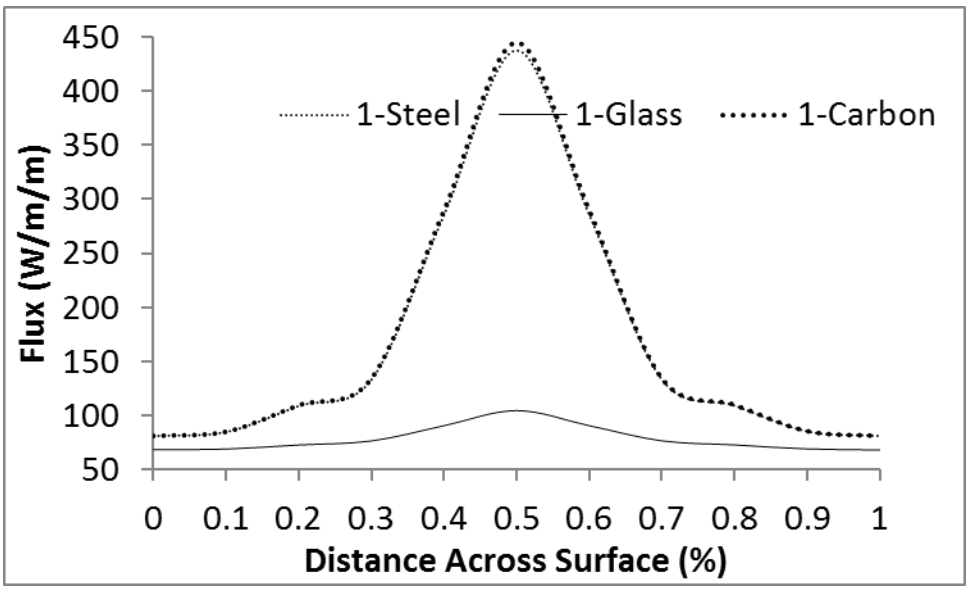

Figure A-11: Glass Dowel Connector Flux Comparison

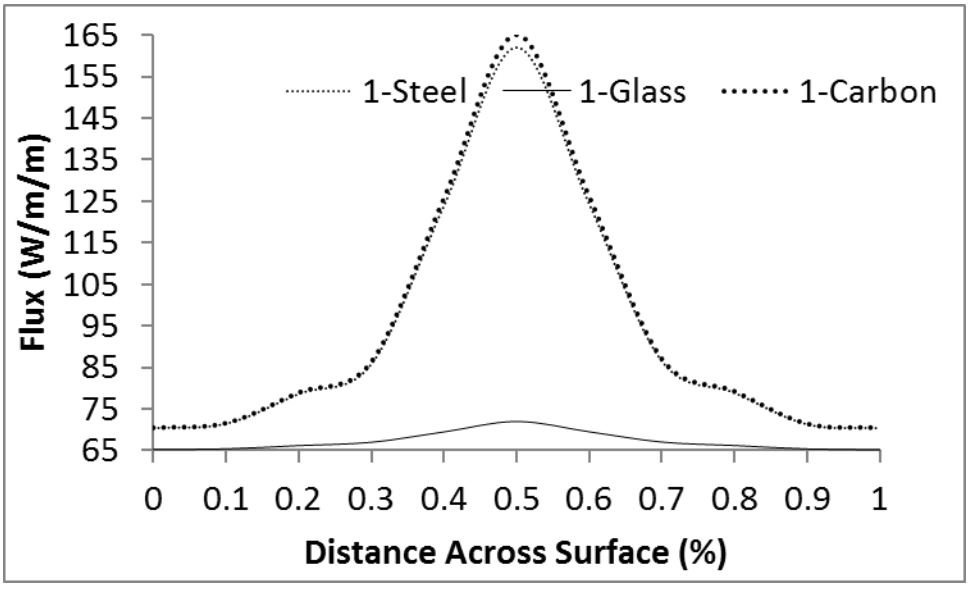

Figure A-12: Carbon Bar Connector Flux Comparison

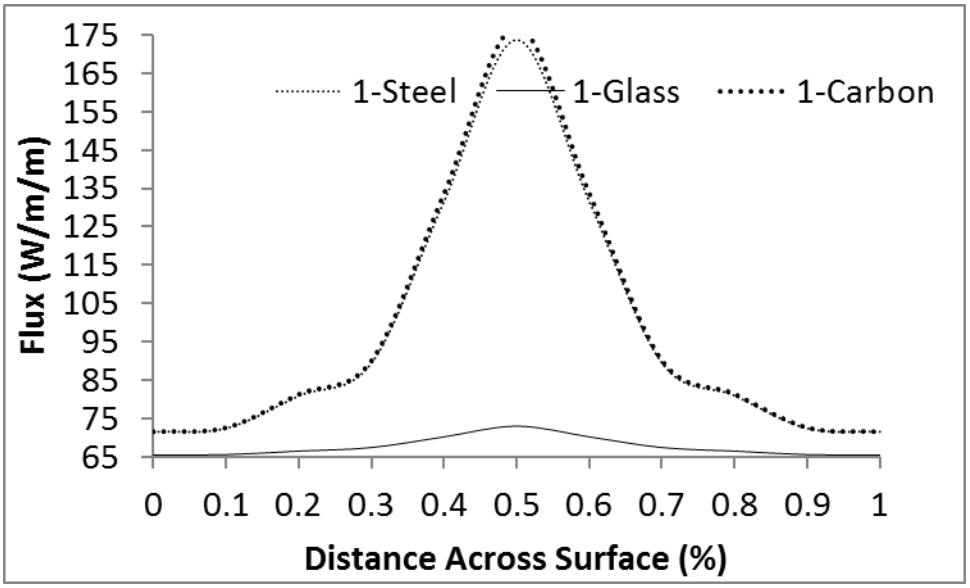

Figure A-13: Carbon Strip Connector Flux Comparison

a)

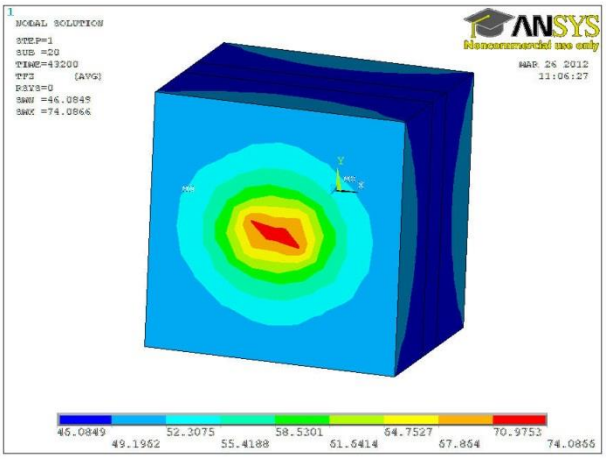

b)

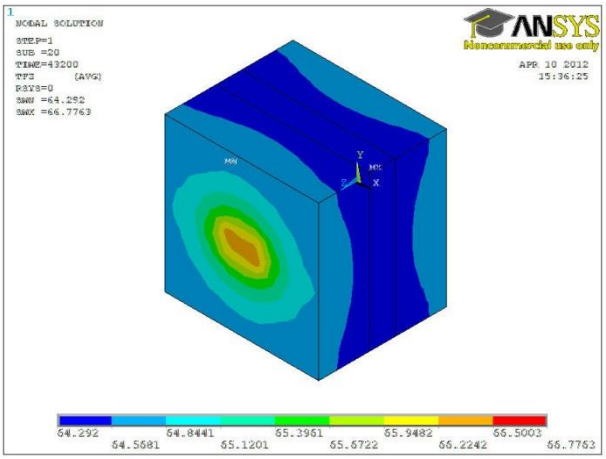

c)

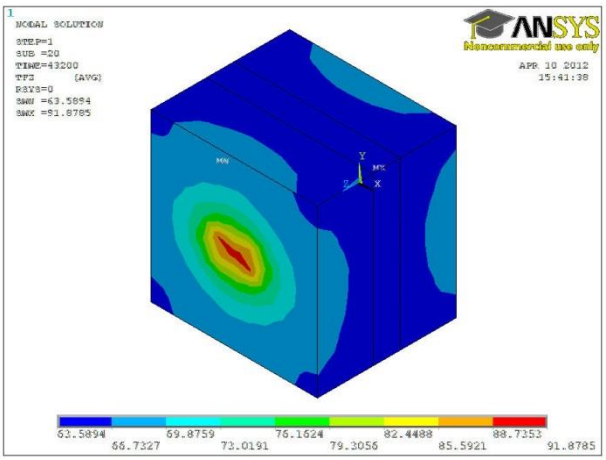

Figure A-14: One W Connector Flux; a: Steel, b: GFRP, c: CFRP

a)

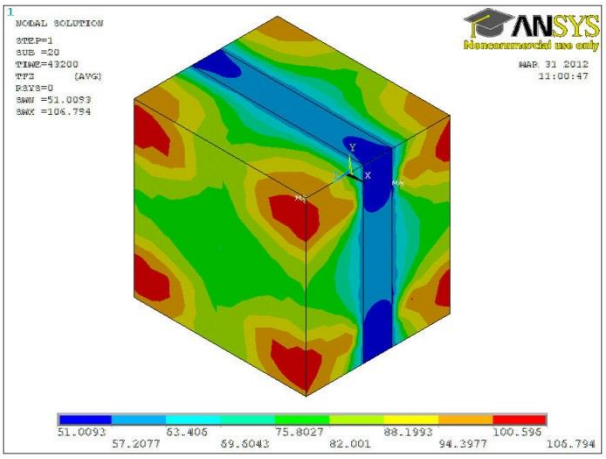

b)

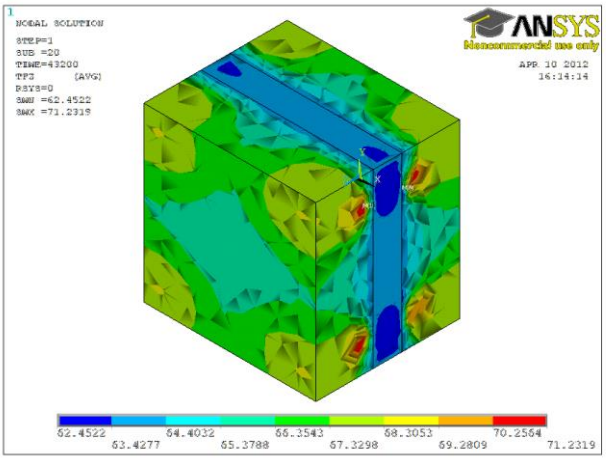

c)

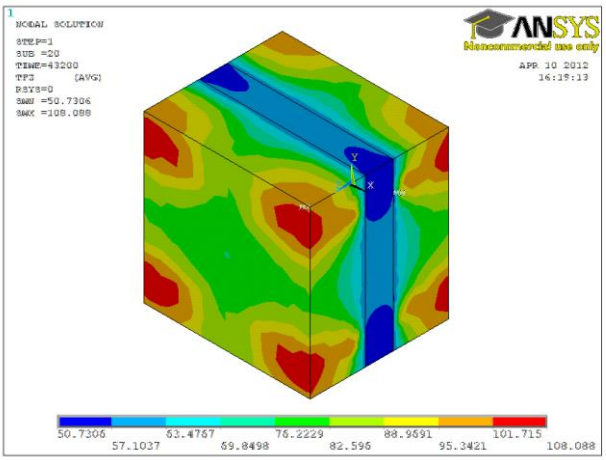

Figure A-15: Four W Connector Flux; a: Steel, b: GFRP, c: CFRP

a)

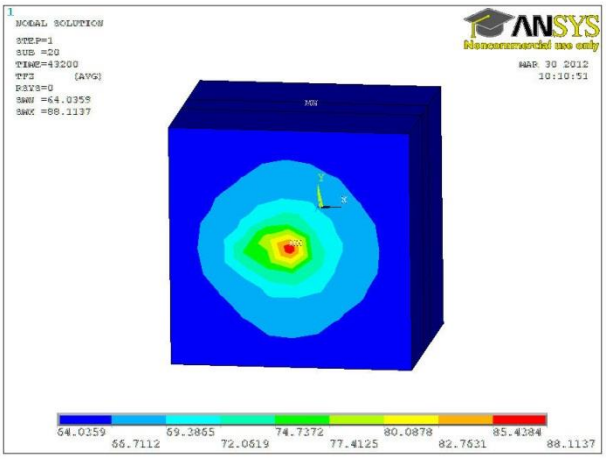

b)

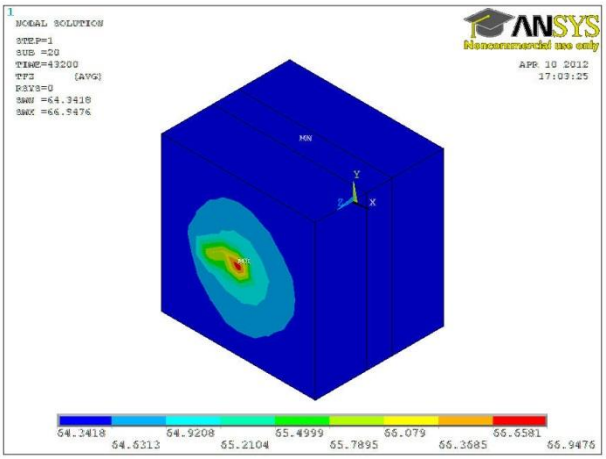

c)

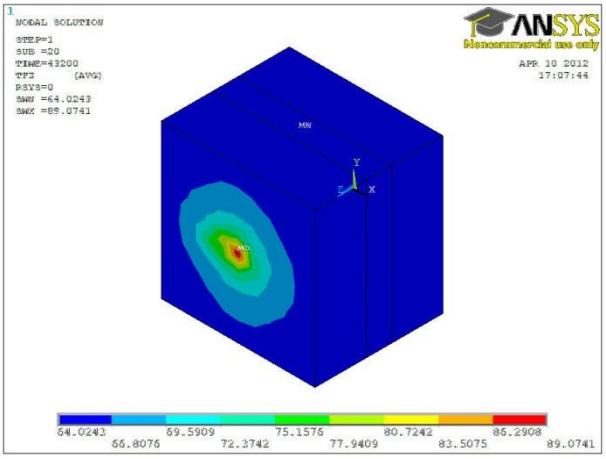

Figure A-16: One Z Connector Flux; a: Steel, b: GFRP, c: CFRP

a)

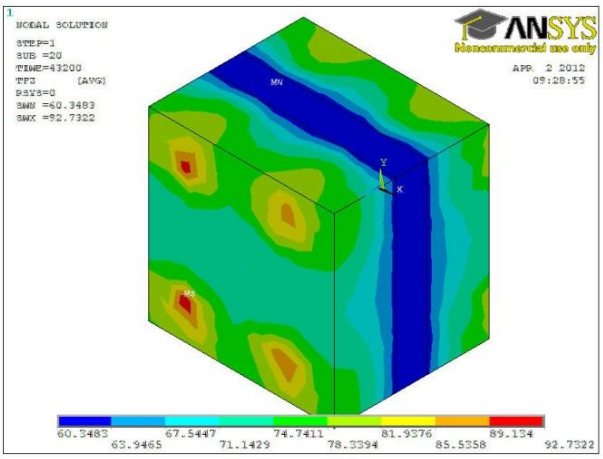

b)

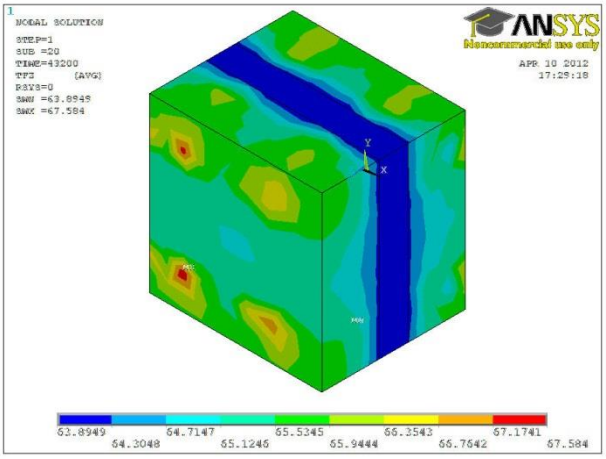

c)

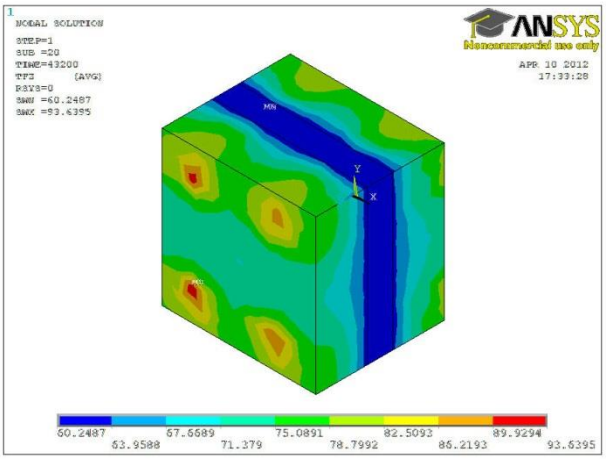

Figure A-17: Four Z Connector Flux; a: Steel, b: GFRP, c: CFRP

a)

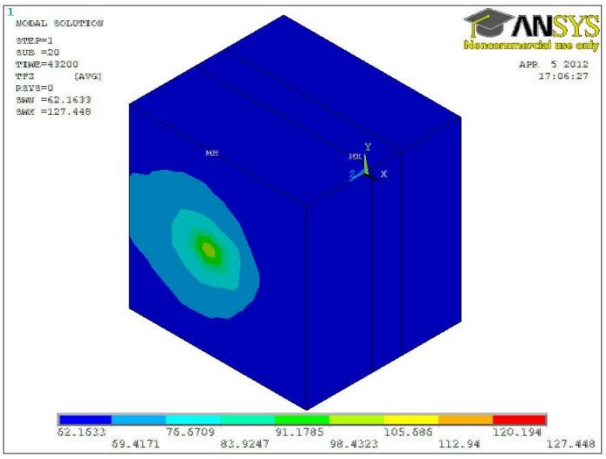

b)

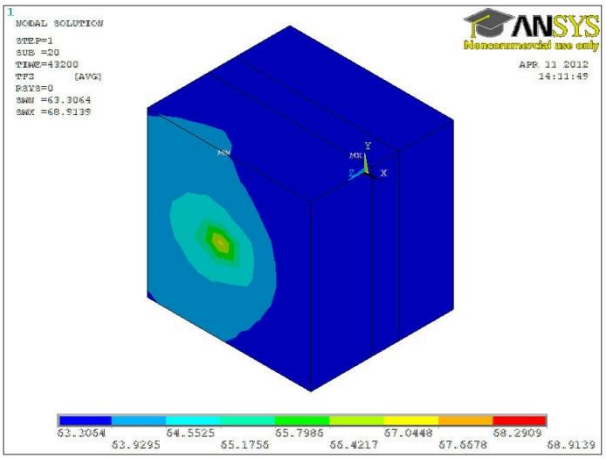

c)

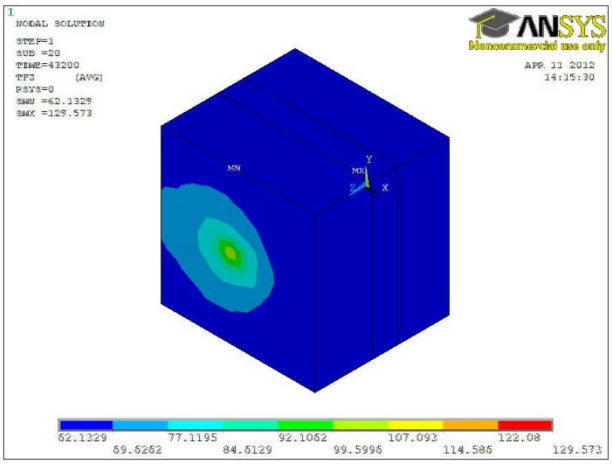

Figure A-18: One J Connector Flux; a: Steel, b: GFRP, c: CFRP

a)

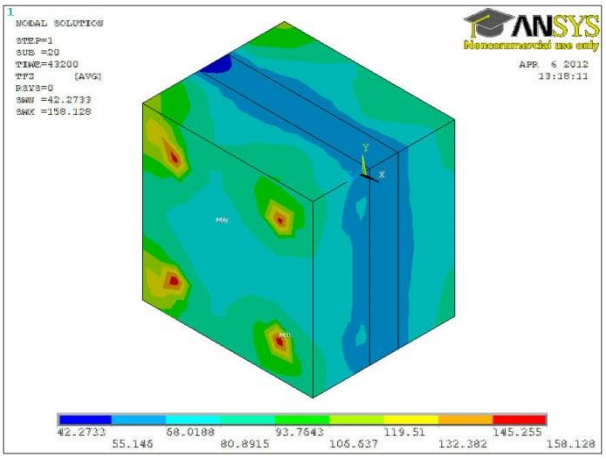

b)

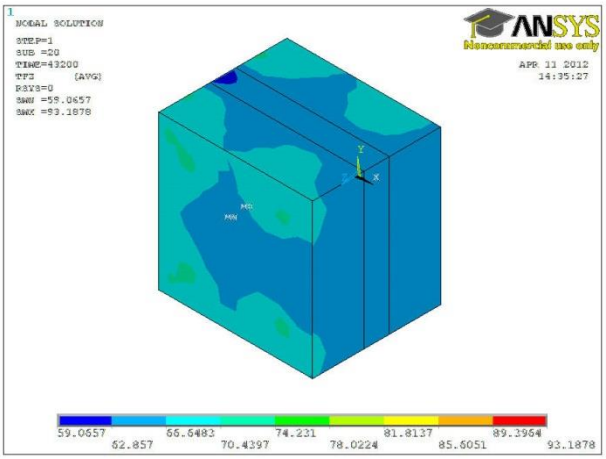

c)

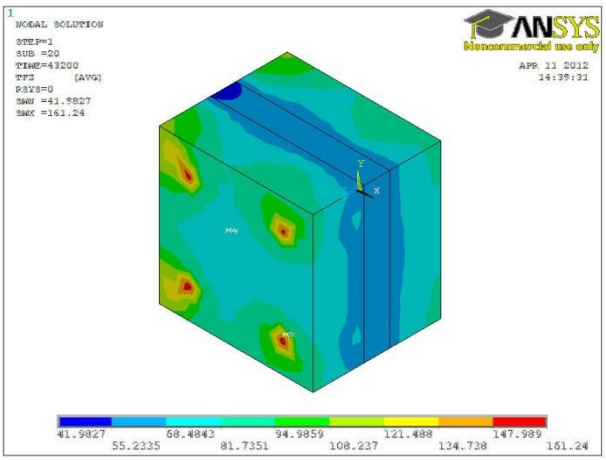

Figure A-19: Four J Connector Flux; a: Steel, b: GFRP, c: CFRP

a)

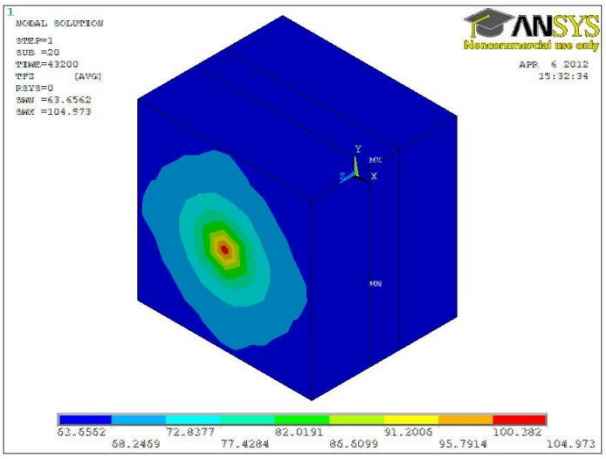

b)

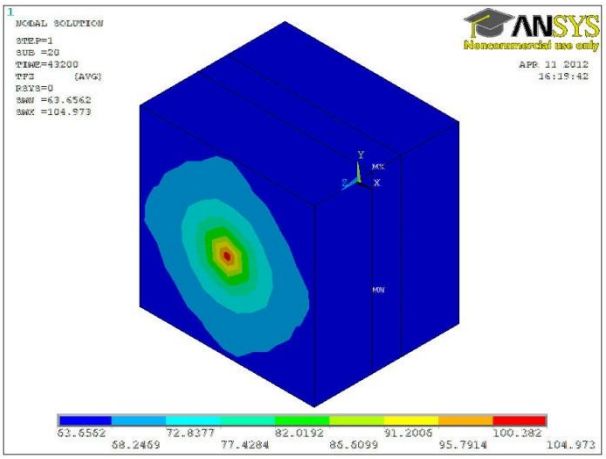

c)

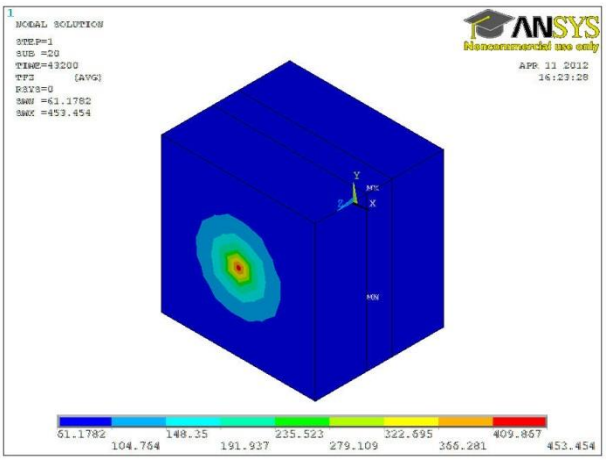

Figure A-20: One Dowel Connector Flux; a: Steel, b: GFRP, c: CFRP

a)

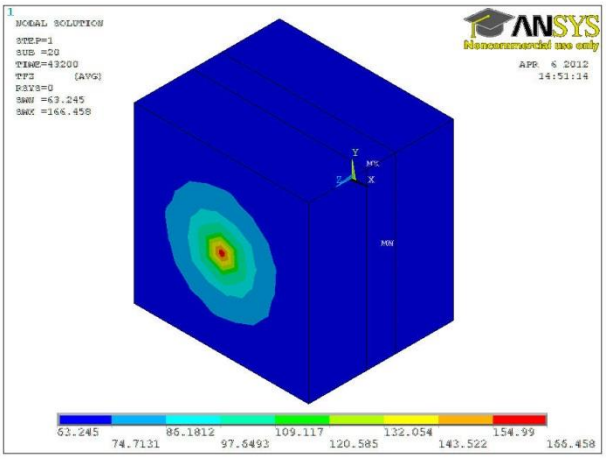

b)

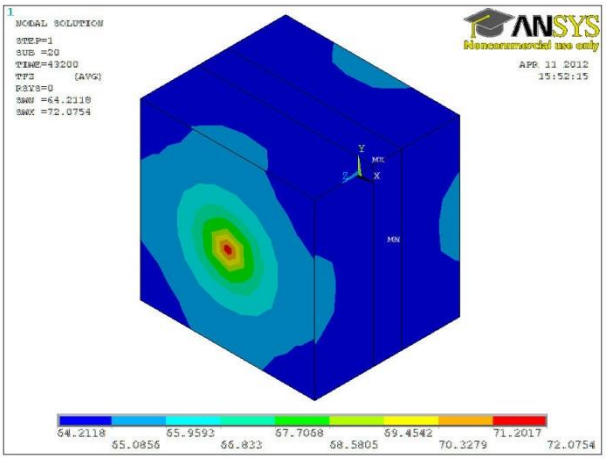

c)

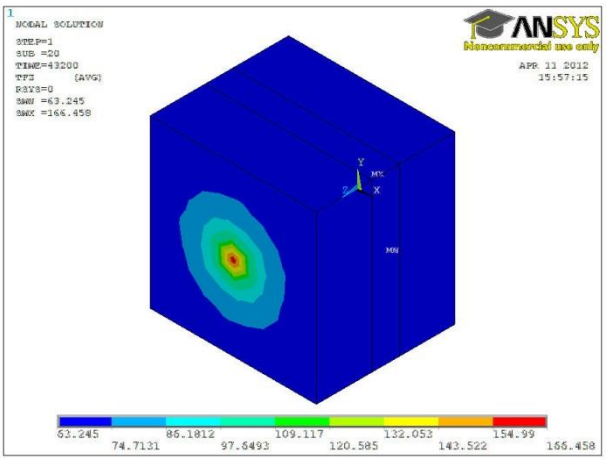

Figure A-21: One Bar Connector Flux; a: Steel, b: GFRP, c: CFRP

a)

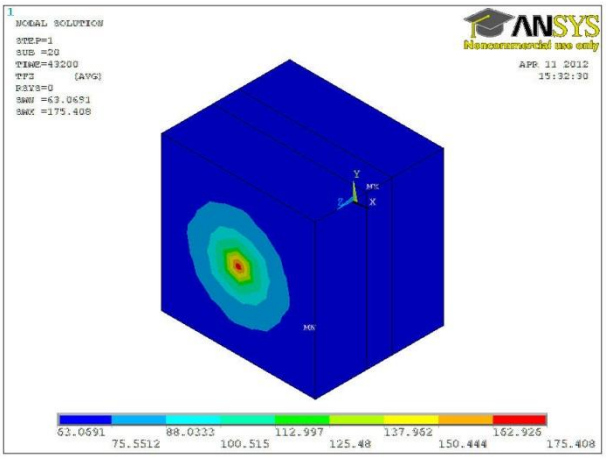

b)

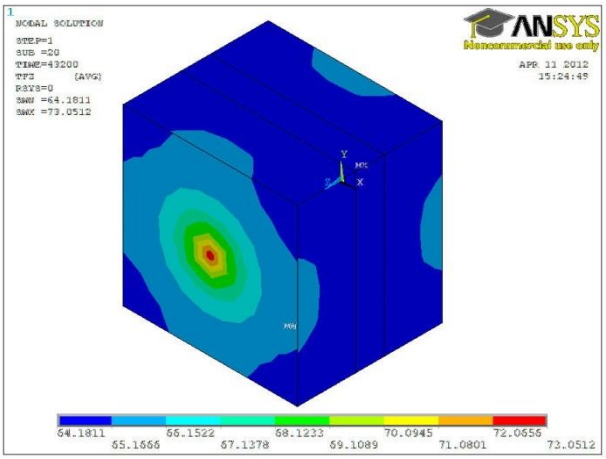

c)

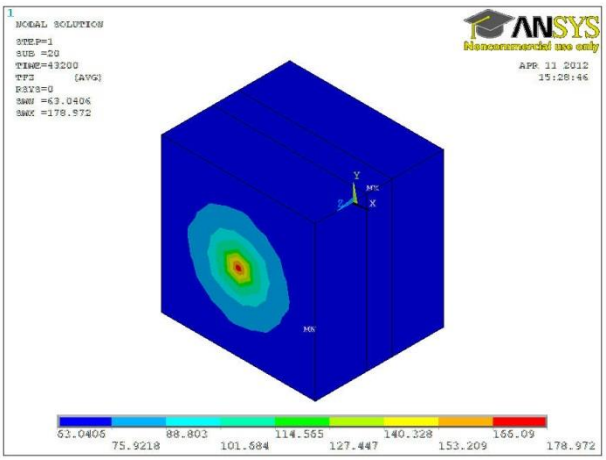

Figure A-22: One Strip Connector Flux; a: Steel, b: GFRP, c: CFRP